TRANSIENT BEHAVIOR OF WIND DRIVEN SYNCHRONOUS MACHINES

By

ABDUL QAVI QAZI

Bachelor of Engineering
University of Karachi
Karachi, Pakistan
1964

Magister Electro-Energeticae
Universitas Studiorum Zagrabiensis
Zagreb, Yugoslavia
1967

Submitted to the Faculty of the
Graduate College of the
Oklahoma State University
in partial fulfillment of
the requirements for
the Degree of
DOCTOR OF PHILOSOPHY
December, 1977

TRANSIENT BEHAVIOR OF WIND DRIVEN

SYNCHRONOUS MACHINES

Thesis Approved:

R. Ramakumar
Thesis Adviser

D K McLaughlin

Richard L. Cummins

Wm. S. Hughes

Norman N Durham
Dean of the Graduate College

ACKNOWLEDGMENTS

I bow my head in respect and gratitude to Professor Dr. R. Ramakumar, my thesis adviser; who made me think hard, work hard, grow and flourish. Dr. Ramakumar has given unsparingly of himself toward the building up of this thesis.

I owe a particular debt of gratitude to Dr. J. P. Chandler, who helped me to construct the computer programs, which made the simulation work possible. I wish to express my sincere appreciation to this scholar and gentleman.

I wish to acknowledge the help and assistance extended by Dr. W. L. Hughes, member of my Doctoral Committee, who devoted his time and effort on several academic and personal matters.

I would also like to thank Dr. Shair Ahmad and Dr. Roger Schoeppel for their assistance as Committee members. Special thanks are due Dr. Dennis McLaughlin and Dr. Richard L. Cummins for their critical examination of this thesis and for many valuable comments.

I take this unique opportunity to express my sincere thanks to Leslie Graham, Nancy Caldwell, Mike Leppela and Dr. Suresh Babu for their encouragement, advice, courtesy and cordiality.

I can only partially acknowledge the unbound love, and goodness of my wife Nasim Qazi, my daughter Fuaaza Qazi and son Abdul Qadir Qazi, who stayed and waited with patience and understanding in Pakistan while I was pursuing my doctoral program for four long years.

I am extremely grateful to the Government of Sind (Pakistan) who sponsored me for this program and financed my education.

Finally, I dedicate this work to the peasants, workers, laborers and intellectuals of the entire world who are striving to set up a classless society.

TABLE OF CONTENTS

LIST OF TABLES

LIST OF FIGURES

LIST OF SYMBOLS

A	the swept area of aeroturbine, m^2
C_d	the damping constant of flexible coupling, N·m·s/rd
C_{ddl}	the non-dimensional damping constant, dimensionless
C_p	the wind rotor power coefficient, dimensionless
E	the voltage of the infinite bus, p·u
E_e	the energy ratio of additional output to the additional input over an interval, dimensionless
E_{ex}	the exciter voltage referred to armature winding, p·u
E_g	the energy actually delivered to grid over an interval, Ws
E_{gd}	the ratio (Eg/Er), dimensionless
E_i'	the internal e·m·f behind direct-axis transient reactance x_d', p·u
E_q	the fictitious quadrature-axis voltage, p·u
E_q'	the quadrature-axis voltage behind transient reactance, p·u
E_{qo}	the fictitious quadrature-axis voltage at a time t=o-, p·u
E_r	the energy that would be delivered to grid over an interval at rated power, Ws
E_w	the energy contained in the wind in an interval, Ws
E_{wd}	the ratio (E_g/E_w), dimensionless
E_{wr}	the energy extracted by the wind rotor over an interval, Ws
G	the generator rating at full load, kVA
H_g	the generator inertia constant, s

H_w the wind rotor inertia constant, s

I_d the direct-axis component of load current, p·u

J_1 the inertia of the input gear, $N \cdot m \cdot s^2$

J_2 the inertia of the output gear, $N \cdot m \cdot s^2$

J_g the inertia of the electrical generator, $N \cdot m \cdot s^2$

J_w the inertia of the wind rotor, $N \cdot m \cdot s^2$

k the reactance ratio, dimensionless

k_1 the equivalent of identity as given by (4.4), dimensionless

k_T the ratio of maximum torque to the rated torque in eddy-current coupling, dimensionless

K_{ex} the excitation system forward gain, p·u

K_{st} the derivative feedback gain, p·u

n the gearing ratio, dimensionless

N_w the speed of wind rotor, r/min

p the number of poles, dimensionless

P_d the generator damping power, p·u

P_d^* the generator damping power, kW

P_{dd} the direct-axis damping power, p·u

P_{qd} the quadrature-axis damping power, p·u

P_s the generator synchronising power, p·u

P_s^* the generator synchronising power, kW

P_w power of the wind rotor, kW

R_w the radius of wind rotor, m

s the Laplace operator, $^1/s$

S_c the stiffness constant of the rigid and flexible couplings, N·m/rd

S_{cdl} the non-dimensional stiffness constant, dimensionless

t	the time, s
T_1	the torque at the input gear, N·m
T_2	the torque at the output gear, N·m
T_d	the generator damping torque, N·m
T'_{do}	the direct-axis transient open-circuit time constant, s
T''_{do}	the direct-axis subtransient open-circuit time constant, s
T_{ex}	the exciter time constant, s
T_g	the generator electromagnetic torque, N·m
T_m	the maximum (eddy-current coupling) torque, N·m
T''_{qo}	the quadrature-axis subtransient open-circuit time constant, s
T_r	the rated torque of generator, N·m
T_s	the generator synchronising torque, N·m
T_{st}	the feedback time constant, s
T_w	the torque developed by wind rotor, N·m
V	the wind speed, m/s
V_p	the peak wind speed, m/s
V_r	the rated wind speed, m/s
V_{ref}	the reference voltage, p·u
V_{st}	the stabilizer feedback voltage, p·u
V_t	the generator terminal voltage, p·u
x	the ratio of ω_m to ω_r as given by (4.3), dimensionless
x'_d	the direct-axis system transient reactance, p·u
x'_{dg}	the generator direct-axis transient reactance, p·u
x''_{dg}	the generator direct-axis subtransient reactance, p·u
x_e	the system external reactance, p·u
x_{e1}	the reactance of transmission line 1, p·u
x_{e2}	the reactance of transmission line 2, p·u

x_q	the system quadrature-axis reactance, p·u
x'_{qg}	the generator quadrature-axis transient reactance, p·u
x''_{qg}	the generator quadrature-axis subtransient reactance, p·u
x_{t1}	the reactance of step up transformer 1, p·u
x_{t2}	the reactance of step up transformer 2, p·u
X_k	the linear voltage rise constant, p·u/s
α	ratio of actual torque to the maximum torque at any instant and given by equation (4.3), dimensionless
β	the blade pitch angle, mech·deg
δ	the generator torque angle, elec·rd
δ_o	the generator initial angle, elec·rd
δ_i	the generator internal angle between vectors E and E'_i, elec·rd
δ_m	the generator maximum angle, elec·rd
$\hat{\delta}$	the generator maximum displacement ($\delta_m-\delta_o$), elec·rd
ε	the error signal, p·u
η_g	the efficiency of gearing, dimensionless
Θ_1	the mechanical angular displacement of input gear, mech·rd
Θ_2	the mechanical angular displacement of output gear, mech·rd
Θ_{gm}	the mechanical angular displacement of generator, mech·rd
Θ_w	the mechanical angular displacement of wind rotor, mech·rd
$\dot{\Theta}_1$	the mechanical angular velocity of input gear, mech·rd/s
$\dot{\Theta}_2$	the mechanical angular velocity of output gear, mech·rd/s
$\dot{\Theta}_{gm}(\omega_{gm})$	the mechanical angular velocity of generator rotor, mech·rd/s
$\dot{\Theta}_w(\omega_w)$	the mechanical angular velocity of wind rotor, mech·rd/s
$\ddot{\Theta}_1$	the mechanical angular acceleration of input gear, mech·rd/s^2
$\ddot{\Theta}_2$	the mechanical angular acceleration of input gear, mech·rd/s^2

$\ddot{\theta}_{gm}$ the mechanical angular acceleration of generator rotor, mech·rd/s^2

$\ddot{\theta}_{w}$ the mechanical angular acceleration of wind rotor, mech·rd/s^2

λ the tip speed to wind speed ratio, dimensionless

ρ the density of air, kg/m^3

ω the (eddy-current coupling) slip at any instant, p.u

ω_o the angular speed of synchronously rotating axis, elec·rd/s

ω_m the (eddy-current coupling) slip at the maximum torque, p.u

ω_r the (eddy-current coupling) slip at the rated torque, p.u

$\omega_{syn}(\dot{\theta}_{gms})$ the synchronous angular velocity of generator, rd/s

CHAPTER I

INTRODUCTION

1.1 Historic Works in Wind Power

Wind as a source of energy has been known from early times of civilization and human beings have used it for pumping water, irrigation purposes and so on. By the turn of the 19th century, windmills were contributing electrical power (though in small amounts) in Europe, most notably in West Germany, Denmark and Holland. At the end of the 19th Century, Professor LaCour began his systematic investigations into the possibilities for production of electricity, utilizing, among other things, a wind turbine generator at Askov in Denmark (1). Later efforts towards utilization of wind energy followed towards the close of First World War and immediately after it. Scientists in France, Germany and Russia became interested in developing a modern theory of the windmill in conjunction with war-born progress in the theory of the air-screw. Joukowsky, Drzewieki, Krassovsky and Sabinin in Russia; Prandtl and Betz in Germany; and Constantin and Eiffel in France are considered as the architects of modern windmill theory. Savonius in Finland, Kumme and Bilau in Germany, Darrieus in France and Fales in the United States evolved various windmill designs (2). Juul, a former collaborator of Professor LaCour, continued the work after 1950 with a wind power unit of 13 kW rating in Vester. He also put in operation on the island of

Bogϕ a three phase 45-kW unit employing a three-blade assembly 13 meters in diameter (3). In 1957, the Danish Wind Power Committee, set up by the Danish Power Station Association, built the 200-kW Gedser mill. It had a swept area of 450 m^2 with 3 blades and a horizontal axis. It employed a low-slip (1 percent) induction generator. The Gedser mill produced rated power at a wind speed of 15 m/s and worked very satisfactorily (4).

Most of the recent German contribution to wind power is accredited to Hütter of Stüttgart, who designed windmills rated in the 10-100 kW range from 1950 to 1960. One example of his design is the 100-kW test facility at Stötten in Germany. It had a propeller area of 910 m^2 with a propeller diameter of 34 m, and produced rated power at 8 m/s. Honeff and Hütter concentrated on the mechanical and structural design aspects along with emphasis on cost economics of windmills (5) (6).

In England, Golding has contributed significantly towards the advancement of wind power. The English had an extensive program from 1945 to 1960, one important example being the 100-kW Enfield-Andreau wind turbine with a propeller diameter of 24 m. Golding (7), in his design analysis of large wind-power generators for electric-utility use, has adopted a low-slip induction machine instead of a conventional synchronous machine.

During the period 1958 - 1966, three large windmills were developed and tested in France, the largest windmill, Saint-Remy-des-Landes, had a rated power of 800 kW. It ran without problems for seven months. The tests with this machine ended in June 1964 due to breaking of the shaft and by this time, in France, it had been decided that continued wind-energy research would not be undertaken (8).

Most of the recent American effort is inspired by the Smith-Putnam experiment and is stimulated by the energy crisis. Present thinking is focused on two basic approaches: (i) constant speed constant frequency (CSCF) approach, in which the aeroturbine drives the synchronous generator (or an induction generator), which operates in parallel with power grids, locks into synchronism and maintains a constant (or nearly constant) rotational speed which is independent of the wind speeds; (ii) variable speed constant frequency (VSCF) approach, in which the aeroturbine operates at varying speeds while the output is maintained at constant frequency by means of a variable-speed, constant-frequency generation scheme (9).

In the last four years, extensive efforts have been undertaken in these two directions. The CSCF approach appears to have drawn more attention, both in private and public sectors. This is possibly due to the fact that considerable experience and technology in design and operation of synchronous and induction machines already exists. Two programs are underway to materialize the CSCF approach. These two programs are different in technical application: one employs a horizontal axis wind rotor and the other (Darrieus), a vertical axis (egg-beater-type) wind rotor. Essentially, horizontal axis wind turbine employs the technology and thinking of the Smith-Putnam machine, influenced somewhat by Hütter's designs. Such a program is underway at the NASA-Lewis Research Center (10). Testing of the prototype MOD-0 100-kW machine at NASA's Plum Brook Station started in 1976. Synchronous operation, in phase with the local utility network was first achieved on October 17, 1976. The NASA proposal calls for installation of two 200-kW versions of this unit (MOD-0A) in 1977 and 1978.

For large systems operating in parallel with utility grids to supplement the energy generated and save fuel, the horizontal axis wind turbine program is being extended. General Electric Company has been selected to undertake final design and fabrication of the MOD-1 1.5-MW wind turbine under the direction of the NASA-Lewis Research Center. This system with a rotor diameter of 61 m, will be the largest wind turbine ever constructed. It is to be optimized for 8.04 m/s average wind sites. This is to be followed by MOD-2 wind turbine, which will have a 91.44 m rotor and be optimized for lower (6.25 m/s) wind sites (11).

The vertical axis wind turbine (VAWT) program constitutes the second and contemporary part of the CSCF approach. This program patronizes the Darrieus, vertical axis (egg-beater-type) wind turbine which is being developed at Sandia Laboratories. It appears to be the most promising advanced system in terms of potential for early implementation and increased energy output per unit-cost. Emphasis is being laid on development and testing of a 17 m unit which is already in operation at Albuquerque, New Mexico. Efforts towards the development of VAWT program are fully reported in the literature published by Sandia Laboratories (12)(13).

The second approach, which is relatively new, has emerged in the form of development of several VSCF electrical generation schemes. Such schemes have been developed by judiciously synthesizing rotating machines with switching devices such as thyristors and diodes. The following schemes are being actively pursued for wind energy applications: (a) field modulated generator systems (14)(15) (b) AC-DC-AC link (16) (c) double output induction generators (17) and; (d) AC commutator generator (18).

1.2 Works on Electrical Stability of Wind-Driven Machines

One important aspect of wind electric conversion systems is that of electrical stability. Stability may be defined as the condition of an electrical system to deliver the load and remain in synchronism, or "in step" with the rest of the system (19) when the system is subject to external disturbances such as wind gusts or electrical faults. It may also be defined as the tendency of a power system or its component parts to develop forces to maintain synchronism (20). As wind driven systems grow in size and capacity, the dynamics of such machines and their interaction with utility grids shall assume special importance. Before treating this subject further, it would be appropriate briefly to review prior efforts on the subject of stability.

Transient stability of wind electric systems has come into focus only recently. Romanelli (21), recognizes an earlier letter of P. C. Brown and sets up a second order differential equation, which is very similar to that of a synchronous generator driven by a classical prime mover running at constant speed (22), excepting that the constant input torque is replaced by wind torque which varies with time. He proposes control to limit the accelerating torque to 0.8 per unit.

Johnson and Smith (23), in their recent pioneering paper, attack the problem using the classical Park equations (24)(25) and solve the sets of appropriate equations to examine the behavior of power and load current variations to an input gust function for various system configurations. This paper does not deal directly with problems of stability.

Pantalone and Potter (26), in a contemporary work, have dealt

with dynamic stability of a simple model with the help of state space equations. They study the dynamics of a wind generating system for small oscillations, using block diagrams, frequency response and time response techniques. A linearized model for the generator has been used and blade pitch control mechanism is represented by a transfer function having a second-order denominator. The model does not deal with disturbances of higher severity as would be the case with sharp wind gusts, short circuits and automatic switching. Martinez and Sanchez (27), consider the static and dynamic characteristics of multi-pole 3-phase alternators, with emphasis on the transient behavior. The transfer function from torque and excitation changes to angular deviations of the alternator rotor is derived for a typical salient-pole machine. An order-of-magnitude estimate of the dominant frequency (that for hunting oscillations) is made to show that the hunting mode can be excited by a variety of disturbing torques.

Lingelbach (28) examines the power-flow dynamics of a wind turbine driving different types of generators by means of analog computer simulation. A quasi-steady state model is used for electrical power developed by the generators. Damping is included only in the mechanical dynamics with electrical losses considered as a part of the electrical power developed by the generator. This paper gives an insight into elements of stability of electrical machines driven by wind rotors.

Hwang and Gilbert (29)(30), in their two most recent papers have studied the problem of random synchronization of a synchronous generator driven by a wind rotor. They simulate solutions for rotor speed, generator power angle, electromagnetic torque, wind turbine torque, blade pitch and output current by solving the sets of relevant non-

linear equation. Machine is represented fully as formulated by Olive (31). They include blade pitch control and simulate the torque and torque angle versus time. They do not deal with slower mechanical transients such as the ones caused by frequently-occurring wind gusts. These papers are of great experimental value, as the authors use the actual data obtained from NASA-Lewis MOD-0 system to verify their simulation results.

1.3 Factors Affecting the Dynamics of Wind-driven Electrical Machine

Contrary to conventional thermal and hydropower plants, wind-driven synchronous machines are faced with more complex problems involving machine dynamics. This complexity is caused by various factors such as varying wind inputs, aeroelastic and aerodynamic properties of wind rotor, type of mechanical coupling, electrical and mechanical parameters of the machine and parameters related to interconnection with the utility grid. Performance of constant speed constant frequency wind energy conversion systems is aggrevated by transient disturbances such as wind gusts, short circuits, opening and reclosing of lines or some combination of the these. Criteria for satisfactory performance of such a system are therefore more difficult to establish under such conditions. Besides the wind gust, which is characterized by the amplitude and duration of the gust function, the following system parameters affect the transient behavior of a wind driven synchronous machine connected to utility grid: inertia constant of wind rotor H_w; power coefficient characteristic of wind rotor; type and characteristics of mechanical coupling; generator rotor inertia H_g;

generator electrical damping; generator transient reactance, x'_{dg}; and overall external reactance, x_e. All these factors affect the dynamic behavior of wind-driven synchronous machines connected to utility grids. A critical examination of the influence of these factors is necessary to determine and suggest solutions to problems associated with design and performance of constant speed constant frequency wind electric conversion systems.

1.4 Problem Description

The transient behavior of wind driven synchronous machines connected to utility grids is affected by several parameters, as discussed in the previous section. The wind gust function is generally characterized in terms of amplitude, duration and frequency of occurrence. These characteristics are highly variable in nature and depend on the geographic location of the wind energy system and the nature of the wind. Specifically, there is no single and universal wind gust model. Analytical research is therefore based on an assumed gust model or recorded gust model. Results are therefore applicable to similar models only. Aerodynamic and aeroelastic reactions of wind rotors are very involved. Parameters of interposed couplings, such as type, stiffness, damping and torque-slip curve make the formulation of problem more involved. Characteristics of machine and connecting links, coupled with the transient state (as in gusts and faults) lead to a system of nonlinear differential equations. A simple system such as one wind driven synchronous machine connected to a utility grid (with a suitable mechanical coupling interposed between low torque gear and generator) leads to two sets of second

order nonlinear differential equations. Solution of these equations by suitable numerical methods should lead to the prediction of dynamic behavior of such systems under transient conditions of gusts and faults for an assumed gust model.

1.5 Model and Associated Assumptions

In order to establish a foundation for examining the transient behavior of wind driven synchronous machines, and to develop understanding of the subject in a systematic manner, it is desirable to set up a mathematical model of the physical system under study. One such physical configuration which would frequently occur with the emergence of wind energy systems is a wind driven synchronous machine connected to a utility grid of very large capacity whose voltage and frequency are fixed. In this thesis attention will be focused on such a system.

In order to simplify the analysis, several idealizing assumptions are made. These assumptions are consistent with the earlier results and (current) engineering practice. With the progress of the thesis, one or more of these assumptions would be relaxed to study the changes in the results. These assumptions are made with the following objectives in mind: (a) that no part of important information would be lost, (b) essential physical aspects of the system being examined are retained and (c) studies could be simplified to gain clear insight into the subject.

With these objectives in mind and as a first step in the transient stability analysis, the following assumptions would be made.

(a) Wind power is instantaneously transferred to the blades of wind rotor on contact.

(b) Blade pitch mechanism will not respond to short duration

gusts of 1 and 2 seconds.

(c) During periods of gusting and faults, the aeroturbine will be swinging on an appropriate C_p vs λ curve corresponding to a fixed blade pitch angle.

(d) At time t=0-, the system is in dynamic equilibrium. Output of the aeroturbine is equal to the mechanical input to generator, accounting for gearing efficiency. This implies no acceleration or decceleration at this time.

(e) The machine under study is of the salient pole type with damper windings and will be represented by a constant quadrature axis transient voltage E_q' (which is proportional to flux linkage) as is customary in stability studies for disturbances of short duration.

(f) For gusts of longer duration, field flux linkage ψ_f and hence Eq' varies with voltage regulator action. Such a regulator and exiter would be represented by a linear variation in the excitation voltage.

(g) Changes in stator flux linkages and speed variations would be neglected.

With the above assumptions, following physical system configurations would be studied:

(i) Wind driven synchronous generator connected to utility grid; stiff coupling interposed between synchronous generator and low-torque gear.

(ii) Wind driven synchronous generator connected to utility grid; flexible coupling with damping interposed between synchronous generator and low-torque gear.

(iii) Wind driven synchronous generator connected to utility grid; eddy-current coupling interposed between synchronous generator and low-torque gear.

1.6 Method of Analysis

The following sequence will be followed to develop the subject matter of this thesis.

(i) To formulate mathematical equations which govern the behavior of physical configurations as outlined in 1.5. These will be sets of coupled non-linear differential equations along with auxilary algebraic equations.

(ii) To solve these equations simultaneously with the help of an appropriate numerical technique.

(iii) To extract the necessary information from computer simulation and predict the behavior of systems when subject to transient disturbances by plotting a series of curves for each system.

(iv) To interpret these curves and draw some useful conclusions.

(v) To establish some guidelines for further research and study.

1.7 Organization of the Thesis

Chapter II deals with the first system configuration, a wind-driven synchronous machine connected to utility grid with a stiff coupling interposed between generator and the low-torque gear. This chapter forms the basis for further studies on the transient behavior of models of more complex systems (configurations). Influence of important system parameters such as system inertia, electrical damping, stiffness of the shaft, machine reactance, external reactance and generator excitation is examined under conditions of one-and two-second duration wind gusts by simulating generator torque angle as a function of time. Some basic conclusions are drawn from curves which form the guide for work in chapters III and IV.

Chapter III deals with the second configuration, a wind-driven synchronous machine connected to utility grid with a flexible coupling interposed between the generator and low-torque gear. The influence of stiffness constants and damping constants is examined in detail. The concept of nondimensional parameters is introduced to make the study more general and widely applicable. Excitation control is included in studies with two-second gusts to make the mathametical models more realistic and complete. Simulation results are presented in the

form of torque angle versus time curves. A set of nondimensional ($\hat{\delta}$ versus k) curves are developed from the simulation results. These curves provide valuable information regarding certain design parameters of the systems.

Chapter IV deals with the third physical system, in which an eddy-current coupling is employed instead of flexible coupling with damping. In addition to stability aspects, attention is focused on energy collection and energy delivery aspects of the system. The concept of nondimensional energy analysis is introduced to make the studies widely applicable. Computer simulations are carried out to study the system behavior for various coupling characteristics. Conclusions are drawn as regards the application and design parameters (k_T and ω_r) of eddy-current couplings.

Chapter V attempts to handle faults and gusts occurring simultaneously, with an eddy-current coupling in the mechanical interface. Some basic conclusions are drawn on the potential of eddy-current couplings for use in wind generating systems.

The thesis concludes with the presentation of the summary of results and suggestions for further work in Chapter VI.

CHAPTER II

STUDIES ON WIND-DRIVEN SYNCHRONOUS MACHINES EMPLOYING STIFF COUPLINGS

2.1 Introduction

This chapter deals with the dynamics of a wind-driven synchronous machine connected to a large utility grid, with stiff coupling interposed between the generator and the high-speed (low-torque) shaft of the step-up gear. Absence of mechanical damping and high stiffness of shaft make this configuration very conservative and severe in terms of transmitting torque fluctuations onto the electrical generator. In spite of these factors, a study of this system should provide an insight into the fundamentals of the dynamics of wind-driven synchronous machines. This system will help in understanding the dynamics of simple couplings and, above all, a formulation of equations in the case of this configuration is easily obtained. Equations established for this case could easily be modified to handle subsequent physical systems (as will be shown in Chapters III and IV). With this view in perspective, governing equations for the stated configuration will be developed with the help of block schematics and free-body diagrams.

2.2 System Configuration and Governing Equations

The system under investigation consists of an aeroturbine, a step-up gearing mechanism, a stiff coupling, and a synchronous generator

connected to a large utility grid (infinite bus) of fixed voltage and frequency. The system schematic is shown in Figure 1, in which a physical configuration and the corresponding free-body diagrams are illustrated. The schematic and free-body diagrams are self-explanatory.

From free-body diagrams,

$$T_w = J_w\ddot{\theta}_w + J_1\ddot{\theta}_1 + T_1 \tag{2.1}$$

Rearranging Equation (2.1) and taking $\theta_w = \theta_1$ for a rigid shaft of large diameter, Equation (2.1) can be written as:

$$T_w = T_1 + \ddot{\theta}_w(J_w + J_1) \tag{2.2}$$

Also,

$$T_2 - J_2\ddot{\theta}_2 = S_c(\theta_2 - \theta_{gm}) \tag{2.3}$$

and

$$S_c(\theta_2 - \theta_{gm}) = J_g\ddot{\theta}_{gm} + T_g \tag{2.4}$$

Neglecting gearing and shaft inertia (which are negligible as compared to system inertia):

$$T_w = T_1 + J_w\ddot{\theta}_w \tag{2.5}$$

$$T_2 = S_c(\theta_2 - \theta_{gm}) \tag{2.6}$$

$$S_c(\theta_2 - \theta_{gm}) = J_g\ddot{\theta}_{gm} + T_g \tag{2.7}$$

Equating work done on both sides of the gearing and accounting for gearing efficiency η_g:

$$\eta_g T_1\theta_w = T_2\theta_2 \tag{2.8}$$

Rearranging Equation (2.8):

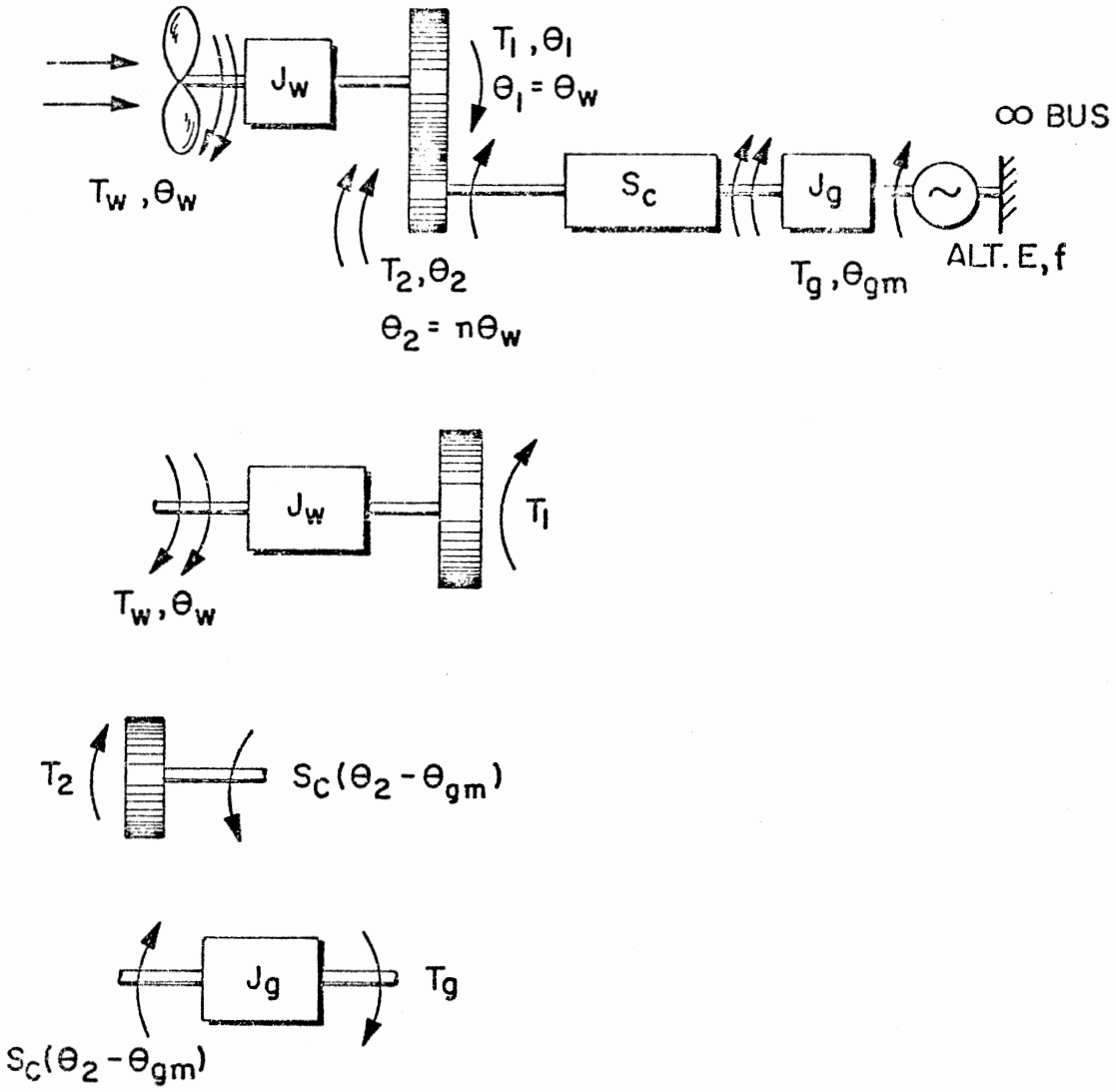

Figure 1. Schematic of the System Employing Stiff Coupling

$$T_1 = T_2 \left(\frac{\theta_2}{\theta_w}\right) \frac{1}{\eta_g} \tag{2.9}$$

but,

$$\frac{\theta_2}{\theta_w} = n$$

where n is the gearing ratio (n > 1). Putting

$$\frac{\theta_2}{\theta_w} = n$$

in Equation (2.9):

$$T_1 = T_2 \, n \, \frac{1}{\eta_g} \tag{2.10}$$

Elimination of T_1 from Equation (2.5) with the help of Equation (2.10) leads to:

$$T_w = T_2 n \, \frac{1}{\eta_g} + J_w \ddot{\theta}_w \tag{2.11}$$

Remembering that $\theta_w = \frac{\theta_2}{n}$, Equation (2.11) can be rearranged as:

$$T_2 = \eta_g \left(\frac{T_w}{n} - J_w \ddot{\theta}_w \frac{1}{n}\right) \tag{2.12}$$

Eliminating T_2 from Equation (2.12) by equating it to Equation (2.6):

$$S_c(\theta_2 - \theta_{gm}) = \frac{\eta_g}{n} (T_w - J_w \ddot{\theta}_w) \tag{2.13}$$

Knowing that $\theta_2 = n\theta_w$:

$$\frac{n}{\eta_g} S_c(n\theta_w - \theta_{gm}) = T_w - J_w \ddot{\theta}_w \tag{2.14}$$

Rearranging Equation (2.14) and multiplying both sides of the same by ω_w:

$$\omega_w J_w \ddot{\theta}_w = \omega_w \left[T_w - \frac{1}{n_g} S_c(n^2\theta_w - n\theta_{gm})\right] \tag{2.15}$$

Recognizing that $\omega_w T_w = P_w$, rearrangement of Equation (2.15) leads to the expression for the acceleration of the wind rotor given by:

$$\ddot{\theta}_w = \frac{1}{\omega_w J_w}\left[P_w - \omega_w S_c\ (n^2\theta_w - n\theta_{gm})\right] \tag{2.16}$$

In this square bracket, P_w is the power of the wind given by:

$$P_w = 0.5\rho\, AV^3 C_p \tag{2.17}$$

and

$$\omega_w = \dot{\theta}_w \tag{2.18}$$

Again from Equation (2.7) and $\theta_2 = n\theta_w$:

$$S_c(n\theta_w - \theta_{gm}) = T_g + J_g\ddot{\theta}_{gm} \tag{2.19}$$

where T_g is the total generator electromagnetic torque, and:

$$T_g = T_s + T_d \tag{2.20}$$

From Equations (2.19) and (2.20):

$$J_g\ddot{\theta}_{gm} = S_c(n\theta_w - \theta_{gm}) - T_s - T_d \tag{2.21}$$

Multiplying both sides of Equation (2.21) by ω_{gm} and rearranging:

$$\ddot{\theta}_{gm} = \frac{1}{\omega_{gm} J_g}\left[\omega_{gm} S_c\ (n\theta_w - \theta_{gm}) - (P_s^* + P_d^*)\right] \tag{2.22}$$

Often in practice, the terms P_s and P_d are known as "per-unit" powers and not the actual quantities. This practice will be followed throughout this study.

Defining G to be the generator rating in kVA, Equation (2.22) can be modified and written as:

$$\ddot{\theta}_{gm} = \frac{1}{\omega_{gm} J_g} [\omega_{gm} S_c (n\theta_w - \theta_{gm}) - 1000\, G(P_s + P_d)] \tag{2.23}$$

where

$$\omega_{gm} = \dot{\theta}_{gm}, \text{ and} \tag{2.24}$$

$$P_s = \frac{E'_q E \sin\delta}{x'_d} + \frac{E^2 (x'_d - x_q) \sin 2\delta}{2 x'_d x_q} \tag{2.25}$$

$$P_d = P_{dd} + P_{dq} \tag{2.26}$$

$$P_{dd} = \frac{E^2 T''_{do} (x'_{dg} - x''_{dg}) \dot{\delta} \sin^2\delta}{(x_e + x'_{dg})^2} \tag{2.27}$$

$$P_{dq} = \frac{E^2 T''_{qo} (x'_{qg} - x''_{qg}) \dot{\delta} \cos^2\delta}{(x_e + x'_{qg})^2} \tag{2.28}$$

$$\delta = \frac{p}{2} \theta_{gm} - \omega_o t \tag{2.29}$$

$$\lambda = \frac{R_w \dot{\theta}_w}{V} \tag{2.30}$$

and finally,

$$C_p = f(\lambda, \beta) \tag{2.31}$$

is known from the shape of the "C_p vs. λ" characteristic of the wind rotor.

Equations (2.25) through (2.29) constitute the mathematical model of the synchronous machine under transient conditions. This model, originally due to Park, is reduced and simplified by Kimbark. It is applicable if the transformer voltage terms are assumed to be small compared

to speed voltages in the stator windings and if variations in speed are small (less than $\pm 3.5\%$). Machine models and their applications are further discussed in the Appendix.

2.3 State Variable Representation

Equations (2.1) through (2.31) fully describe the dynamics of the physical system. A closer look at these equations will show that they form a coupled, nonlinear, fourth-order system. The order of the system will be higher if voltage-regulator action, stabilizer action, complete machine representation (see Appendix), and blade pitch control are included in the study. Since the purpose of this chapter is to develop understanding of the elements of system dynamics and essentials of transient stability study, the above set of equations will suffice and will adequately represent the dynamics of the system configuration.

Solution of these equations should provide the necessary information regarding transient behavior of the system when subjected to short-duration wind gusts of one and two seconds. The set of equations given by Equations (2.1) through (2.31) can be put in the state variable representation as follows.

Define a solution vector $\vec{Z}(t)$ and a function vector $\vec{F}(\vec{Z},t)$, such that:

$$\vec{Z}(t) \equiv \begin{bmatrix} Z(1) \\ Z(2) \\ Z(3) \\ Z(4) \end{bmatrix} \equiv \begin{bmatrix} \theta_w(t) \\ \dot{\theta}_w(t) \\ \theta_{gm}(t) \\ \dot{\theta}_{gm}(t) \end{bmatrix} \tag{2.32}$$

$$\vec{F}(\vec{Z},t) \equiv \dot{\vec{Z}}(t) \equiv \begin{bmatrix} \dot{Z}(1) \\ \dot{Z}(2) \\ \dot{Z}(3) \\ \dot{Z}(4) \end{bmatrix} \equiv \begin{bmatrix} f_1(\vec{Z},t) \\ f_2(\vec{Z},t) \\ f_3(\vec{Z},t) \\ f_4(\vec{Z},t) \end{bmatrix} \tag{2.33}$$

For the preliminary mathematical model, f_1 through f_4 are given by Equations (2.18), (2.16), (2.23), and (2.24) with necessary substitutions of auxiliary Equations (2.17) and (2.18) in Equations (2.16) and (2.25), and Equations (2.25), (2.27) and (2.28) in Equation (2.23).

2.4 Choice of Numerical Method and Digital Simulation

Earlier works by Kimbark and Crary (32) have employed "step-by-step" methods for solution of the well-known swing equations. Stagg and El-Abiad (33) have described a variety of numerical methods for solution of higher-order differential equations occurring in power-system analysis. When the system is "stiff," many of the ordinary numerical methods do not give a solution with reasonable step size. "Stiffness," in the numerical sense, is roughly defined as the ratio of the largest time constant in the system to the smallest time constant in the system. As systems become stiffer, popular numerical methods tend to become unstable and one has to resort to absolutely stable or A-stable methods such as Treanor's method or Lawson's methods, which can transform a stiff system to a nonstiff one (34). Explicit methods are complex and much more difficult to program, and one must choose between smaller step size and a more complex program.

In this study the fourth-order Runge-Kutta method will be used to solve the appropriate sets of Equations (2.1) through (2.31). The fourth-order Runge-Kutta method is (computationally) more efficient than some other methods, such as the Euler and the modified Euler method. It is highly accurate and most widely used for the solution of differential equations (35). A basic advantage of the method is that it needs only the initial values to generate the entire solution for the state vector $\vec{Z}(t)$ (36). The fourth-order Runge-Kutta method is also readily adopted to digital simulation.

In order to simulate the solution vector $\vec{Z}(t)$, Equations (2.1) through (2.31) need to be solved simultaneously (in a proper sequence). The computer program developed for this study can handle any number of elements in the state vector $\vec{Z}(t)$. The program designed for this stiff coupling is flexible and could be modified easily to handle the couplings to be treated in subsequent chapters. A program with these qualifications has been prepared to achieve generality, accuracy and flexibility. The flow chart of such a program for computer simulation is shown in Figure 2. This program uses three subroutines, RUK, FUNC and CYPY, to simulate the solution vector $\vec{Z}(t)$. In this process the subroutine CYPY provides an instantaneous value for the coefficient of performance corresponding to a previously computed value of λ. As pointed out earlier, the aeroturbine is assumed to be operating on a given C_p vs. λ curve for a fixed blade pitch angle (Figure 3) during conditions of gusting.

In order to conduct test studies, the data given in Table I is used for simulation. Values of the machine reactances and the time constants are chosen from literature (38) to conform to the normal practice. Air density is taken as 1.2 kg/m^3. Generator rotor inertia is estimated to

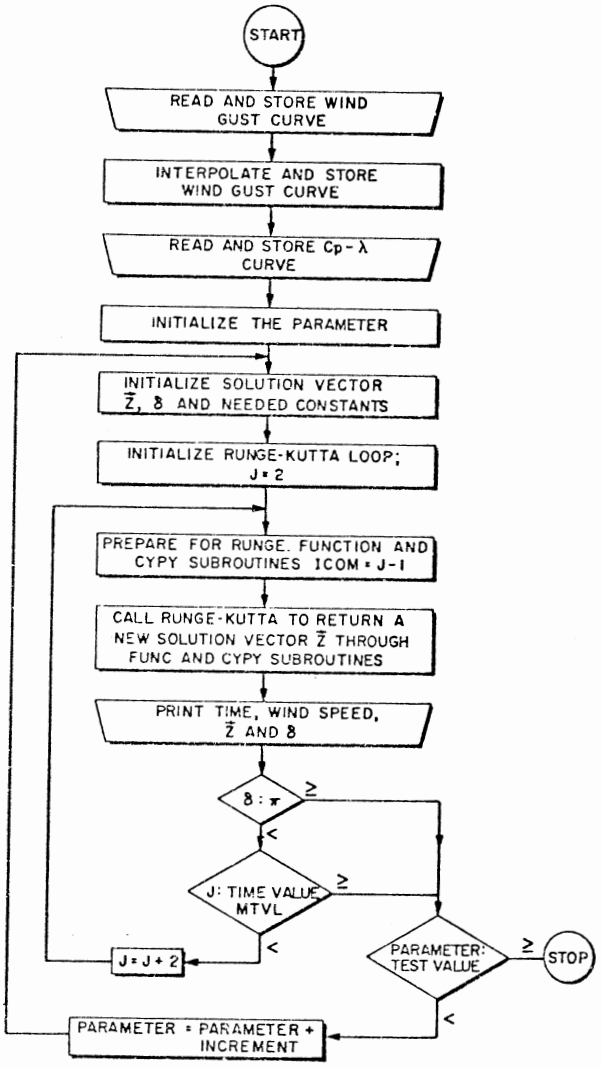

Figure 2. Computer Simulation Flow Chart

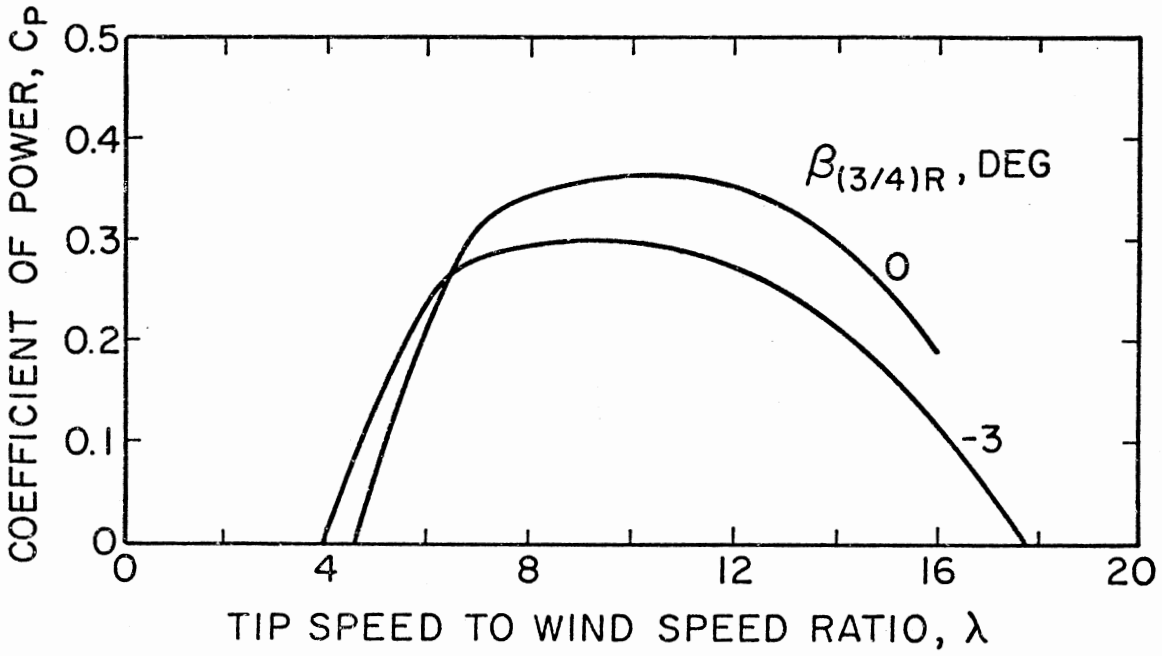

Figure 3. Model Power Coefficient

TABLE I

PARAMETERS OF SYSTEM UNDER STUDY (37)

Wind Rotor	
Blade Power, kW	133.000
Desired Rated Power Coefficient	0.375
Rated Wind Speed, m/s	8.048
Number of Blades	2
Diameter of Wind Rotor, m	37.500
Rotor Revolutions, r/min	40.000
Generator	
Type: Salient Pole Synchronous With Damper Windings	
Rated kVA	125.000
Rated Power Factor	0.800
Frequency, Hz	60
Terminal Voltage, V	480.000
Weight of Machine, kg	646.400
Generator Revolutions, r/min	1800.000
Number of Poles	4
$x_{dg} = 0.6$; $x_{qg} = 0.4$; $x'_{dg} = 0.2$; $x'_{qg} = 0.4$; $x''_{dg} = 0.13$	
$x''_{qg} = 0.23$; $T'_{do} = 1.5$; $T''_{do} = 0.01$; $T''_{qo} = 0.01$	
Coupling	
Type: Stiff Shaft	
Stiffness Constant, N.m/rd	3×10^4

be 12.5 N.m-s^2. This corresponds to an H value of 1.85 at rated speed for the generator. As discussed earlier, a stiff coupling is assumed in this initial study with a view that it would lead to more conservative results as compared to the flexible coupling with damping or eddy-current coupling and that the influence of the system parameters will be pronounced.

Two wind gust models, as suggested in Reference (21), are employed in the study reported in this chapter. They are illustrated in Figure 4. Both the one-second and two-second wind gust models used in full-load simulation have the same peak wind speed. The step size selected in this study is 0.01 second, which is of the order of magnitude of the smallest system time constant (open circuit direct axis subtransient time constant T''_{do}).

2.5 Parametric Variation

The system parameters are changed, one at a time, to study their effect on the overall operation. A single parameter variation is adopted in this initial study to make the chapter systematic and pedagogic and to see if a particular parameter exercised strong influence on the dynamic behavior of the system. The influence of electrical damping, stiffness coefficient of coupling, machine reactance, external reactance, and the voltage behind transient reactance is studied by simulating the generator torque angle as a function of time during and immediately after (for an additional period of two seconds) the occurrence of a wind gust.

In the study of transient behavior of synchronous machines, it is customary to assume the voltage behind transient reactance as constant immediately following a disturbance. However, with smooth wind gust

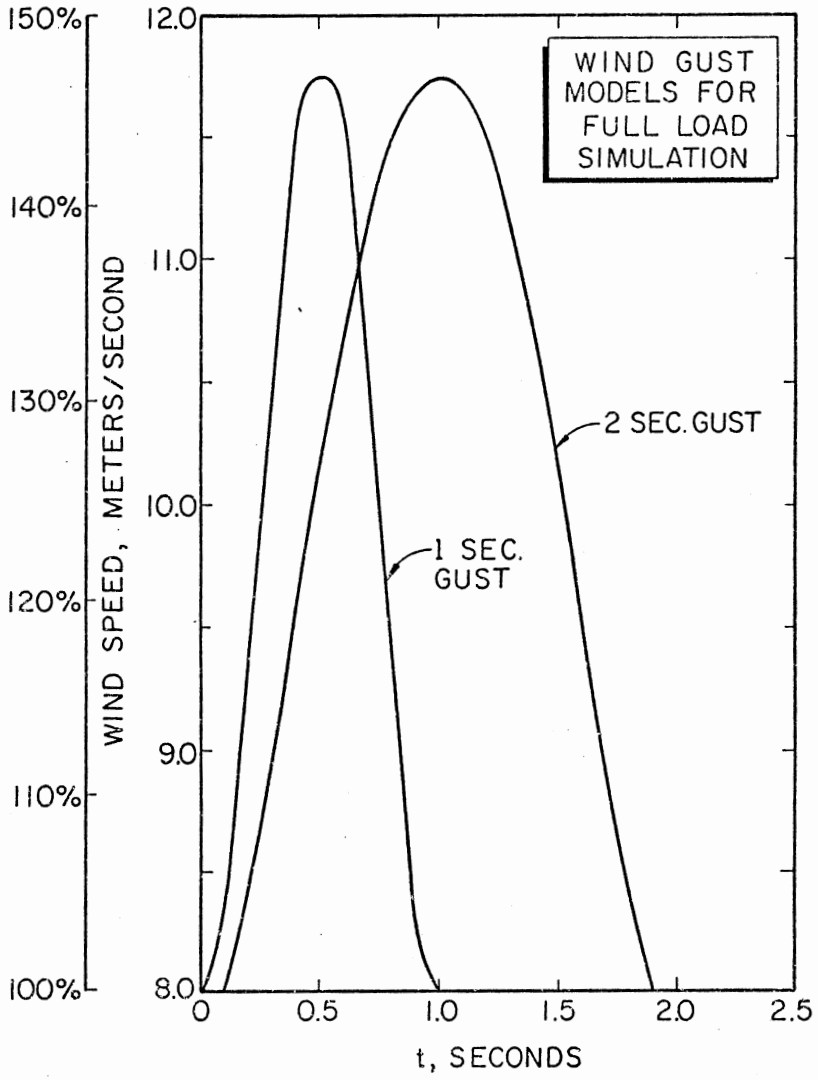

Figure 4. Wind Gust Models for Full Load Simulation

models extending over a period of one to two seconds (which is comparable with the transient open-circuit field time constant of 1.5 seconds), such an assumption may not be strictly valid. Variations in E'_q can be included in the analysis by incorporating the following equations in the mathematical model.

$$E_q = E'_q + (x_d - x'_d)I_d \tag{2.34}$$

$$\dot{E}'_q = (E_{ex} - E_q)/T'_{do} \tag{2.35}$$

E_{ex} itself may be held constant by voltage regulator action or may vary with time in a suitable manner. In this initial study a simple linear variation is considered.

$$E_{ex} = E_{qo}(1 + X_k t_k) \tag{2.36}$$

If X_k is zero, then the voltage regulator is holding E_{ex} constant and equal to E_q computed prior to the disturbance (denoted by E_{qo}), and if X_k is positive, the regulator is forcing a linear build-up of E_q. The solution vector and the function vector defined by Equations (2.32) and (2.33) must now be expanded by adding a fifth element, $Z(5) = E'_q$ and $f_5(\vec{Z},t) = \dot{E}'_q$, given by Equation (2.35). Computer simulation is carried out exactly as before from this point onwards. This assumption of linear build-up will be relaxed in the next chapter to include a transfer function for the generator voltage regulator with a feedback from stabilizer to make the model more realistic and complete. This would lead to further expansion of the state vector $\vec{Z}(t)$, as will be shown later.

2.6 Results and Discussion

An overall examination of the results of computer simulation indicates that the stability problems worsen with sharpness of gust. Any

mild disturbance immediately following a sharp gust has the potential to force the system out of synchronism.

The influence of system inertia on the swing curves is shown in Figures 5 and 6 for one- and two-second gusts. Other conditions remaining the same, the longer gust results in milder swings and smaller subsequent oscillations of the generator torque angle. However, there appears to be an optimum combination of the inertia, damping, stiffness constant of coupling, and the machine and the system parameters that results in minimal oscillations in δ after the initial swing (see Figure 5; J_g = 8.3 N.m-s^2). The dynamic interaction between the electromagnetic torque and the wind rotor torque via the stiff coupling produces "kinks" in the swing curve as illustrated in Figure 6. These are the result of the simultaneous acceleration and deceleration of the generator rotor and the wind rotor, respectively and vice versa. Earlier simulations with the rigid shafts did not exhibit this behavior.

The provision of the electrical damping reduces the amplitude of the torque angle oscillations after the initial swing and increases the rate of decay of oscillations, as shown in Figure 7. The amount of electrical damping is a somewhat easily adjustable parameter in the machine design, and a proper choice will improve the overall performance of the system.

The generator (transient) reactance plays a significant role in the operation of wind-electric systems under gusty conditions. This is illustrated in Figures 8 and 9. The smaller the reactance, the stiffer the system in the electrical sense. Referring to Figure 8, a reactance value of 0.5 pu makes the system unstable with a one-second gust; a value of 0.37 pu results in motoring once during each cycle of torque angle

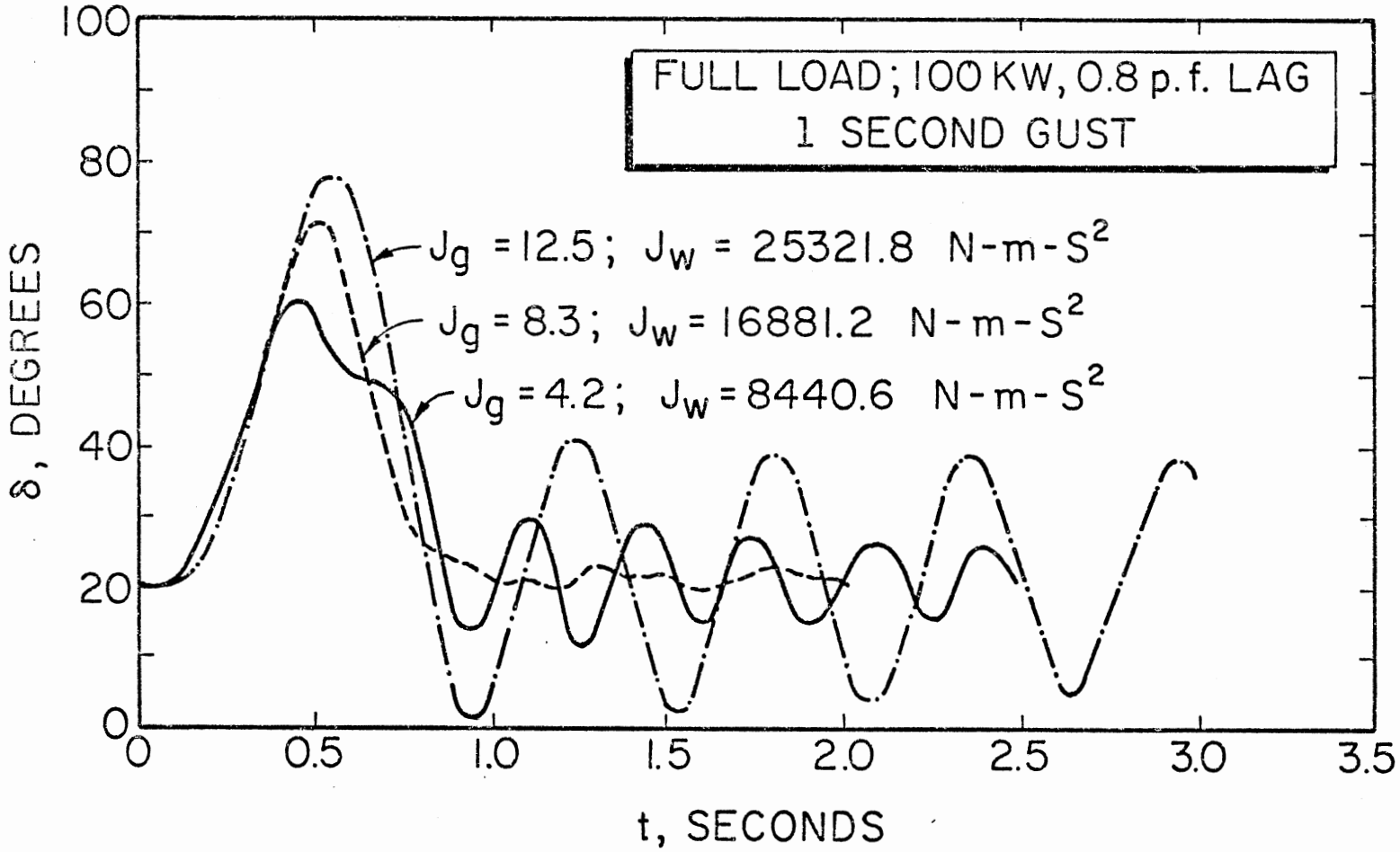

Figure 5. Influence of Inertia; One Second Gust

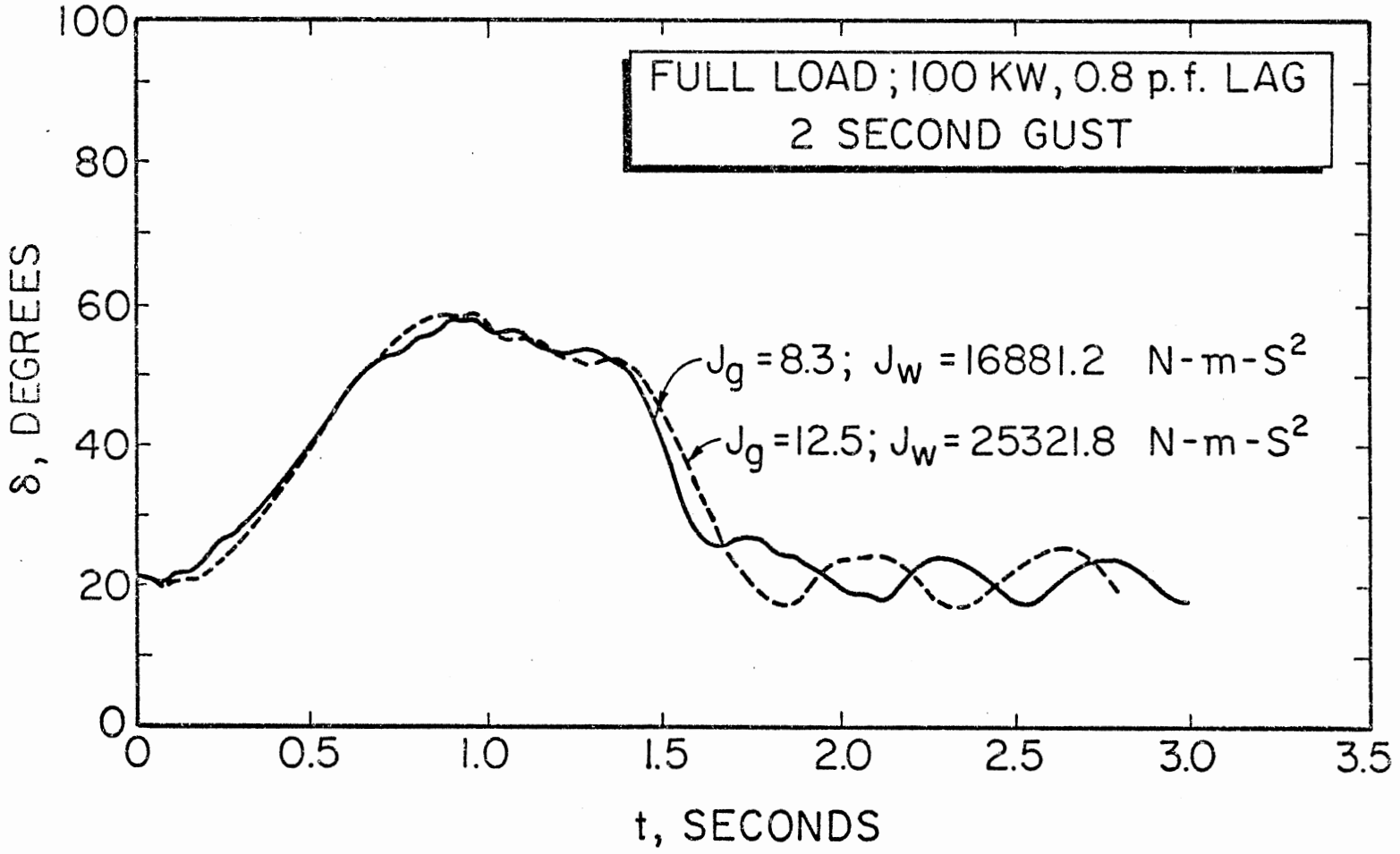

Figure 6. Influence of Inertia; Two Second Gust

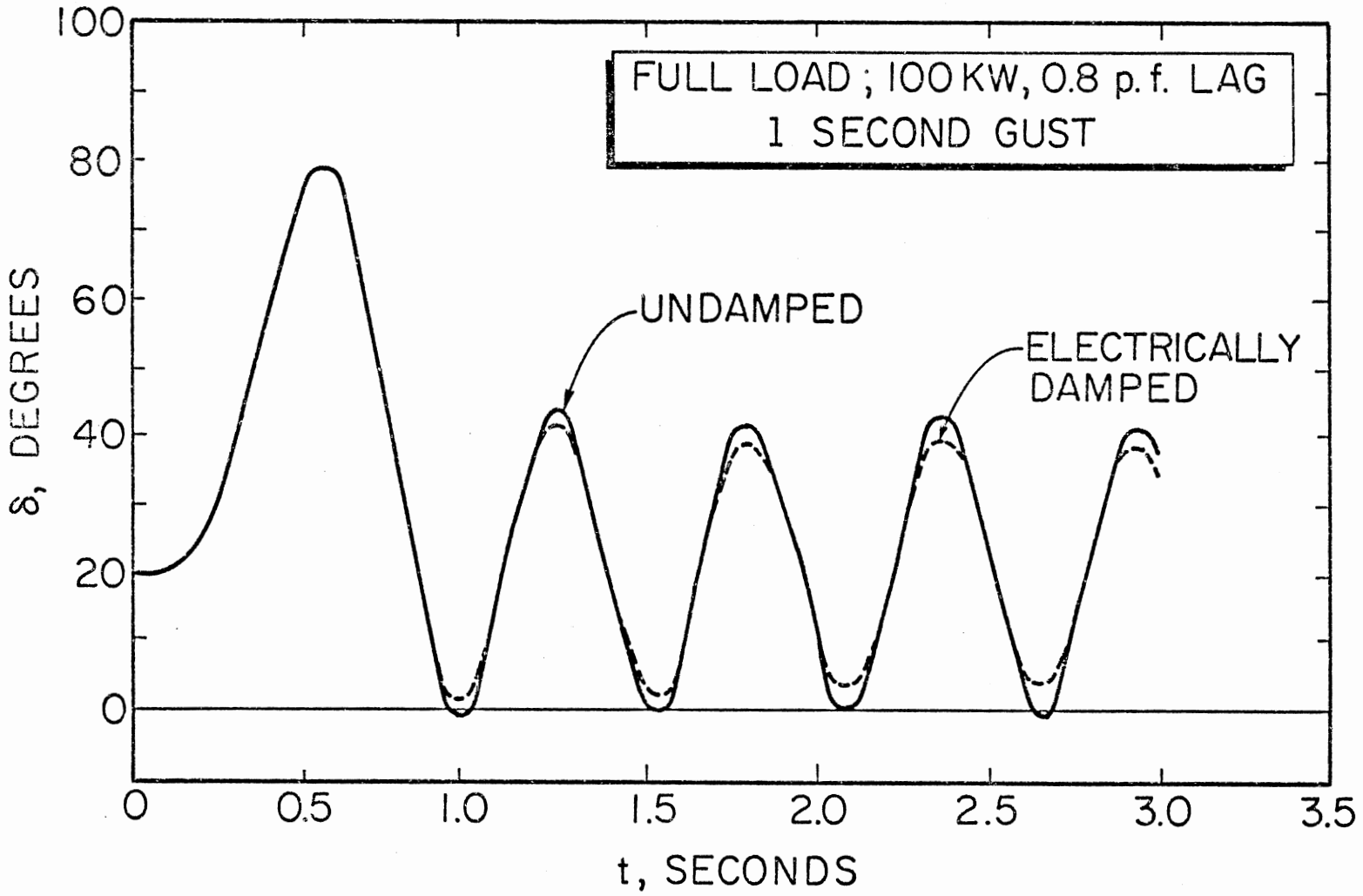

Figure 7. Influence of Electrical Damping

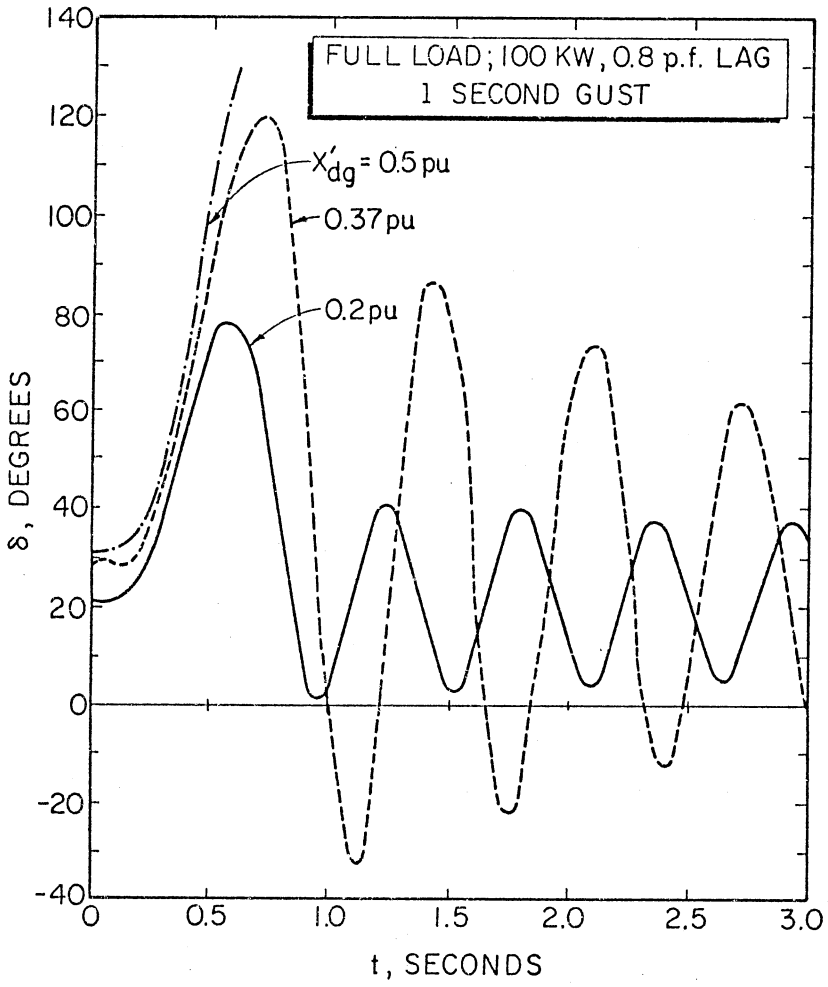

Figure 8. Influence of Generator Transient Reactance; One Second Gust

swing and a value of 0.2 pu leads to stable operation. Behavior with a two-second gust has similar characteristics, though less severe as shown in Figure 9.

Large wind-electric systems are generally expected to be situated in remote locations and therefore the reactance of the line (with or without intermediate transformers) connecting the wind system to a point in the utility grid (where it can be approximated as a infinite bus) becomes an important parameter to be considered. The effect of varying the external reactance is shown in Figures 10 and 11. The influence appears to be greater than the one experienced with changes in machine transient reactance. One explanation of this lies in the fact that an increase in the external reactance not only makes the electrical coupling soft but also decreases the effective electrical damping (see Equations (2.27) and (2.28)). As usual, a one-second gust creates larger swings than a two-second gust.

The effect of three different variations of the voltage behind generator transient reactance is presented in Figure 12. With X_k equal to zero, both E_q and E'_q vary during gusting, but the excitation voltage is held constant. A simple linear excitation voltage variation is considered with $X_k = 0.5$. These two cases are compared with the results obtained for a constant value of E'_q. Obviously, proper excitation voltage control improves the performance by decreasing the amplitudes of torque angle swings which then decay rapidly. This observation is in conformity with the suggestions of Park and Bunkers (39) and the conclusions of Furst (40). Voltage regulator action is much more complex than the simple case considered here and will be investigated further in Chapters III and IV.

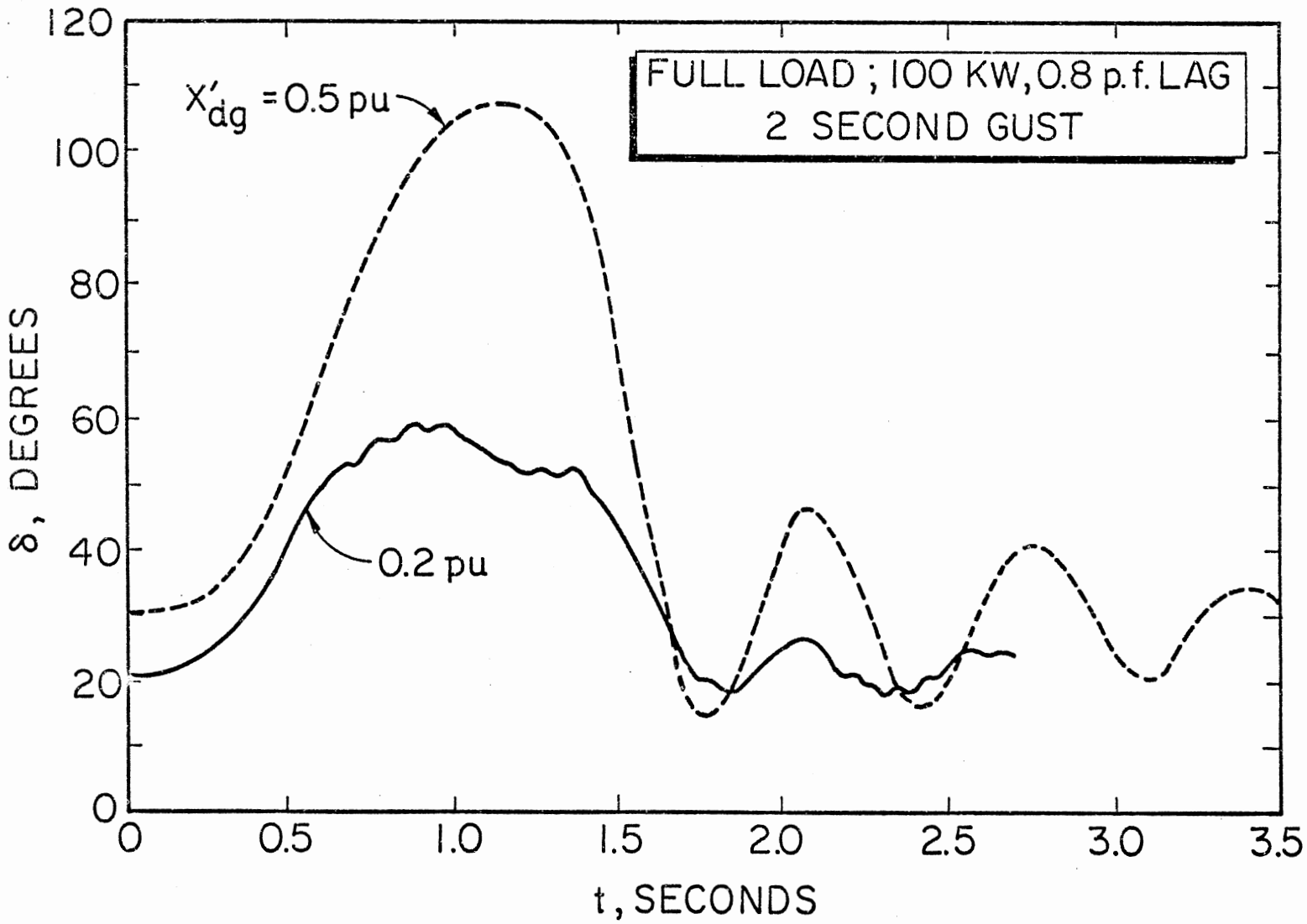

Figure 9. Influence of Generator Transient Reactance; Two Second Gust

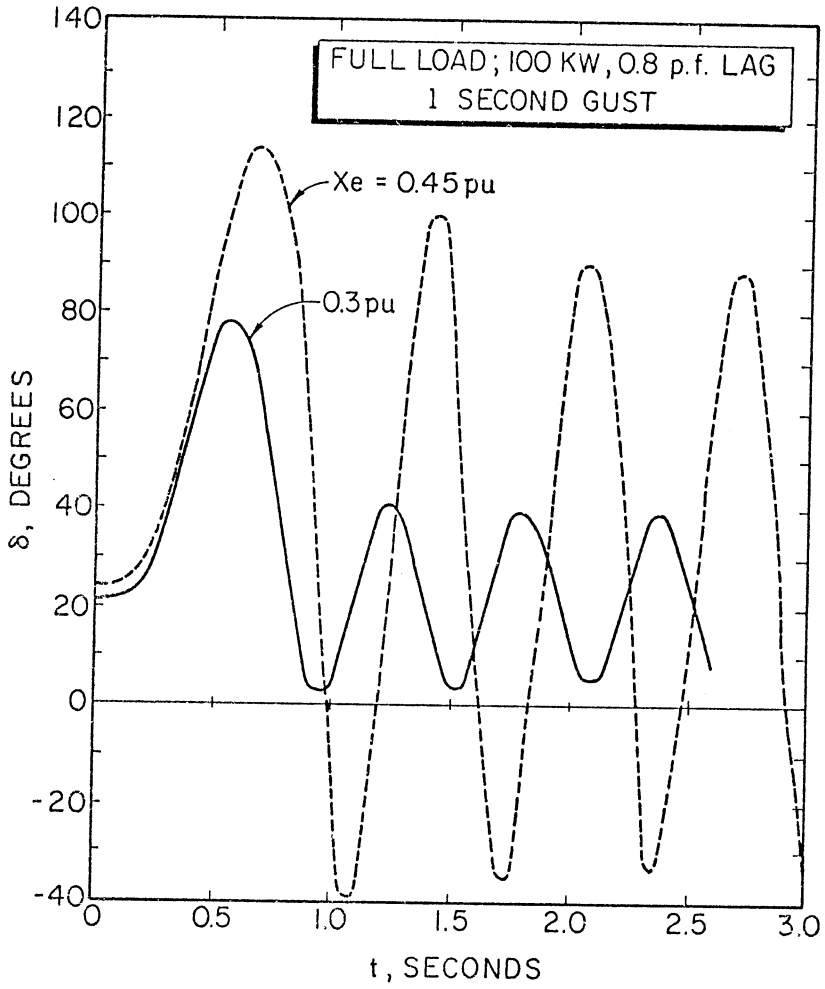

Figure 10. Influence of System External Reactance; One Second Gust

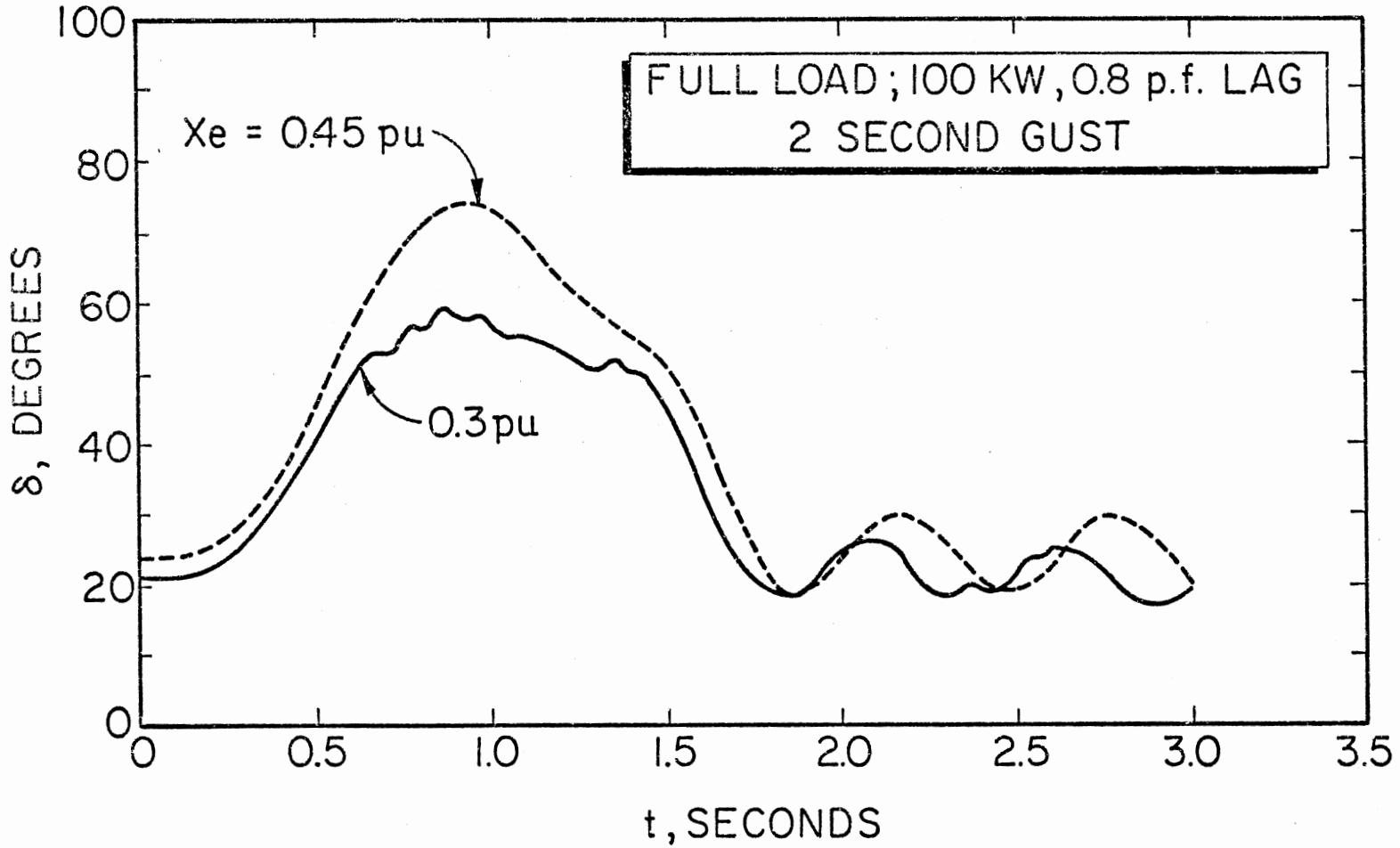

Figure 11. Influence of System External Reactance; Two Second Gust

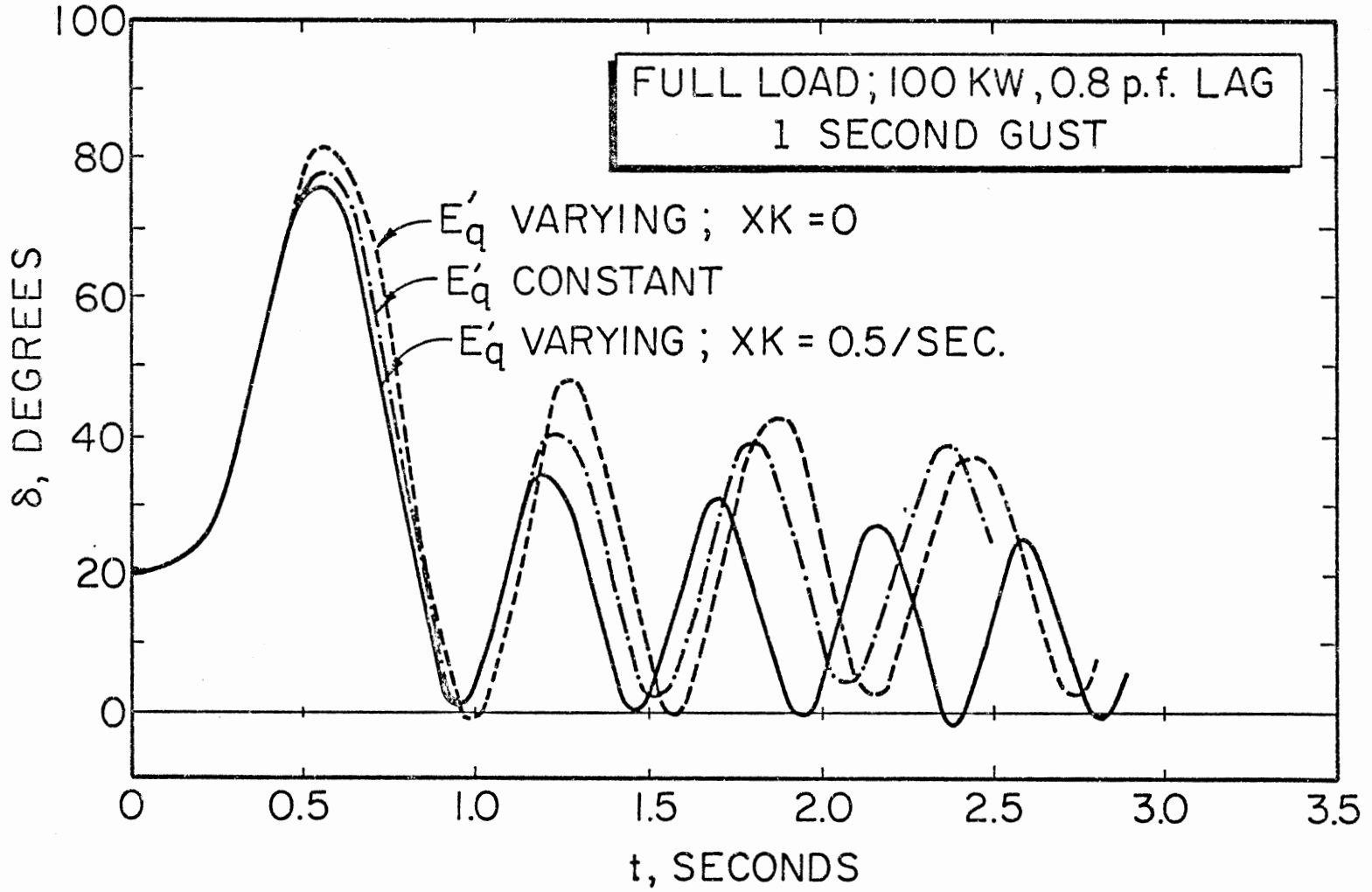

Figure 12. Influence of Different Variations in E'_q

It was found during the several simulation runs that the stiffness-constant of the stiff coupling-shaft did not appreciably alter the behavior of the system, even with an order of magnitude (10 to 1) change in the stiffness constant. The only visible difference was the appearance (or not) and the size of the "kinks" in the swing curve (see Figure 6). Therefore, no results are presented in this connection.

The influence of stiffness-constant and mechanical damping constants would be a subject of considerable detail in Chapter III, whence the flexible shaft with damping would be employed instead of the stiff coupling.

2.7 Concluding Remarks

Dynamic behavior of wind-driven synchronous machines operating in parallel with infinite bus bars is analogous to the behavior of similar conventional prime-mover driven systems, except that the wind gusts occur repeatedly and in varying strengths and durations.

Although the present study has assumed just one gust interposed between periods of steady winds and has made several other idealizing assumptions listed in previous sections, some basic conclusions are evident from an examination of the results. Shorter duration wind gusts are more severe than longer duration gusts. The amplitude, frequency, and the duration of the wind gusts play an important role in determining the behavior and the stability of the wind-electric systems and as such, the wind gust models should be defined clearly and realistically. As expected, strong electrical damping improves the dynamic performance of the system. There appears to be an optimum combination of the inertia, damping, coupling stiffness coefficient, and the system reactances that

results in minimal oscillations in the generator torque angle after the initial swing. Effects of the changes in external reactance (between generator output and infinite bus) on the dynamic behavior are more severe than the effects of the changes in generator reactances. Proper voltage regulator action improves the dynamic performance in terms of stability, and smaller and rapidly decaying oscillations in δ during and immediately after gusting.

CHAPTER III

STUDIES ON WIND-DRIVEN SYNCHRONOUS MACHINES EMPLOYING DAMPED FLEXIBLE COUPLINGS

3.1 Introduction

Studies on wind electric systems employing synchronous machines and stiff couplings have shown that the synchronous generator frequently operates as a motor during and following the wind gusts of high severity. If the gusts are frequent, this could cause serious operational and stability problems, especially with multi-unit systems. In the absence of additional mechanical damping (although the system may have some inherent damping) the oscillations caused by the gust may continue for several seconds. This is undesirable from the viewpoint of electrical stability and the quality of the energy supply. This chapter is therefore devoted to the study of the wind electric systems employing couplings which, in addition to transmitting the torque by virtue of torsional wind up, introduce damping to improve the overall performance of the system.

3.2 System Configuration and Governing Equations

The system under study consists of an aeroturbine, a step-up gearing mechanism, a flexible shaft with damping and a synchronous generator connected to a large utility grid (infinite bus) of fixed voltage and frequency. The schematic of the system is shown in Figure 13.

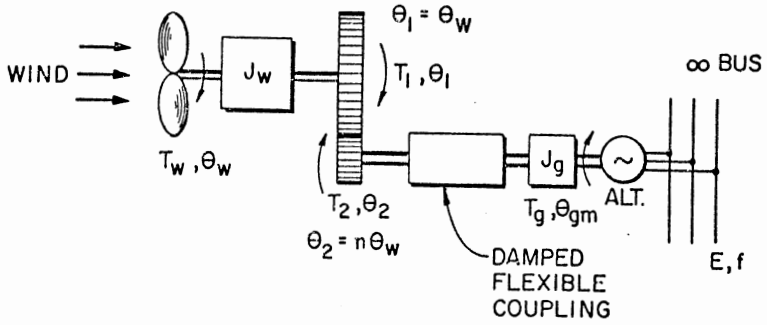

Figure 13. Schematic of the System Employing Damped Flexible Coupling

Performance equations for the model employing damped flexible coupling can be easily obtained from the set of Equations (2.1) through (2.31) with some modifications. Additions of damping term $C_d(\dot{\theta}_2 - \dot{\theta}_{gm})$ in Equations (2.3) and (2.4) yield the following equations:

$$T_2 - J_2\ddot{\theta}_2 = S_c(\theta_2 - \theta_{gm}) + C_d(\dot{\theta}_2 - \dot{\theta}_{gm}) \tag{3.1}$$

$$S_c(\theta_2 - \theta_{gm}) + C_d(\dot{\theta}_2 - \dot{\theta}_{gm}) = J_g\ddot{\theta}_{gm} + T_g \tag{3.2}$$

Following the procedure outlined in section 2.2 and with the above additions, the following performance equations are obtained:

$$\ddot{\theta}_w = \frac{1}{\omega_w J_w}\left[P_w - \frac{n\omega_w}{\eta_g}\{S_c(n\theta_w - \theta_{gm}) + C_d(n\dot{\theta}_w - \dot{\theta}_{gm})\}\right] \tag{3.3}$$

$$\ddot{\theta}_{gm} = \frac{1}{\omega_{gm} J_g}\left[\omega_{gm}\{S_c(n\theta_w - \theta_{gm}) + C_d(n\dot{\theta}_w - \dot{\theta}_{gm})\} - 1000\, G(P_s + P_d)\right] \tag{3.4}$$

3.3 Introduction of Nondimensional Parameters

In stability studies it is customary to use per-unit quantities whenever possible. These quantities have the advantage that they do not vary largely from one system to the other and are almost the same for most of the electrical machinery of a particular type, irrespective of the machine ratings.

Also, per-unit quantities are easy to handle and compare in any study. In order to make the study in this work more general and widely applicable, the concept of nondimensional parameters is introduced and used in further discussions.

Let the wind rotor inertia constant H_w be defined as the ratio of the wind rotor energy stored in kJ at the rated speed to the rated wind

rotor power output in kW. Let S_{cdl} be the normalized stiffness constant, defined as the ratio of the actual shaft stiffness constant S_c to the rated torque T_r. Let the normalized damping constant C_{ddl} be defined as the ratio of the product of actual damping constant C_d and the synchronous angular speed ω_{syn} to the rated torque T_r. Finally, the reactance ratio k is defined as the ratio of the per-unit external reactance x_e to the per-unit generator transient reactance x'_{dg}.

Consider a wind-driven synchronous machine which has a rated power output of 1500 kW at a synchronous speed of 1800 r/min. The rated torque of this machine is 7957.75 N.m and its rated angular speed is 188.5 rd/s. Let it be driven by a wind rotor of inertia J_w. Let the value of the newly-defined quantity H_w be equal to 5. Then the actual inertia of the wind rotor, which is running at a rated speed (N_w) of 30 r/min, is obtained from the formula:

$$H_w = \frac{5.48 \cdot 10^{-6} \cdot (N_w)^2 \, J_w}{\text{Rating in kW}}$$

From this, the value of the wind rotor inertia J_w is found to be 1.52 x 10^6 N.m.s^2.

It may be noted here that, although J_w (depending on the rotor mass, blade diameter, etc.) and the rated power can vary over a wide range, the value of H_w will lie between 2.0 and 6.0. The parameter H_w is analogous to the well-known inertia constant H_g of the synchronous machine. For synchronous machines, this quantity lies between 2.0 and 8.0 (41).

To illustrate this concept further, let a flexible coupling of stiffness constant 6.5 x 10^5 N.m/rd and damping constant of 1000

N.m.s/rd be interposed between the synchronous machine and the low torque gear. The normalized stiffness constant S_{cdl} and the normalized damping constant C_{ddl} can be computed as shown below.

$$S_{cdl} = \frac{S_c}{T_r} = \frac{6.5 \times 10^5}{7957.75} = 81.68$$

$$C_{ddl} = \frac{C_d \cdot \omega_{syn}}{T_r} = \frac{1000 \times 188.5}{7957.50} = 23.69$$

Given any set of normalized parameters S_{cdl} and C_{ddl}, the actual values of S_c and C_d can be easily determined by reversing the procedure outlined above.

3.4 Selection of Torsional Couplings With Damping

While selecting the torsional couplings with damping for application in wind-driven electrical systems, it is important to know the upper limit of torque reached when the system is subjected to wind gusts. This consideration assumes special importance for the cases when the wind gust has a sharp peak and is of short duration. Maximum torques may reach four to five times the rated torque. These high torques must be withstood by the coupling, although a good part (up to 50%) of the same may be taken up by damping.

It is useful to know the torque-wind speed curve for the given wind turbine. This curve can be easily estimated in the following way: assuming that ω_w is constant (in fact, ω_w does not vary much before synchronism is lost) tip speed to wind speed ratio (λ) can be easily estimated from Equation (2.30) for a given value of wind speed. The coefficient of performance (C_p) corresponding to this value of λ can be found from C_p vs λ characteristic of the wind rotor. Knowing C_p, instantaneous power

can be obtained from Equation (2.17). Knowing the wind power (P_w), torque of wind (T_w) can easily be estimated for each value of the wind speed. A number of torque values can be thus obtained, each value corresponding to one given value of the wind speed. From this set of points obtained, a curve can be plotted. From this curve, maximum torque can be estimated after allowing for a reasonable safety factor (1.2 or more of estimated torque). Figure 14 shows a typical torque-wind speed curve. It is clear that the maximum torque reached is more than three times the rated torque. It is on the basis of this maximum torque that the coupling with suitable torsional and damping characteristics must be selected for a specific application. Procedures for selecting a flexible, damped coupling along with the relevant data can be found in the literature (42) (44).

3.5 Excitation Voltage Control

In the solution technique described in Chapter II, it was tacitly assumed that E'_q was constant and the effects of exciter voltage control on the system response were neglected when dealing with a one-second gust. For a two-second gust, variations in E'_q were accounted for by considering E_{ex} to be a linear function of time as given by Equation (2.36). Such a linear variation was assumed to develop a feeling for the effect of the excitation control on the system behavior. These assumptions (constant E'_q and simple linear increment in E_{ex}) will be replaced (in the case of studies with two-second gusts) by an excitation control scheme of the type encountered in practice. Modern excitation systems are quite complicated and can be represented in many ways. Such representations and the computer simulation are well documented in the

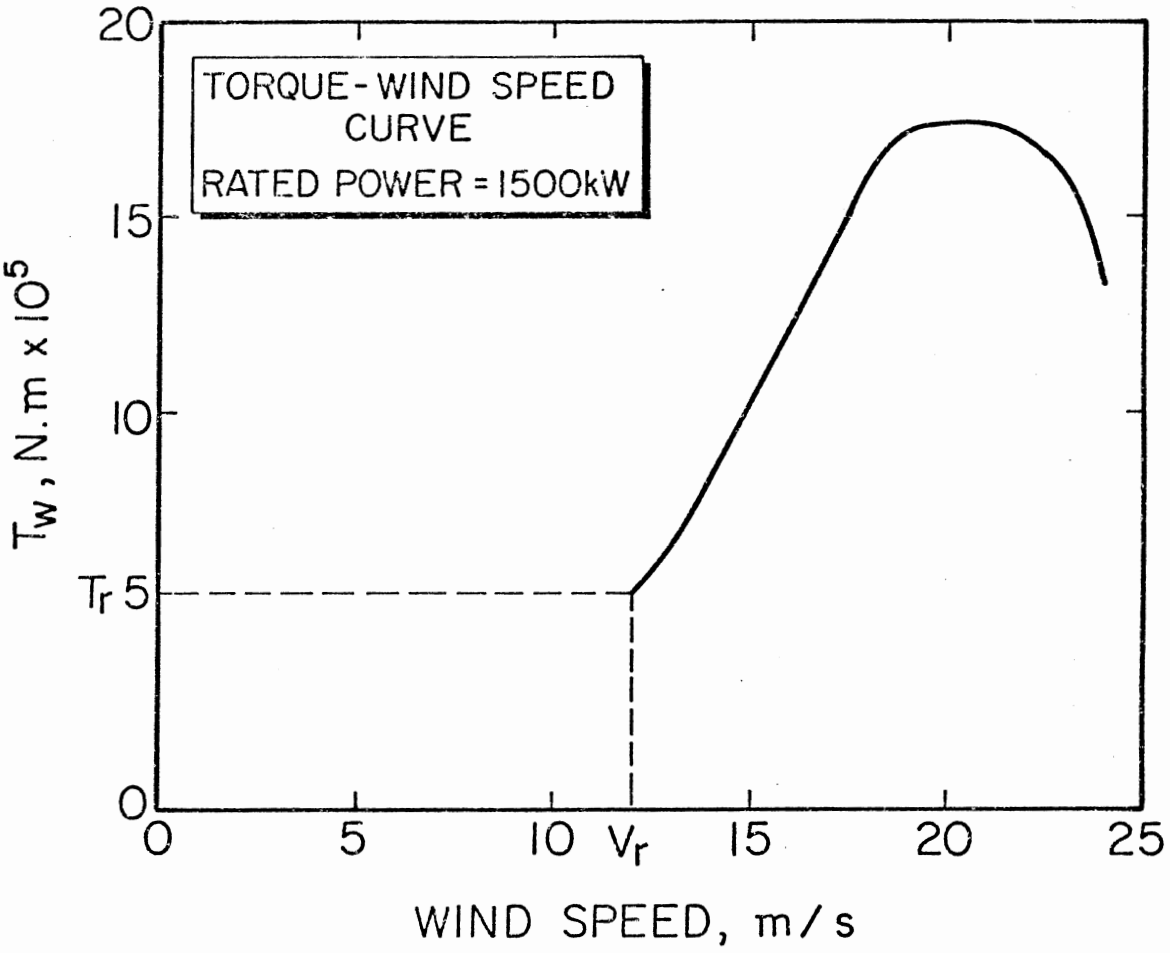

Figure 14. Torque-Wind Speed Curve of Damped Flexible Coupling

literature (45). One such scheme, which adequately represents a modern excitation control will now be described and its performance equations developed. Figure 15 shows a block diagram of the excitation control system used.

The performance equations for the scheme can be set up by simple inspection:

$$\frac{E_{ex}(s)}{\varepsilon(s)} = \frac{K_{ex}}{1 + sT_{ex}} \tag{3.5}$$

$$\frac{V_{st}(s)}{E_{ex}(s)} = \frac{sK_{st}}{1 + T_{st}} \tag{3.6}$$

$$\varepsilon(s) = V_{ref}(s) - V_t(s) - V_{st}(s) \tag{3.7}$$

From Equations (3.5) and (3.6):

$$E_{ex}(s) + sE_{ex}(s)T_{ex} = \varepsilon(s)K_{ex} \tag{3.8}$$

$$V_{st}(s) + sV_{st}(s)T_{st} = sE_{ex}(s)K_{st} \tag{3.9}$$

Simplifying Equations (3.8) and (3.9):

$$sE_{ex}(s) = (K_{ex}\varepsilon(s) - E_{ex}(s))/T_{ex} \tag{3.10}$$

$$sV_{st}(s) = (sK_{st}E_{ex}(s) - V_{st}(s))/T_{st} \tag{3.11}$$

By inverse transformation, the following two differential equations are obtained:

$$\dot{E}_{ex} = (K_{ex}\varepsilon - E_{ex})/T_{ex} \tag{3.12}$$

$$\dot{V}_{st} = (K_{st}\dot{E}_{ex} - V_{st})/T_{st} \tag{3.13}$$

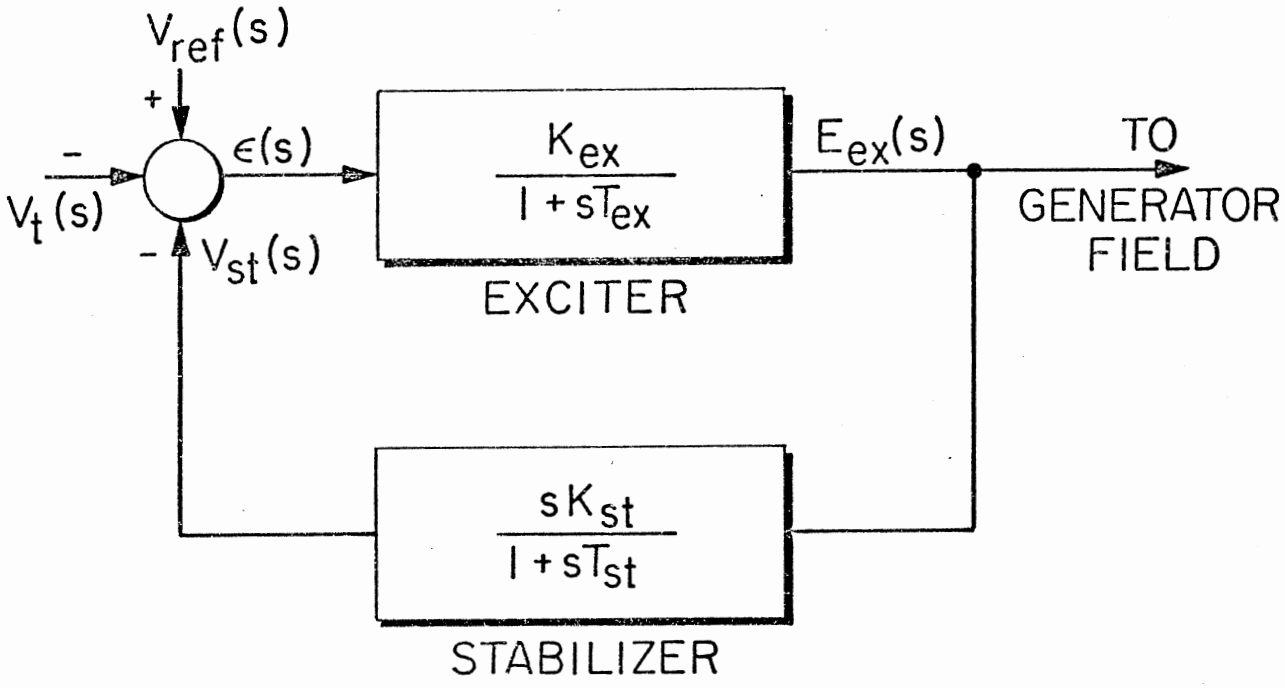

Figure 15. Block Diagram of the Excitation Control System

From Equations (3.12), (3.13), and (2.35), which is the connecting link, the following final form of the excitation control model is obtained:

$$\dot{E}_{ex} = (K_{ex}\varepsilon - E_{ex})/T_{ex} \tag{3.14}$$

$$\dot{V}_{st} = \frac{K_{st}}{T_{st}T_{ex}}(K_{ex}\varepsilon - E_{ex}) - \frac{V_{st}}{T_{st}} \tag{3.15}$$

$$\dot{E}'_q = (E_{ex} - E_q)/T'_{do} \tag{3.16}$$

The initial conditions are given by:

$$E_{ex(i)} = E_{q(i)} = E_{qo} \qquad \text{(value of } E_q \text{ before gust)}$$

$$V_{st(i)} = 0.0$$

$$E'_q = E'_{q(i)} = E'_{qo} \qquad \text{(value of } E'_q \text{ before gust)}$$

Equations (3.14) through (3.16) along with the given initial conditions are sufficient to describe the performance of the control loop.

Satisfactory performance will depend, however, on the proper selection of the constants K_{ex}, T_{ex}, K_{st}, T_{st} and the constants of the system being controlled. Selected values of these constants are given in Table II of section 3.7. These values are typical for a rotating exciter with a stabilizer and are taken from the work of Furst previously quoted (Reference (40)).

3.6 Computer Simulation

The program constructed is modified to conform with the Equations (3.3) and (3.4). The program is further modified to include the automatic voltage regulator action as described by Equations (3.14) through

(3.16). The exciter ceiling voltage has been kept floating with a view to estimate the favorable values of ceiling voltage ratio (CVR) when the system is subjected to severe wind gusts. The state vector $\vec{Z}(t)$ is now extended to have seven elements and is initialized using the values of $E_{ex(i)}$, $V_{st(i)}$, and $E'_{q(i)}$ before the occurrence of the wind gust. The function vector $\vec{F}(\vec{Z},t)$ is similarly extended by the same number of elements by incorporating Equations (3.14) through (3.16) in $\vec{F}(\vec{Z},t)$ as described in section 2.3. The digital simulation is carried out in exactly the same manner as described in section 2.4.

3.7 Test Data and Gust Models

The test data given in Table II is used for the simulation. Air density is taken as 1.1 kg/m^3. The generator rotor inertia is selected as 211.08 $N.m\text{-}s^2$. This corresponds to a H_g value of 2.0, which is typical for a salient pole synchronous generator. A value of 5.0 is selected for H_w. This corresponds to an actual wind rotor inertia of 1520681.27 $N.m\text{-}s^2$ as proposed by Johnson and Smith (23). Two types of couplings are selected for the case studies in this chapter. One of them is an off-the-shelf coupling with a high normalized stiffness constant and a low normalized damping constant and the other is a very flexible coupling with damping (compliant shaft with damping) as suggested by Johnson and Smith. These two couplings are selected with the idea of examining their suitability for application in wind energy conversion systems and to make recommendations in that regard.

Three wind gust models are employed in the case studies presented in this chapter. They are illustrated in Figures 16, 17, and 18. The actual wind gust model (Figure 18) is included to see if such an input drastically changed the system behavior.

TABLE II

PARAMETERS OF SYSTEM UNDER STUDY

Wind Rotor	
Blade Power, kW	1715.000
Desired Rated Power Coefficient	0.359
Rated Wind Speed, m/s	12.000
Number of Blades	2
Diameter of Wind Rotor, m	40.000
Rotor Revolutions, r/min	30.000
Gearing Efficiency	0.870
Generator	
Type: Salient Pole Synchronous With Damper Windings	
Rated kVA	1875.000
Rated Power Factor	0.800
Frequency, Hz	60
Terminal Voltage, V	2400.000
Weight of Machine, kg	114850.000
Generator Revolutions, r/min	1800.000
Number of Poles	4
$x_{dg} = 0.6$; $x_{qg} = 0.4$; $x'_{dg} = 0.2$; $x'_{qg} = 0.4$;	
$x''_{dg} = 0.13$; $x''_{qg} = 0.23$; $T'_{do} = 1.5$; $T''_{do} = 0.01$;	
$T''_{qo} = 0.01$	
Coupling Type 1	
Damped Flexible Coupling	
Normalized Stiffness Constant	80.000
Normalized Damping Constant	25.000
Coupling Type 2	
Very Soft Coupling With Damping	
Normalized Stiffness Constant	1.250
Normalized Damping Constant	100.000

TABLE II (Continued)

Excitation Voltage Control	
Type: Rotating Exciter	
Exciter Gain Constant	900.000
Stabilizer Gain Constant	0.075
Exciter Time Constant, s	0.300
Stabilizer Time Constant, s	2.000
Exciter Ceiling Voltage Ratio (CVR)	Floating
Maximum Voltage Regulator Error Signal, p.u	0.020

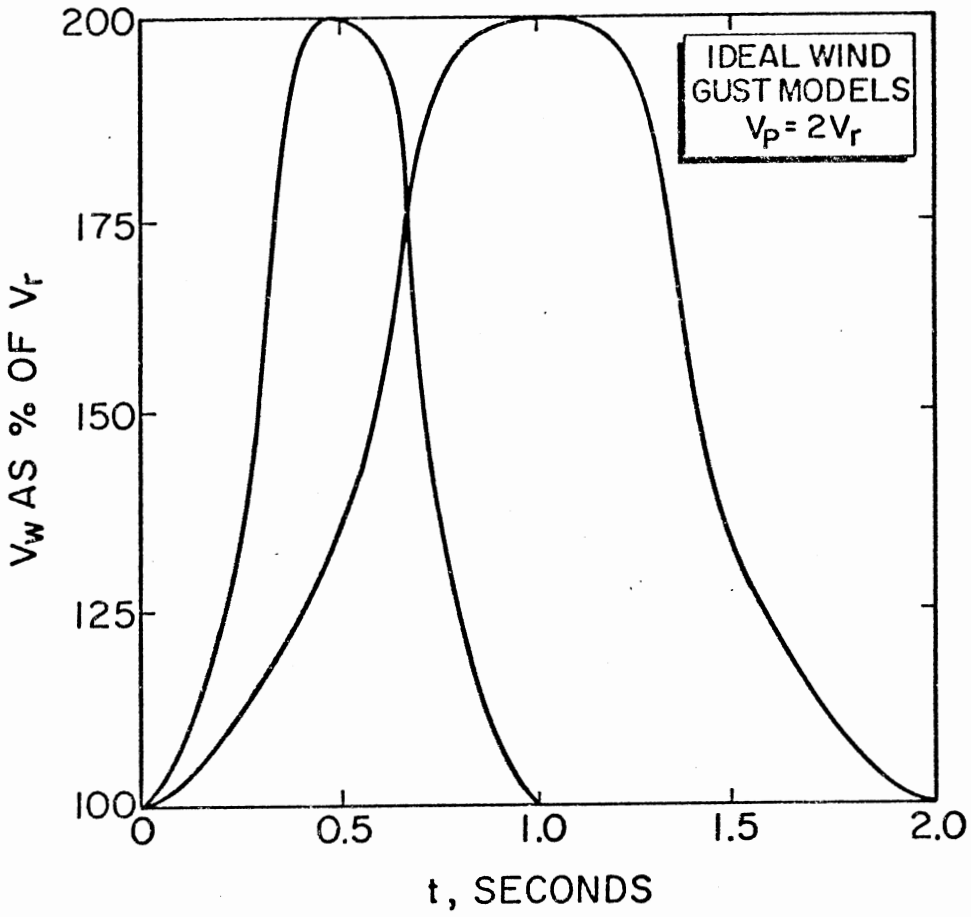

Figure 16. Idealized Wind Gust Models ($V_p = 2V_r$)

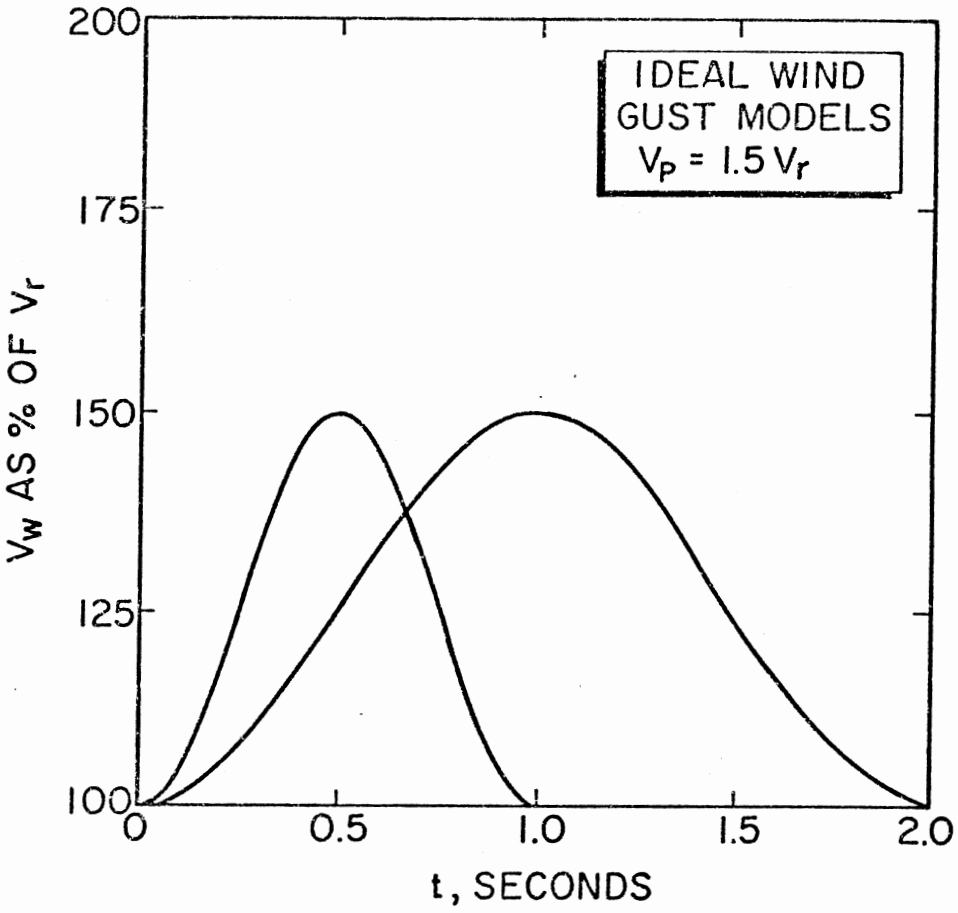

Figure 17. Idealized Wind Gust Models ($V_p = 1.5V_r$)

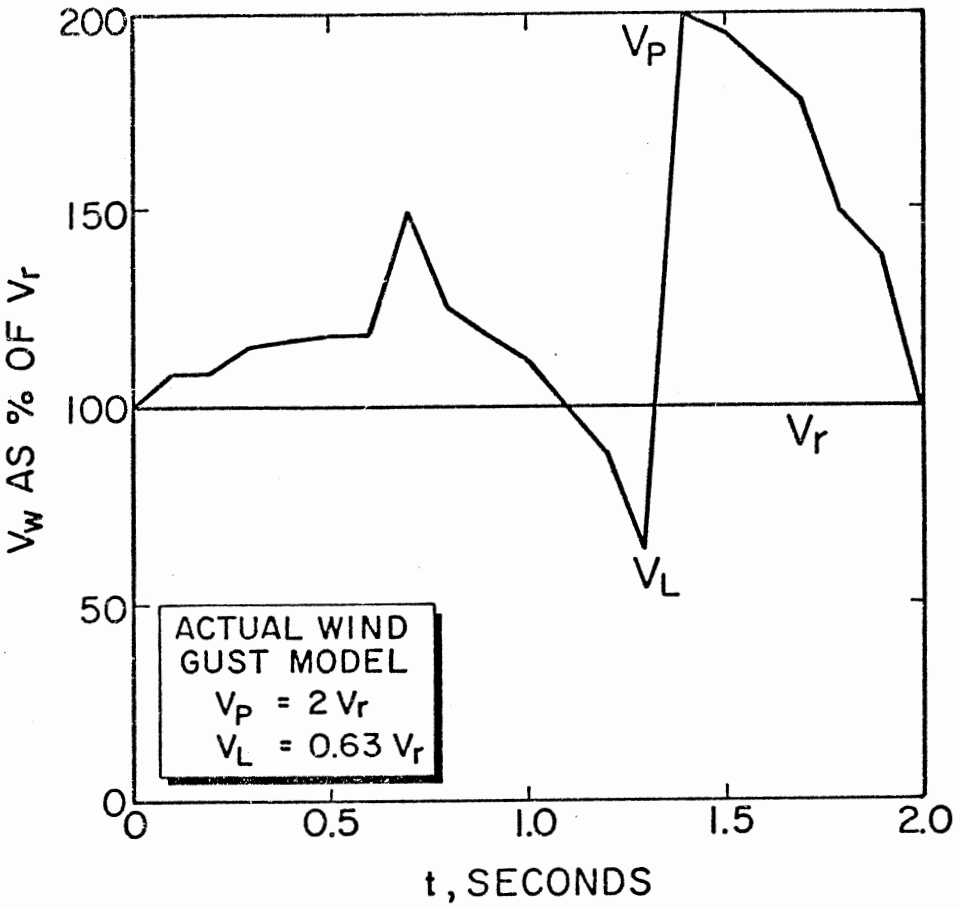

Figure 18. Actual Wind Gust Model ($V_p = 2V_r$ $V_L = 0.63V_r$)

3.8 Results and Discussion

Results and discussion will be subdivided into five parts as follows:

1. General.
2. One-second gust.
3. Two-second gust.
4. Nondimensional curves.
5. Exciter ceiling voltage.

3.8.1 General

Computer simulation results are presented in the form of the following curves.

1. Swing (δ versus t) curves.
2. Dimensionless curves -$\hat{\delta}$ (the maximum angular displacement, given by $\hat{\delta} = \delta_m - \delta_o$) versus the reactance ratio k.

Swing curves are plotted with an objective to see if the system is stable or unstable. These curves will provide information regarding the comparative level of stability and regarding the influence of the important mechanical, electrical and control parameters on the system behavior.

Dimensionless curves ($\hat{\delta}$ versus k) are plotted in the form of families of curves. These provide information regarding the selection of synchronous machine parameters and the system external reactance for a coupling with selected values of parameters. "Critical Line" shows the limit where the system can lose synchronism. The approach used to obtain this line is discussed later in this chapter.

An overall examination of the swing curves reveals that the chances of maintaining system stability worsen with increasing peak of the gust.

Behavior of the system employing a very soft coupling with damping is mild and favorable as compared to the one employing an off-the-shelf (damped flexible) coupling. Generator excitation control remarkably improves the system behavior under gusts of short and long duration, when the parameters of the feedback loop are properly selected. System reactance appears to be the most influential electrical parameter and the peak and the duration of the wind gust are the most important external (input) variables.

3.8.2 One-Second Ideal Gust ($V_p = 1.5V_r$ and $V_p = 2V_r$)

Swing curves comparing the performance of the system with two gusts are shown in Figures 19 and 20. As seen from these plots, the gust with the higher peak ($V_p = 2V_r$) is very severe and throws the system out of synchronism with both the couplings studied.

The gust with a lower peak ($V_p = 1.5V_r$) allows the system to maintain synchronism. Subsequent osciallations die down quickly with a soft coupling (Figure 20) and the system response is very satisfactory. Damped flexible (off-the-shelf) coupling causes undesirable motoring and the generator rotor continues to oscillate for a long time about its equilibrium position. It was found that a 100 percent increase in C_{dd1}, from 25 to 50 (while maintaining S_{cd1} constant at 80) did not change the system behavior significantly and hence no curves are included in this work. It appears that the system would be firm and maintain synchronism if the external reactance is reduced from 0.3 to 0.2 (from k = 1.5 to k = 1.0). It is therefore inferred that if it is necessary to employ off-the-shelf couplings in wind energy system applications, it would be advisable to reduce the system reactance. This can be achieved by

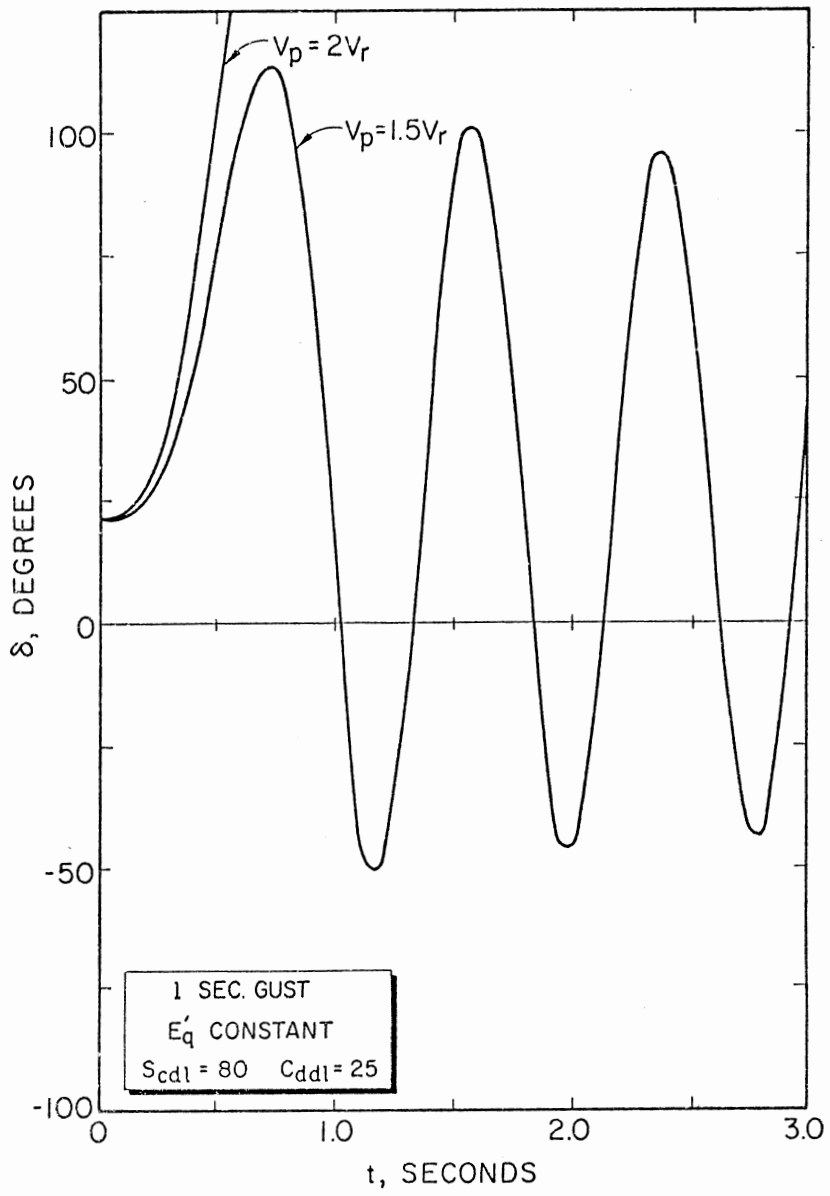

Figure 19. Influence of Peak of Gust; Damped Flexible Coupling

properly selecting the machine parameters or by employing such couplings only in cases in which the distance between the generating system and the main utility grid is very small.

Generator and wind rotor inertias (H_g and H_w) were varied to see if they exercised any significant influence on the system behavior. Changes in H_g from 2 to 4 caused the upper and the lower angles during the swing to increase by about 5° and no other undue changes were noted. Therefore, no curves are reported in this regard. Changes in H_w within reasonable limits (variations from 3 through 5) also did not cause any dramatic differences in the behavior. Higher system inertias cause the system to osciallate for longer durations.

The results of simulation with voltage control are depicted in Figures 21 and 22. Not only is the value of δ_m reduced by 14°, as compared to the case study with constant E'_q (Figure 22), but also motoring is almost eliminated, which is highly desirable from the operation point of view. For the case with a higher peak ($V_p = 2V_r$) there is a considerable difference of stable operation with control and unstable with constant E'_q (Figure 21). It is observed that the voltage control (as compared to assuming a constant E'_q) reduces the rotor angular displacement by approximately 14° (compare curves in Figure 22) when a soft coupling is employed. Summing up, proper voltage control appears to have a very favorable influence on the system performance, especially when soft couplings with damping ($S_{cdl} = 1.25$; $C_{ddl} = 100$) are employed (in the mechanical interface).

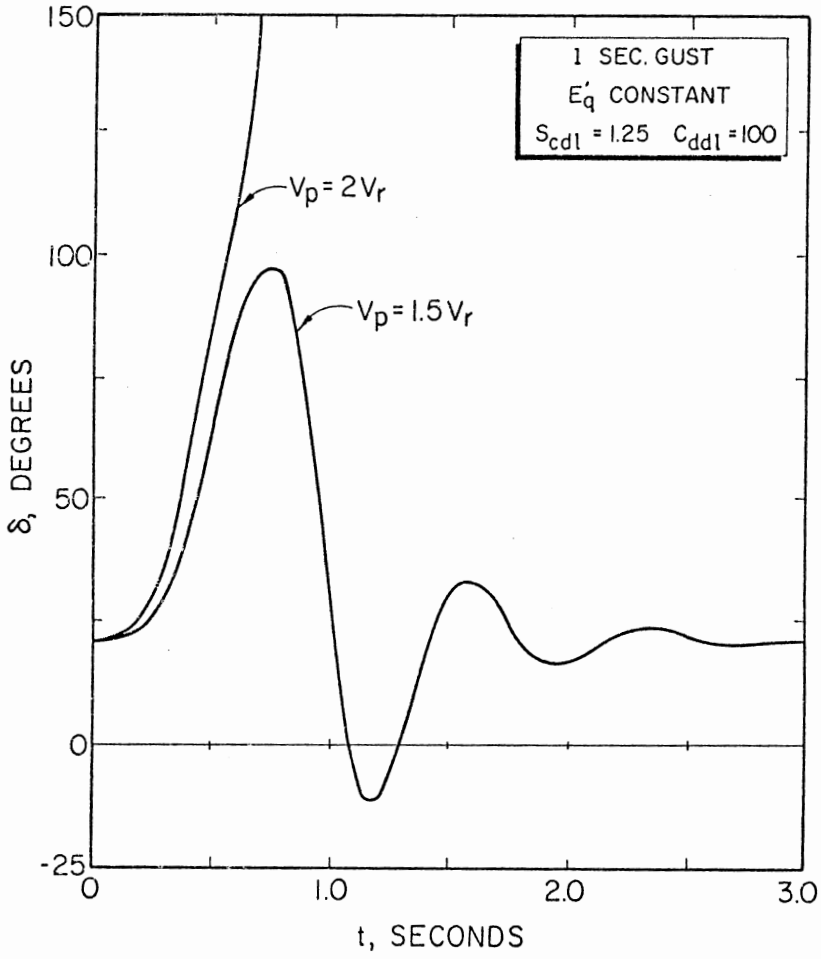

Figure 20. Influence of Peak of Gust; Very Soft Coupling with Damping

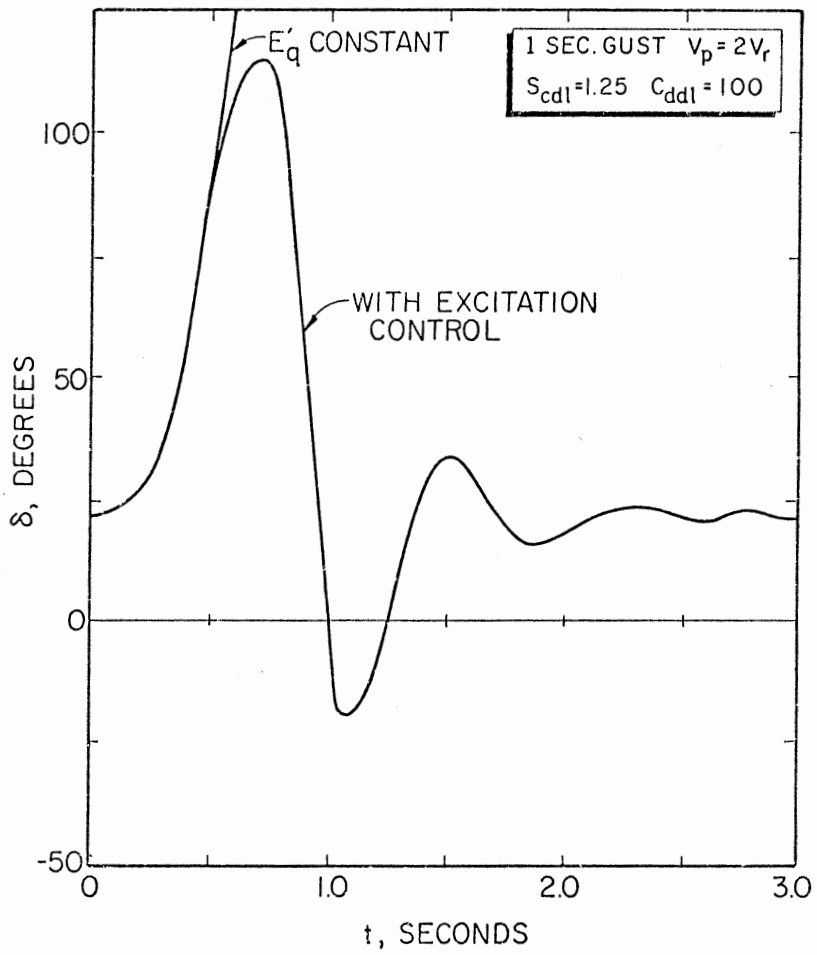

Figure 21. Influence of Excitation Voltage Control; Very Soft Coupling with Damping ($V_p = 2V_r$)

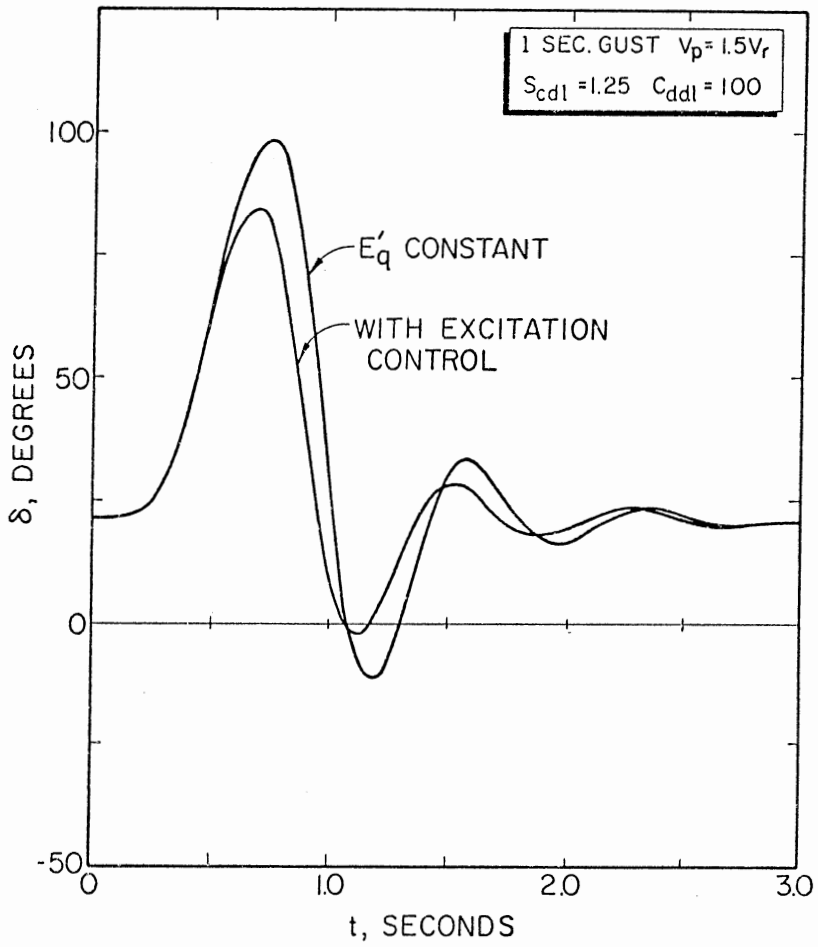

Figure 22. Influence of Excitation Voltage Control; Very Soft Coupling with Damping ($V_p = 1.5V_r$)

3.8.3 Two-Second Ideal and Actual Gusts ($V_p = 2V_r$)

The results of studies on systems employing the two couplings are shown in the form of the swing (δ versus t) curves (Figures 23 to 25). In these simulations, excitation control is included to make the system as close to actual as possible. The control parameters have been selected with a view to get a good response. As discussed in section 2.7, assuming the peaks are the same, a short duration gust is more severe than a long duration gust with all other parameters remaining unchanged (compare Figures 21 and 23), except that the voltage regulator action is included for the two-second gust studies. It is observed that the response of the system with damped flexible coupling ($S_{cdl} = 80$; $C_{ddl} = 25$) is highly unsatisfactory for the case study with x_e equal to 0.3. The oscillations grow in time and synchronism is lost in 2.4 seconds. The damped flexible coupling can be effectively employed if the total reactance of the system is low; this is shown by the simulation results illustrated in Figure 24, wherein the system response is compared for the two types of couplings. Obviously, very soft coupling with damping is a superior choice.

The response of the system, when subjected to a two-second actual wind gust model, is depicted in Figure 25. The behavior of the system is similar to the cases discussed earlier, though the upper rotor angle δ_m is much higher even for a lower value of external reactance ($x_e = 0.0$ per unit). Stability in this case is lower as compared to that in the case of ideal gust of the same duration (compare Figures 24 and 25). System oscillations appear to die down quickly. It is obvious from this plot (Figure 25) that a reduction in the system reactance would assure satisfactory operation of the system under actual wind-gusting conditions.

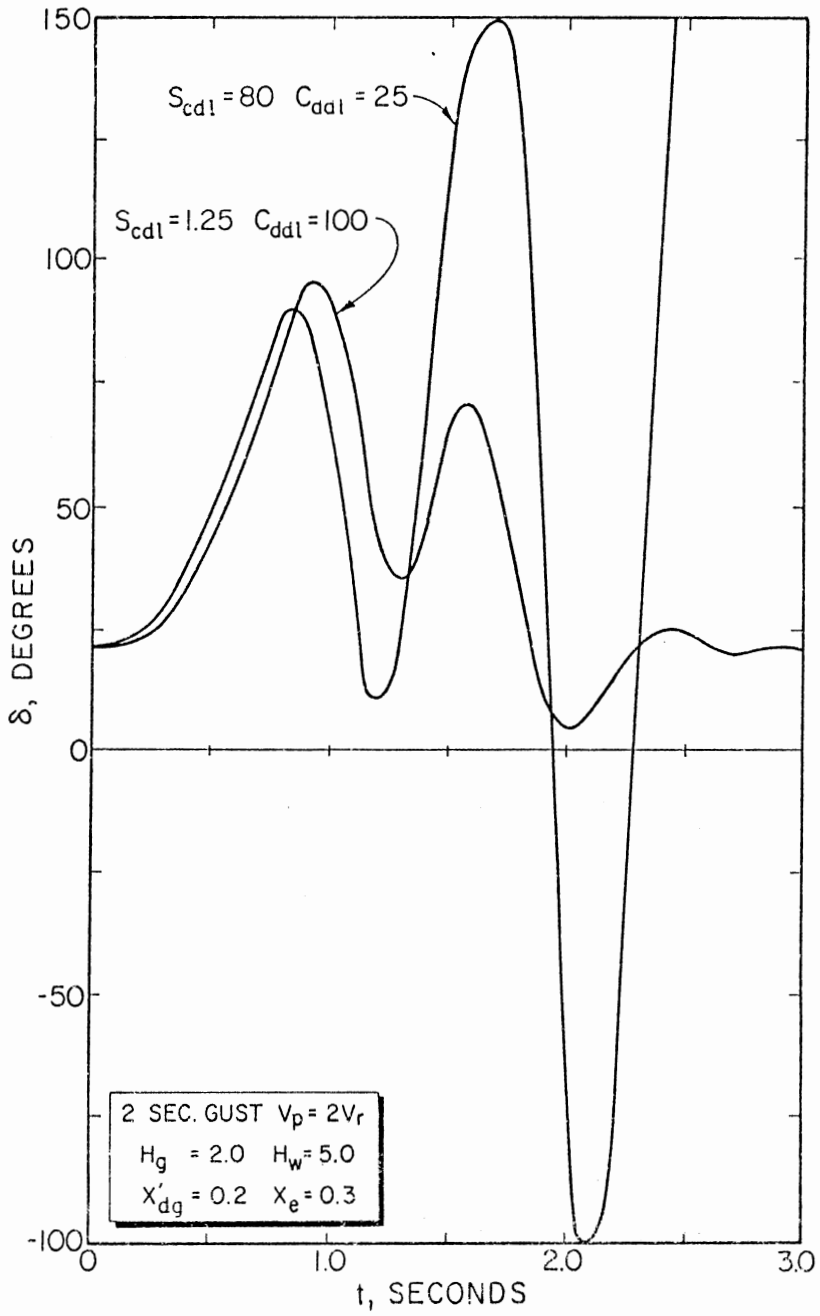

Figure 23. Influence of Normalized Stiffness and Damping Constants; Two Second Gust ($V_p = 2V_r$)

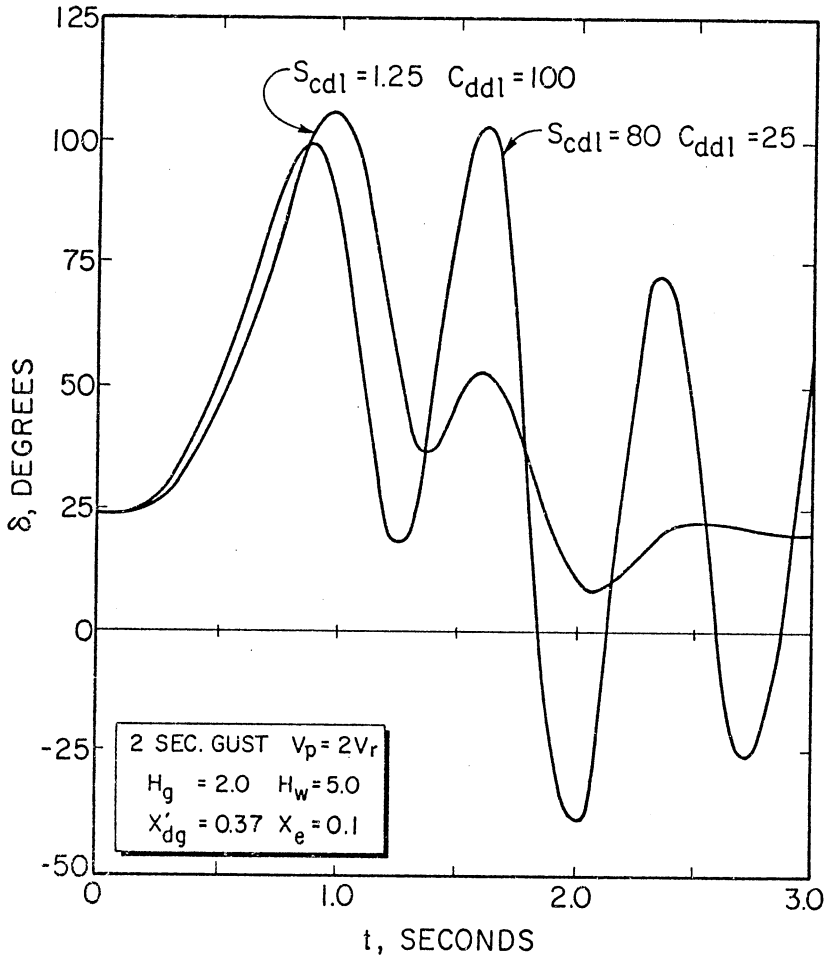

Figure 24. Influence of Normalized Stiffness and Damping Constants; Two Second Gust ($V_p = 2V_r$)

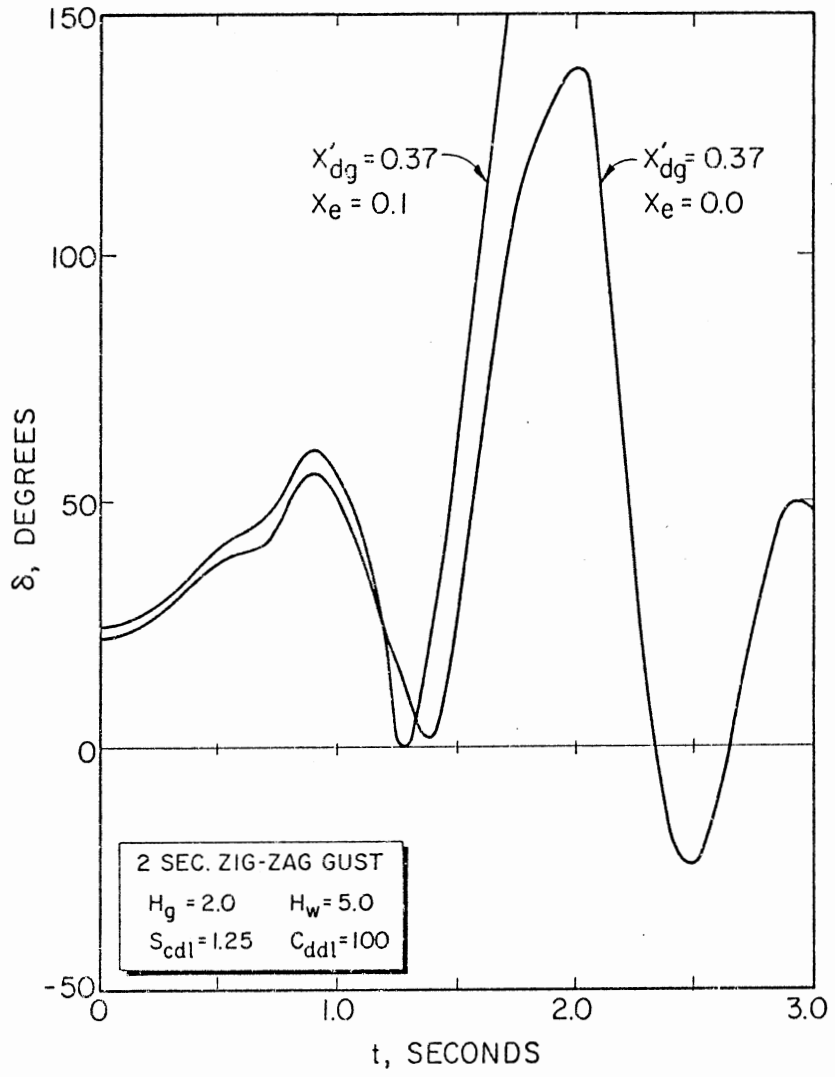

Figure 25. Influence of System External Reactance; Two Second Actual Gust ($V_p = 2V_r$)

3.8.4 Nondimensional Curves

Families of nondimensional curves relating $\hat{\delta}$ and k are presented in Figures 26 through 28. In simulations with a one-second gust, no voltage control is assumed (constant E'_q). Control is included in the studies carried out with two-second ideal and actual gusts ($V_p = 2V_r$).

These curves are obtained by increasing the k of the system in steps (for a given x'_{dg}) up to an optimum value for which the synchronism is lost (or very near to being lost). This process is repeated for three different values (high, medium, and low) of x'_{dg} (0.37, 0.3, and 0.2) which are typical for salient pole synchronous generators.

The nondimensional plots provide the following information:

1. Given the x'_{dg} of the machine, x_e, and the type of coupling, the system designer can assess whether the system will be stable or not.

As an example, let $x'_{dg} = 0.3$, $x_e = 0.2$, and assume a very soft coupling ($S_{cdl} = 1.25$; $C_{ddl} = 100$). The system has a k equal to 0.67. Corresponding to this value of k, $\hat{\delta}$ is found from Figure 28 as equal to 83°. This means that the system is stable with a δ_m in the range of 105° to 110° when subjected to a wind gust of two seconds duration with a peak equal to twice the value of the rated wind speed.

In fact, a series of such curves can be drawn for any value of x'_{dg} and a chosen set of control parameters. Only three representative series have been drawn to illustrate this concept for the two couplings proposed.

It should be remarked at this point that practical systems must be designed with a sufficient margin of safety and operation near the "critical line" should be avoided as far as possible.

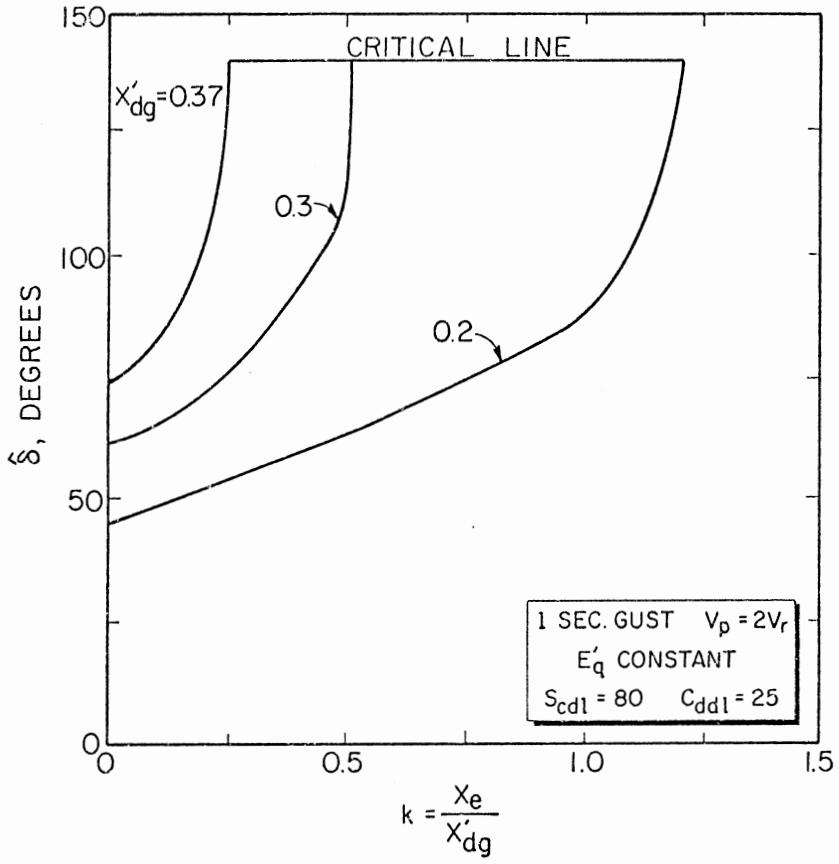

Figure 26. Non-dimensional ($\hat{\delta}$ versus k) Curves of Damped Flexible Coupling ($V_p = 2V_r$ Constant E'_q)

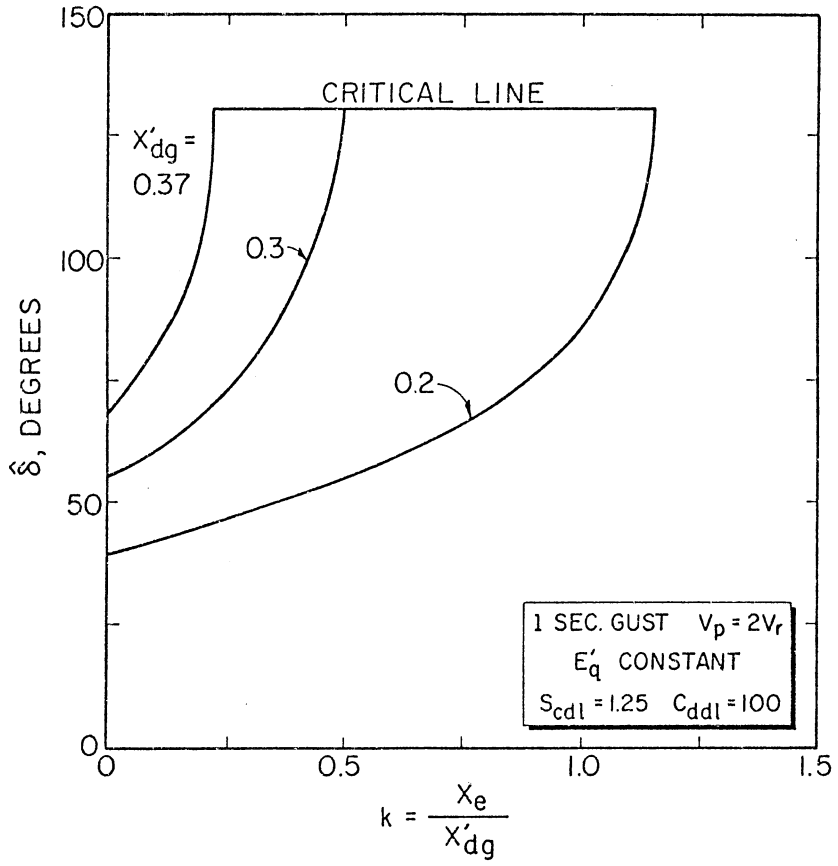

Figure 27. Non-dimensional ($\hat{\delta}$ versus k) Curves of Very Soft Coupling with Damping ($V_p = 2V_r$ Constant E'_q)

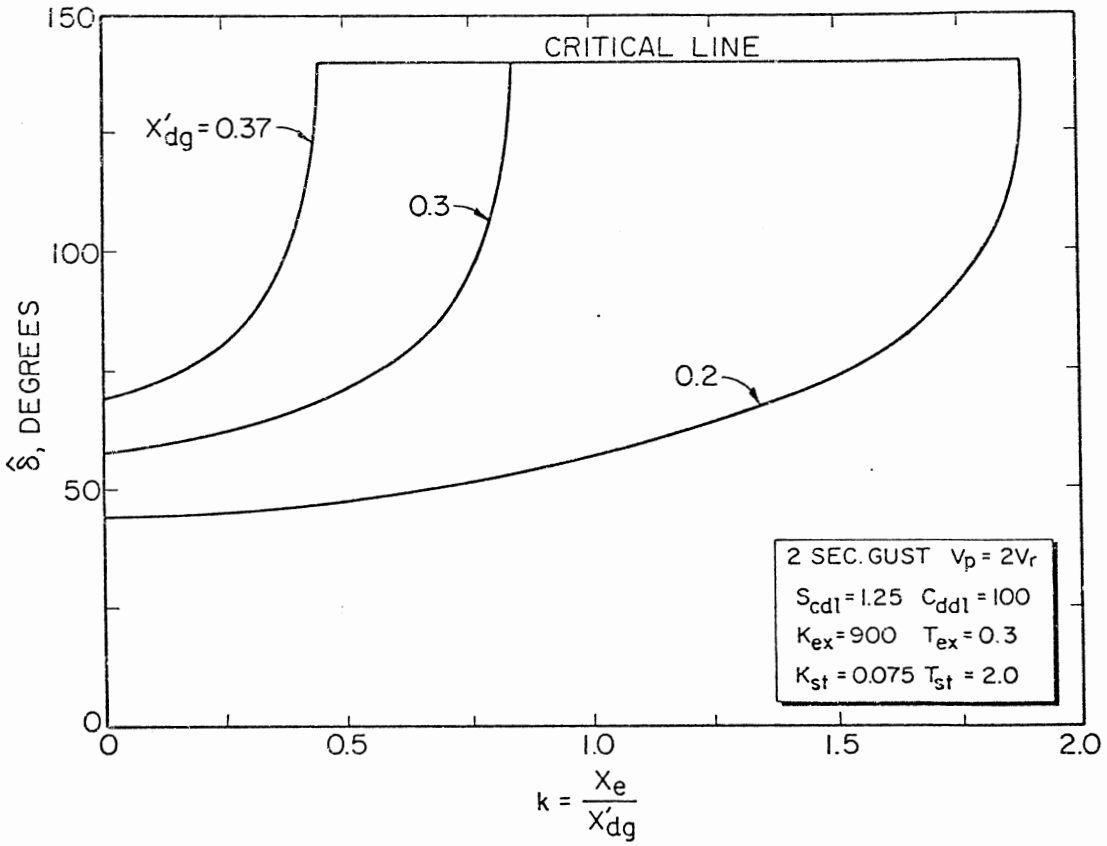

Figure 28. Non-dimensional ($\hat{\delta}$ versus k) Curves of Very Soft Coupling with Damping ($V_p = 2V_r$) including Voltage Control

3.8.5 Exciter Ceiling Voltage

Computer simulations have shown that the excitation voltage E_{ex} reaches values in the range of 3.75 to 4.25 times the initial value with maximum rotor angles of around 114° to 160° with a soft coupling. For unstable cases this value reaches as high as six times the initial exciter voltage. For very stable cases, such as the ones encountered in systems with low reactance, mild gusts ($V_p \leq 1.5V_r$) and soft couplings, E_{ex} is limited within twice the initial value.

3.9 Concluding Remarks

The following conclusions can be drawn from the results and discussion presented in this chapter.

1. Peak and duration of the gust appear to be the most important external variables affecting the performance of wind electric systems.

2. System (machine and external) reactance is the most influential electrical parameter.

3. Soft coupling with damping ($S_{cdl} = 1.25$; $C_{ddl} = 100.00$) appears to be the most effective from the viewpoint of reducing the maximum rotor angle deviations and dampening the oscillations subsequent to the maximum swing.

4. Damped, flexible coupling ($S_{cdl} = 80$; $C_{ddl} = 25$) of the type readily available in the market can be used only if the system reactance is sufficiently low ($x'_d = 0.3$ or lower) and the gusts are mild ($V_p \leq 1.5V_r$).

5. Careful choice of control loop parameters greatly improves the overall system performance. A typical set of recommended values is given below.

K_{ex} = 900.0 p.u T_{ex} = 0.3 s

K_{st} = 0.075 p.u T_{st} = 2.0 s

6. Changes in H_g (from 2.0 to 4.0) and H_w (from 3.0 to 5.0) do not significantly change the system performance, although they affect the upper and lower rotor angles slightly (some 5°). Larger inertias contribute to prolonged oscillations subsequent to the occurrence of gusts.

7. Low system reactance (x'_{dg} = 0.2; x_e = 0.2) and soft coupling with damping (S_{cdl} = 1.25; C_{ddl} = 100.0) restrict the upper angle δ_m to about 80°, prevent motoring, and assure satisfactory operation.

8. If the gusts are more frequent at the location of the wind electric system, very soft coupling must be recommended for satisfactory operation.

9. The families of nondimensional curves presented provide valuable information helpful to the system designer.

10. Under transient conditions, excitation control increases the excitation voltage E_{ex} sharply with increases in generator rotor angle. For normal stable systems the recommended values of CVR lie between 2.0 and 3.0.

CHAPTER IV

STUDIES ON WIND DRIVEN SYNCHRONOUS MACHINES EMPLOYING EDDY-CURRENT COUPLINGS

4.1 Introduction

Chapter II of this thesis dealt with a wind driven synchronous generator employing a stiff coupling in the mechanical interface. Chapter III dealt with the use of flexible coupling with damping wherein the influence of the stiffness constant and damping coefficient were critically examined along with the effect of changing some mechanical and electrical parameters. Concept of non-dimensional constants was introduced and their possible choice recommended in the concluding summary. Attention will now be focused on interposing an eddy-current coupling between the generator and the step-up gear box. Although eddy-current coupling has been known and is available in a variety of forms, it has not been put to effective use in the wind-driven machine applications where input is inherently varying. In most of the practices till to date, the eddy-current coupling has been employed in drives where the prime mover runs at a constant speed and the load is variable speed or fluctuating as for example is the case with the extruders and the textile machinery.

There is considerable literature available that pertains to various aspects of the eddy-current couplings. Gibbs (46), in his very early

paper on this coupling, deals with the nature of losses encountered. Glazenko (47) sets up the formulae that relate the maximum torque and the critical slip and discusses design factors that affect the torque-slip characteristic. Glazenko's equation relating the maximum torque (T_m) to slip at maximum torque (ω_m) and slip at rated torque (ω_r), would be employed in modeling in this chapter. Davies (48) derives the steady state equations of eddy-current couplings with homogeneous ferromagnetic drums and verifies his theory with experimental results. Flack et al (49), discuss possible future applications of this coupling and show the variation of torque-speed curve with excitation. Putnam (Reference (2), page 114) considered using this coupling in his well known Smith-Putnam project, but finally gave up the idea due to the fact that the technology and experience with such couplings were not well established at that time. It is the purpose of this chapter to consolidate all these ideas and proceed with the development of the performance equations of the third configuration which will employ an eddy-current coupling instead of a flexible coupling with damping dealt with in Chapter III.

4.2 Operation of Eddy Current Coupling

A simple eddy-current coupling for the wind energy application is shown schematically in Figure 29. The input shaft is driven by the wind rotor. The field member carries a magnetic pole arrangement as in an alternator. When these poles are excited (with direct current as in the case of synchronous machine) and there is relative motion between the drum and the field member, the pole flux pattern moves past the loss drum at the air gap surface and eddy currents are induced

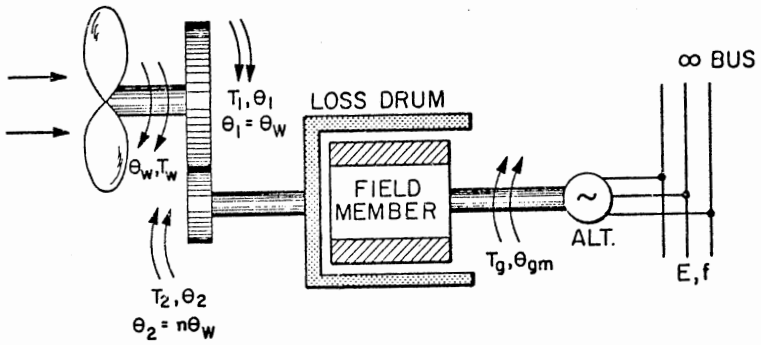

Figure 29. Schematic of System Employing an Eddy Current Coupling

in the drum. Interaction between these currents and the magnetic field results in an electromagnetic coupling and the transmission of torque The magnitude of the eddy currents induced and the associated losses in the drum depend on the frequency (given by the slip speed and the number of poles) and the excitation. Thus the torque transmitted is a function of the field (exciting) current and the slip speed. As excitation is increased, field strength increases and the level of output torque is raised. Effect of varying the excitation on the torque-slip characteristic is shown in Figure 30 for a typical eddy-current coupling.

4.3 Torque-Slip Characteristics

Torque-slip characteristic of an eddy-current coupling is given in non-dimensional form by Glazenko:

$$\frac{T_2}{T_m} = \frac{(2 + \sqrt{2})}{\frac{\sqrt{\omega}}{\sqrt{\omega_m}} + \frac{\sqrt{\omega_m}}{\sqrt{\omega}} + \sqrt{2}} \tag{4.1}$$

At the rated conditions,

$$\frac{T_2}{T_m} = \frac{T_r}{T_m} = \frac{(2 + \sqrt{2})}{\frac{\sqrt{\omega_r}}{\sqrt{\omega_m}} + \frac{\sqrt{\omega_m}}{\sqrt{\omega_r}} + \sqrt{2}} \equiv \frac{1}{k_T} \tag{4.2}$$

Let

$$x = \frac{\omega_m}{\omega_r} \tag{4.3}$$

Using (4.3) in (4.2) one obtains;

$$\sqrt{x} + \frac{1}{\sqrt{x}} = k_T (2 + \sqrt{2}) - \sqrt{2} \equiv k_1 \tag{4.4}$$

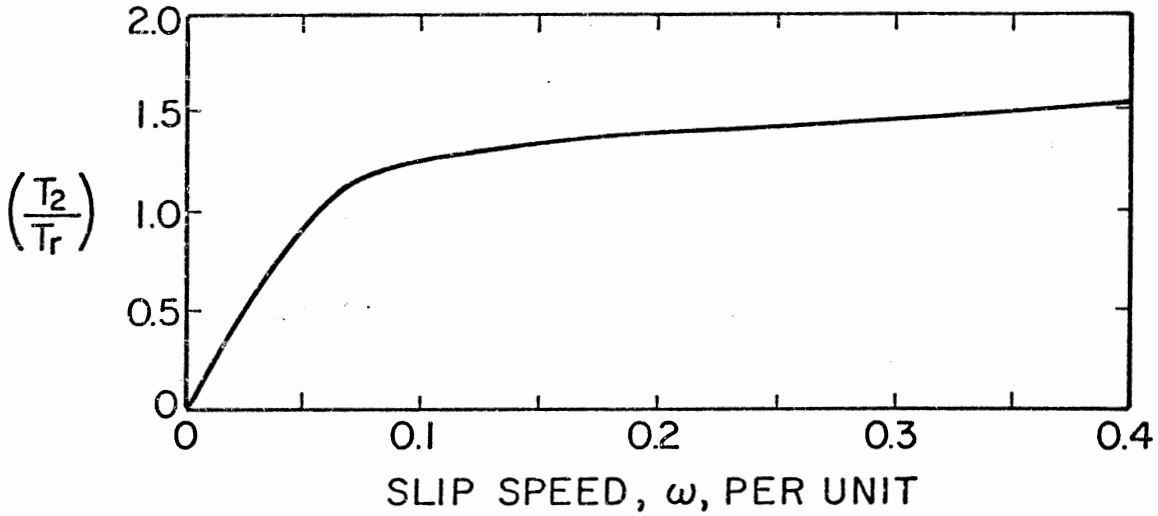

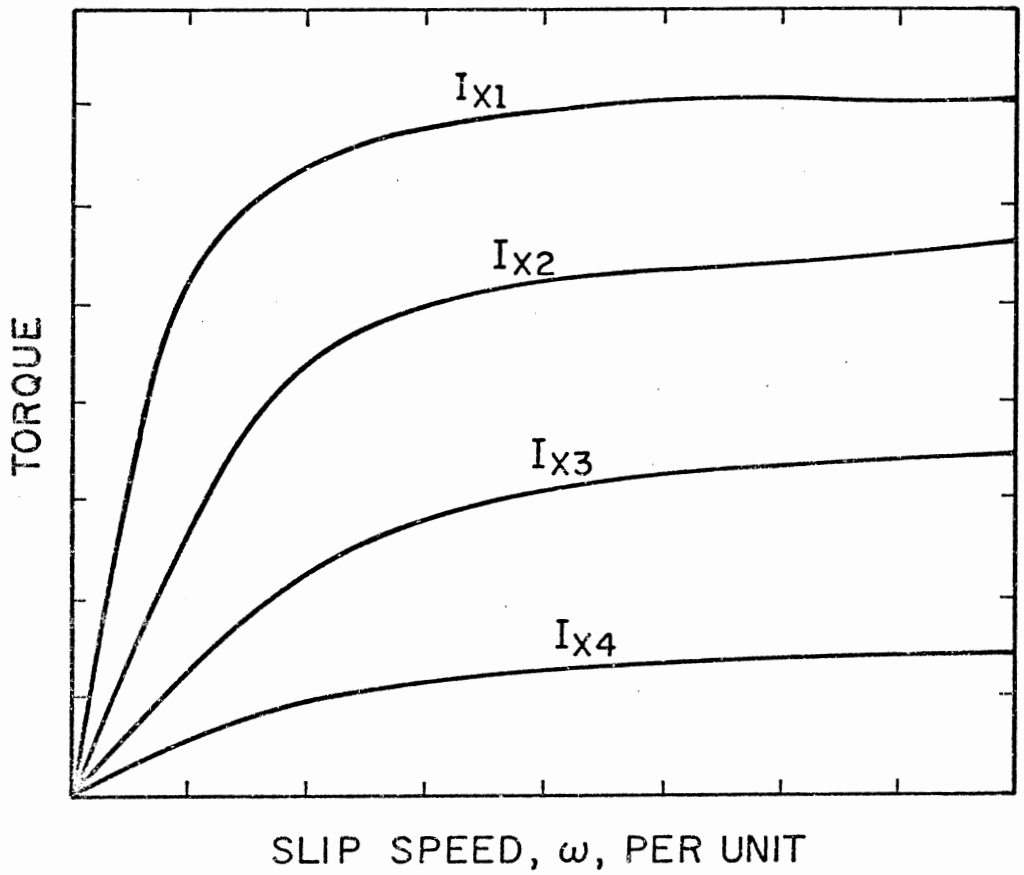

Figure 30. Torque-Slip Speed Characteristics of an Eddy Current Coupling for Varying Field Current

which can be rewritten as:

$$\frac{x + 1}{\sqrt{x}} = k_1 \tag{4.5}$$

Squaring both sides of (4.5) and rearranging, one obtains:

$$x^2 + 2x + 1 = k_1^2 x \tag{4.6}$$

Or,

$$x^2 + x(2-k_1^2) + 1 = 0 \tag{4.7}$$

Solving for x,

$$x = \frac{-(2-k_1^2) \pm \sqrt{\{(2-k_1^2)^2 - 4\}}}{2} \tag{4.8}$$

The quantity x fixes the shape of the torque-slip curve for a given value of k_T. A family of such curves is drawn for ω_r values of 0.025, 0.05 and 0.075 in Figures 31, 32 and 33. It should be noted that for one set of (ω_r, k_T) there is an entire set of values of T_2 versus ω_2, determined by the instantaneous speed difference between loss drum and field member. During actual operation of the wind system employing this coupling ω continues to vary. Instantaneous torque transmitted will also vary corresponding to the variations in ω.

At this point it is important to note that (ω_m, T_m) form only one set corresponding to a set of (ω_r, k_T). If ω_r and k_T are selected the shape of the torque-slip curve is fixed and ω_m is fixed for a given k_T and T_m. Once the shape of the curve is fixed, T_2, which is the output torque at any instant, is a function of ω. The maximum torque T_m may never be reached in actual practice and normally, in the operating range, ω is much less than ω_m and T_2 is much smaller than T_m. Consider, for example, a case with $k_T = 20$. The corresponding value

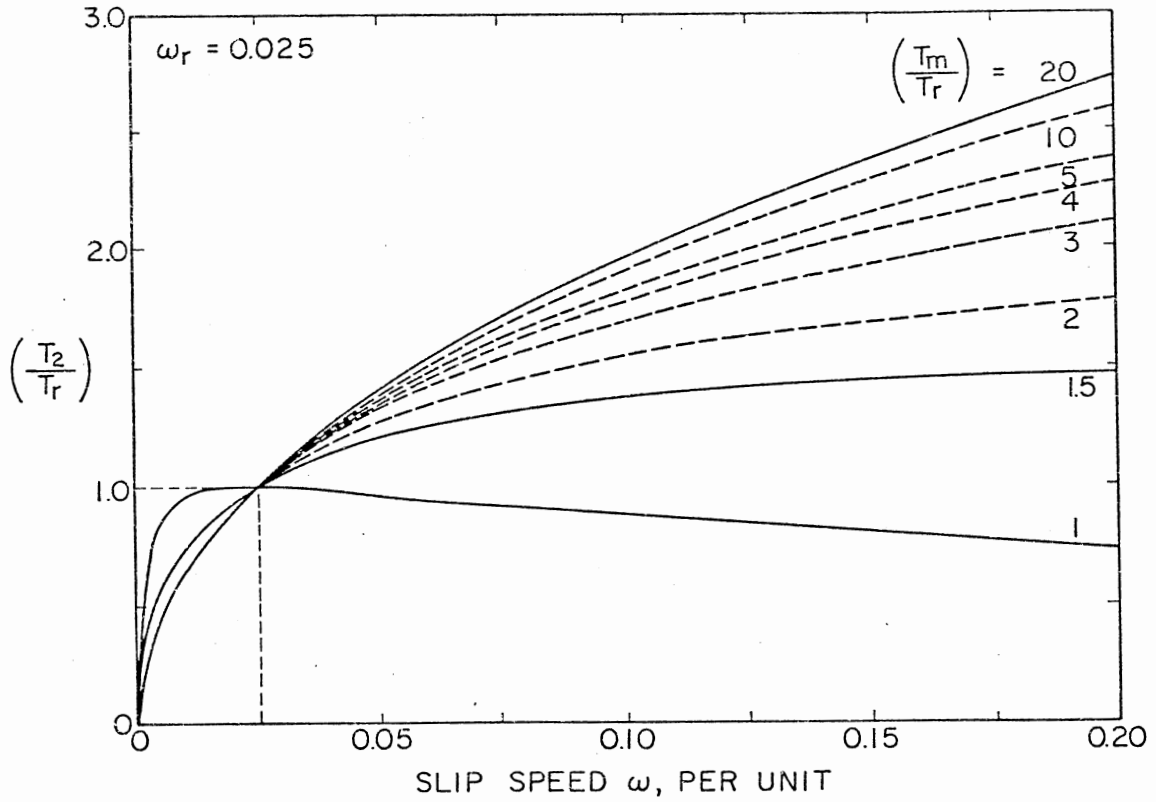

Figure 31. Family of Normalized Torque-Slip Speed Characteristics of an Eddy Current Coupling (ω_r = 0.025)

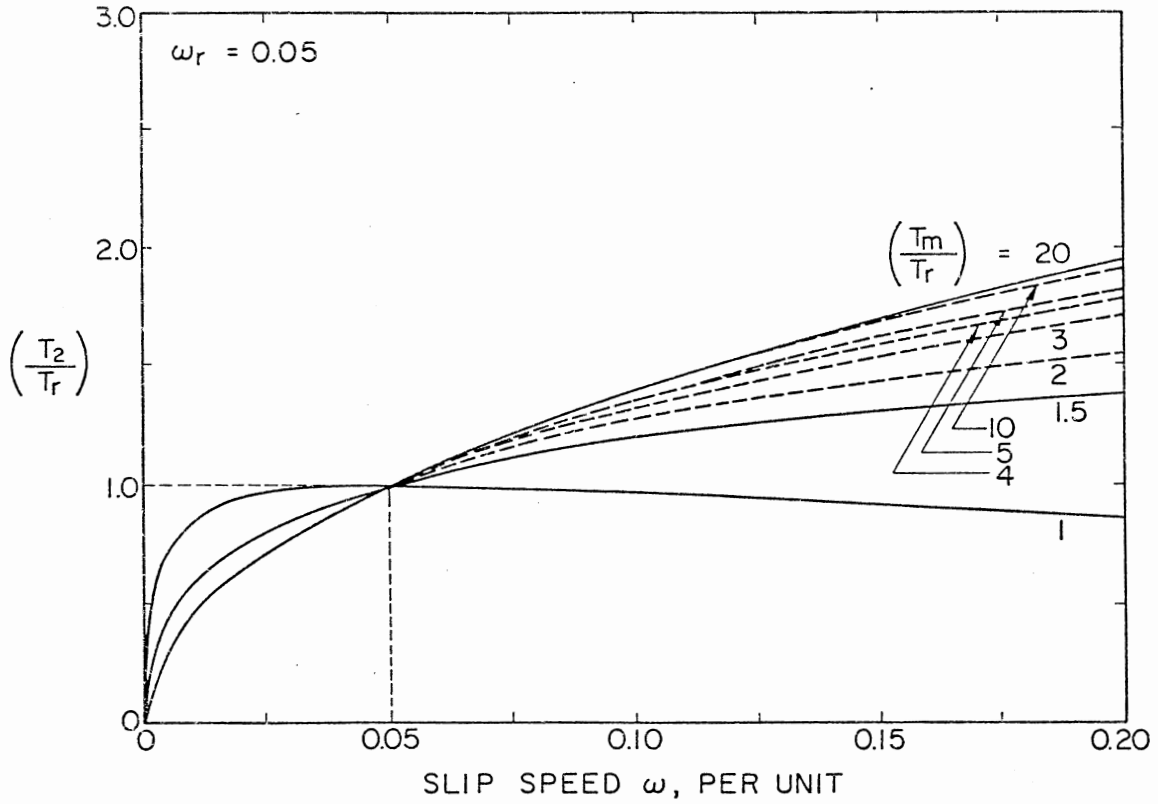

Figure 32. Family of Normalized Torque-Slip Speed Characteristics of an Eddy Current Coupling (ω_r = 0.05)

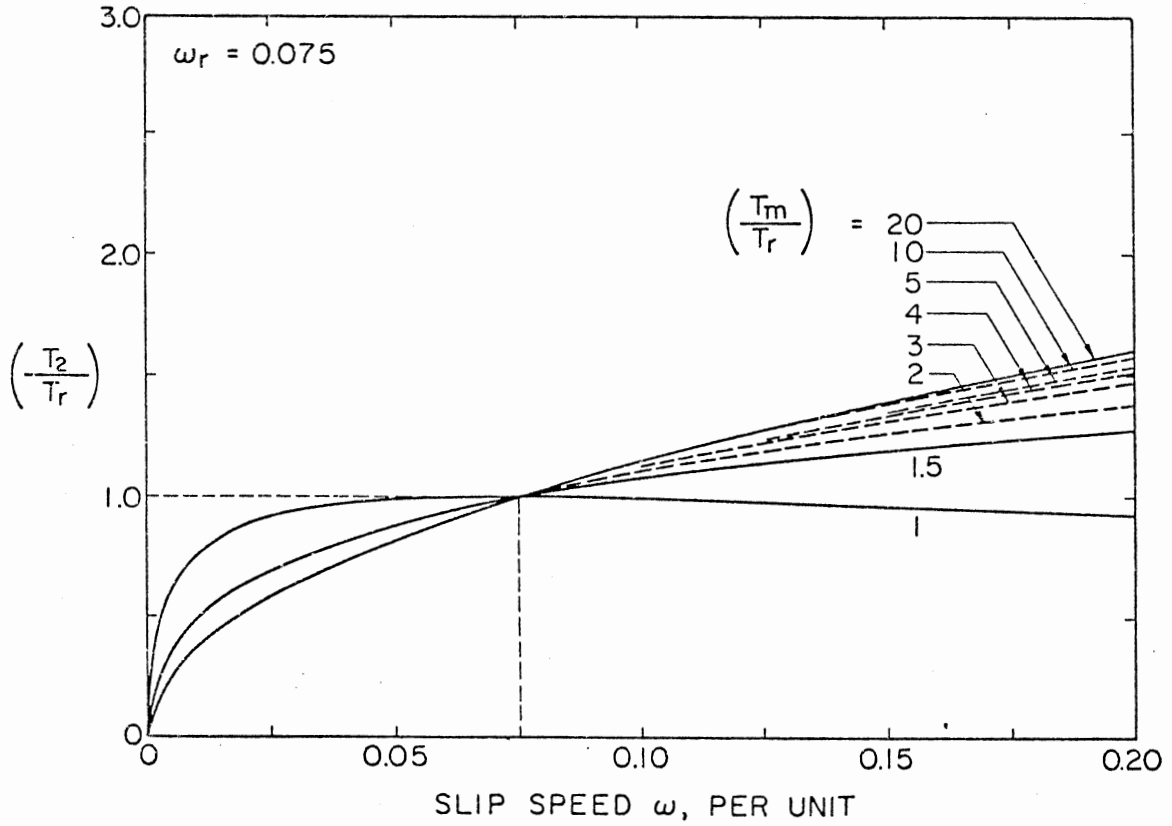

Figure 33. Family of Normalized Torque-Slip Speed Characteristics of an Eddy Current Coupling (ω_r = 0.075)

of x is given by (4.8) as 4469.6. Selecting a rated per unit slip ω_r of 0.05, one obtains the following:

$$\omega_r = 0.05\ \omega_{syn}$$

$$x = \frac{\omega_m}{\omega_r} = \frac{\omega_m}{0.05\ \omega_{syn}} = 4469.6$$

$$\omega_m = 0.05 \times 4469.6 \times \omega_{syn}$$

$$= 223.48\ \omega_{syn}$$

Since one per unit corresponds to the synchronous speed of the alternator, it is seen that maximum torque T_m is obtained at a slip speed equal to 223.48 times the value of synchronous angular speed. This slip, though numerically conceivable, is physically not realizable and can never be achieved in actual practice. Similarly, the maximum torque, which is 20 times the rated torque in this example, will never be reached. In fact, computer print outs show that instantaneous torque does not usually exceed 2 to 3 times the rated torque even when $T_m = 20\ T_r$.

4.4 Performance Equations

Performance equations for the wind-electric system employing an eddy-current coupling can be easily obtained by slightly modifying the equations (2.3) and (2.4).

Replacement of $S_c(\Theta_2 - \Theta_{gm})$ with αT_m in (2.3) and (2.4) yields:

$$T_2 - J_2 \ddot{\Theta}_2 = \alpha\ T_m \tag{4.9}$$

$$\alpha T_m = J_g \ddot{\Theta}_{gm} + T_g \tag{4.10}$$

where

$$\alpha = \frac{(2 + \sqrt{2})}{\left[\frac{\omega_m \dot{\theta}_{gms}}{(\dot{\theta}_2 - \dot{\theta}_{gm})}\right]^{1/2} + \left[\frac{(\dot{\theta}_2 - \dot{\theta}_{gm})}{\omega_m \dot{\theta}_{gms}}\right]^{1/2} + \sqrt{2}} \tag{4.11}$$

as given by Glazenko.

Following the procedure outlined in section 2.2 and with the above replacements, the performance equations are obtained as given below:

$$\ddot{\theta}_w = \frac{1}{\omega_w J_w} \left[P_w - \frac{n}{\eta_g} \omega_w \alpha T_m\right] \tag{4.12}$$

$$\ddot{\theta}_{gm} = \frac{1}{J_g} \left[\alpha T_m - \frac{1000G}{\omega_{gm}} (P_s + P_d)\right] \tag{4.13}$$

4.5 Dimensionless Energy Analysis

As already mentioned, the main objective of this thesis is to concentrate on the performance of the system when subjected to a transient disturbance caused by a wind gust. Following such a disturbance, the generator rotor oscillates about its equilibrium position. These oscillations are of fairly large magnitude if the gust is sharp and continue even after the gust has ceased. Motoring also may take place resulting in reverse power flow. If the gusts are frequent, such oscillations, though not disastrous from the stability point of view, may cause considerable reverse power flow. It is from this view point that in this section in addition to stability, the energy aspects will be discussed. In order to lay the ground work for a general application; quantities of energy and some factors would be defined.

Let E_g by the energy actually delivered to the grid over a time interval in Watt-seconds, E_w the energy contained in wind over the same

time interval in Watt-seconds, E_r the energy that would be delivered to the grid in the same interval of time at the rated power in Watt-seconds.

Let E_{gd} be the ratio (E_g/E_r), E_{wd} the ratio (E_g/E_w) and let E_e be given by the expression:

$$E_e = \frac{(E_{gd}-1)E_r}{E_w \text{ -energy in wind without gust}}$$

It is seen that E_e is the ratio of additional output (over and above rated) to the additional input (over and above rated). A value of E_{gd} greater than one signifies that, for the time interval considered, the energy delivered to the grid with the transient disturbance is more than the energy that would be delivered to the grid if there was no disturbance. E_{wd} is the ratio (E_g/E_w) and it signifies the overall energy collection efficiency of the system for the time period considered. E_{wd} can never be greater than 1; however, higher values of E_{wd} could imply, that a larger fraction of the energy in the wind is converted to electrical form. E_e, which is defined as the ratio of additional output to the additional input can be interpreted as follows; during the transient disturbance the wind input is more (over and above the rated) and rotor angle δ deviates to larger or smaller values causing changes in power flow. During the transients caused by the gust there are two energy processes that are taking place; one is the increase or decrease of the energy delivered to the grid (over and above the rated or below the rated) due to the changes in rotor angle and the other is the increase in wind input due to the gust. The relationship between these two is given by E_e.

4.6 Computer Simulation

Computer simulations are carried out exactly in the same way as described in Chapters II and III. Wind gust models and physical test data are given in section 3.7 of the Chapter III. Program constructed is modified so as to conform with modified equations (4.12) and (4.13). The program is augmented to handle new energy variables by extending $\vec{Z}(t)$ vector by additional three elements - namely, energy in the wind (E_w), energy extracted from wind by wind rotor (E_{wr}), and energy being delivered to the grid (E_g). These new variables are zero at time $t=0_-$. State vector now has ten elements. $\vec{F}(\vec{Z},t)$ also has the same number of elements (equations) as state vector $\vec{Z}(t)$. Control is included only for two-second idealized and actual gusts. For one-second gust, it is assumed that E'_q is constant. This is a well established assumption in stability studies.

4.7 Results and Discussion

Results and discussion will be subdivided into three parts as listed below:

1. General
2. One-second gust; $V_p = 2V_r$ and $V_p = 1.5\ V_r$.
3. Two-second ideal and actual gusts; $V_p = 2V_r$

4.7.1 General

Computer simulation results are presented in the form of the following curves:

i. δ_m versus k_T

ii. % change in ω_w versus k_T

iii. E_{gd} versus k_T

iv. E_{wd} versus k_T

v. E_e versus k_T

These parameters have been selected with the objective of presenting the results in a manner which will provide information from both the design and the energy collection view points.

In addition, the following time-plots are included.

i. δ versus t

ii ω_w versus t

These plots will provide information regarding the rotor angle and the energy absorbed by the wind rotor during disturbance.

An overall examination of the curves reveals that the stability worsens with the sharpness and the peak of the gust and δ_m increases with an increase in the peak of the gust, for a given value of k_T. Stability is not in any danger for sufficiently large values of k_T. Upper angle δ_m is limited to a reasonable level for all types and durations of gusts considered in this study. Dynamic interactions are severe in lower ranges of k_T, and become more and more mild as k_T increases and almost level off for larger values of k_T. Torque angle δ is limited very effectively by the coupling and motoring is prevented in all the cases studied. Generator speed variations are insignificant, but wind rotor speed variations are much more pronounced. E_{gd}, E_{wd} and E_e increase as k_T increases; however, these increases level off with higher values of k_T. Computer print outs clearly indicate that variations in reactance parameter (0.5 to 0.8) do not have any significant influence on the stability of studied system.

4.7.2 One-Second Gust; ($V_p = 2V_r$ and $V_p = 1.5\ V_r$)

The nature of variations of δ_m with k_T for one-second gust is similar with both values of gust peak (refer Figures 34 and 39); evidently the wind gust with higher peak results in larger rotor angle deviations for any given value of k_T. Rotor angle δ_m is higher with lower rated slip ($\omega_r = 0.025$) in both cases ($V_p = 2V_r$ and $V_p = 1.5V_r$) because of the fact that couplings with smaller rated slips are less lossy and energy in the gust is transmitted more effectively and efficiently to the generator rotor. At the same time it may be noted that in the case of the couplings with the smaller rated slips, wind rotor speed variations are minimum (compare Figures 34 and 35). For example when $k_T = 2.5$ and $\omega_r = 0.025$ generator angle reached is 41^o and change in the wind rotor speed is approximately 13 percent. For the other two couplings ($\omega_r = 0.05$ and $\omega_r = 0.075$), angles reached are a little lower but the effect on the wind rotor is higher (14% and 14.5% respectively).

These dynamic studies provide valuable inferences as regards the selection of proper k_T and ω_r which appear to be the predominant parameters in determining the performance of wind systems employing eddy-current couplings. Peak of the gust appears to be the most influential external variable. Behavior of δ_m and ω_w is precisely similar for a given ω_r and k_T; only the reactions are more mild in case of gust with lower peak ($V_p = 1.5V_r$) as compared to the gust with higher peak ($V_p = 2V_r$) (compare Figures 34 with 39 and 35 with 40). It is significant to note that all curves tend to level off between $k_T = 2.0$ to $k_T = 3.0$ leading one to infer that this is the favorable range from the design point of view.

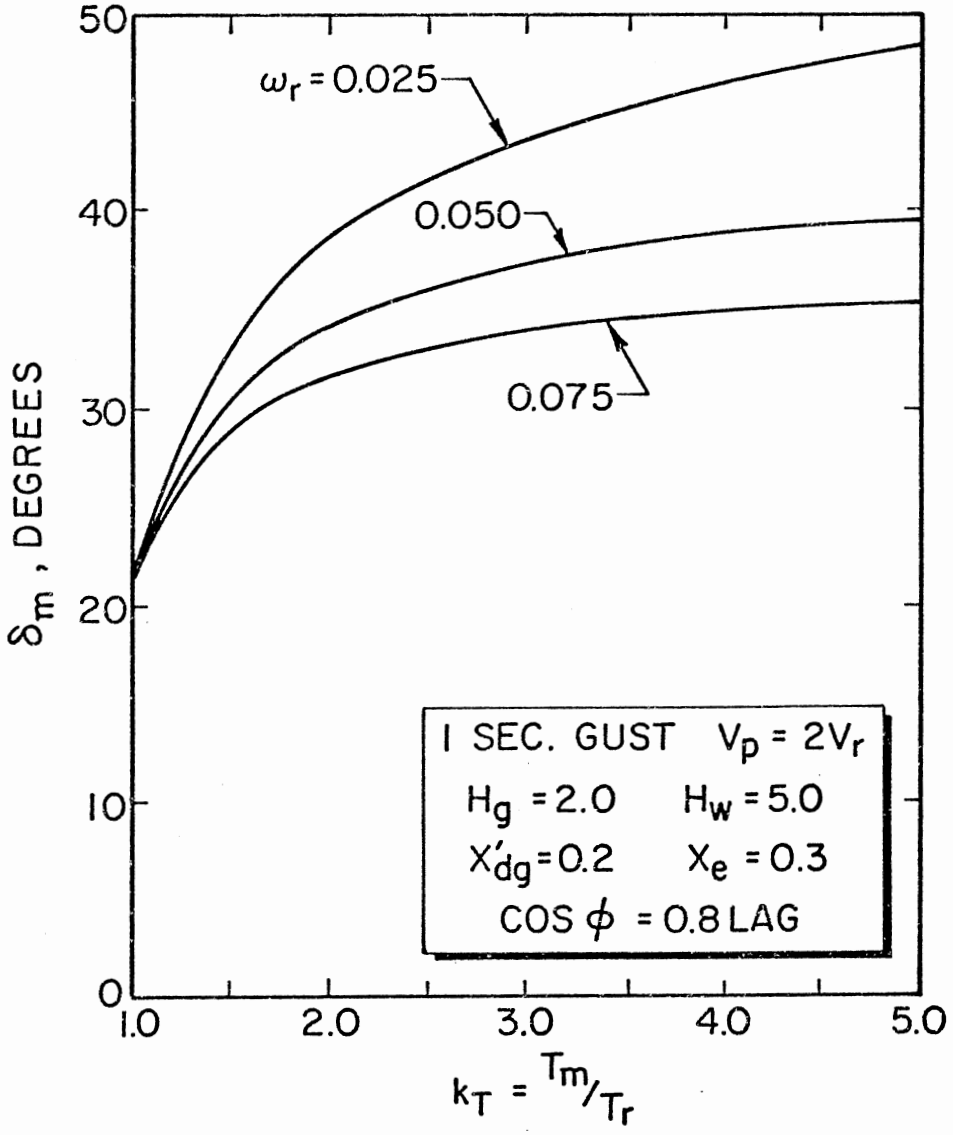

Figure 34. Effect of k_T and ω_r on Maximum Rotor Angle δ_m; One Second Gust ($V_p = 2V_r$)

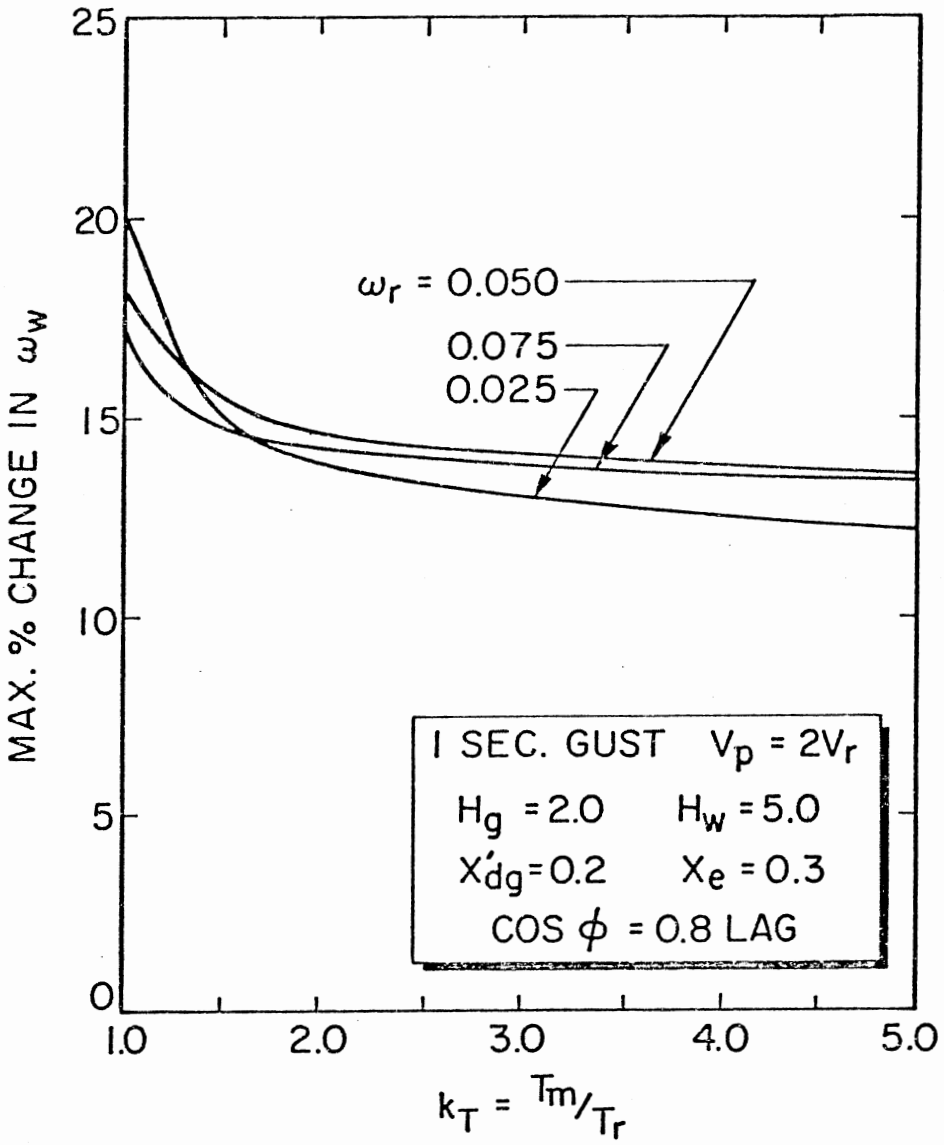

Figure 35. Effect of k_T and ω_r on Speed Variations of Wind Rotor ω_w; One Second Gust ($V_p = 2V_r$)

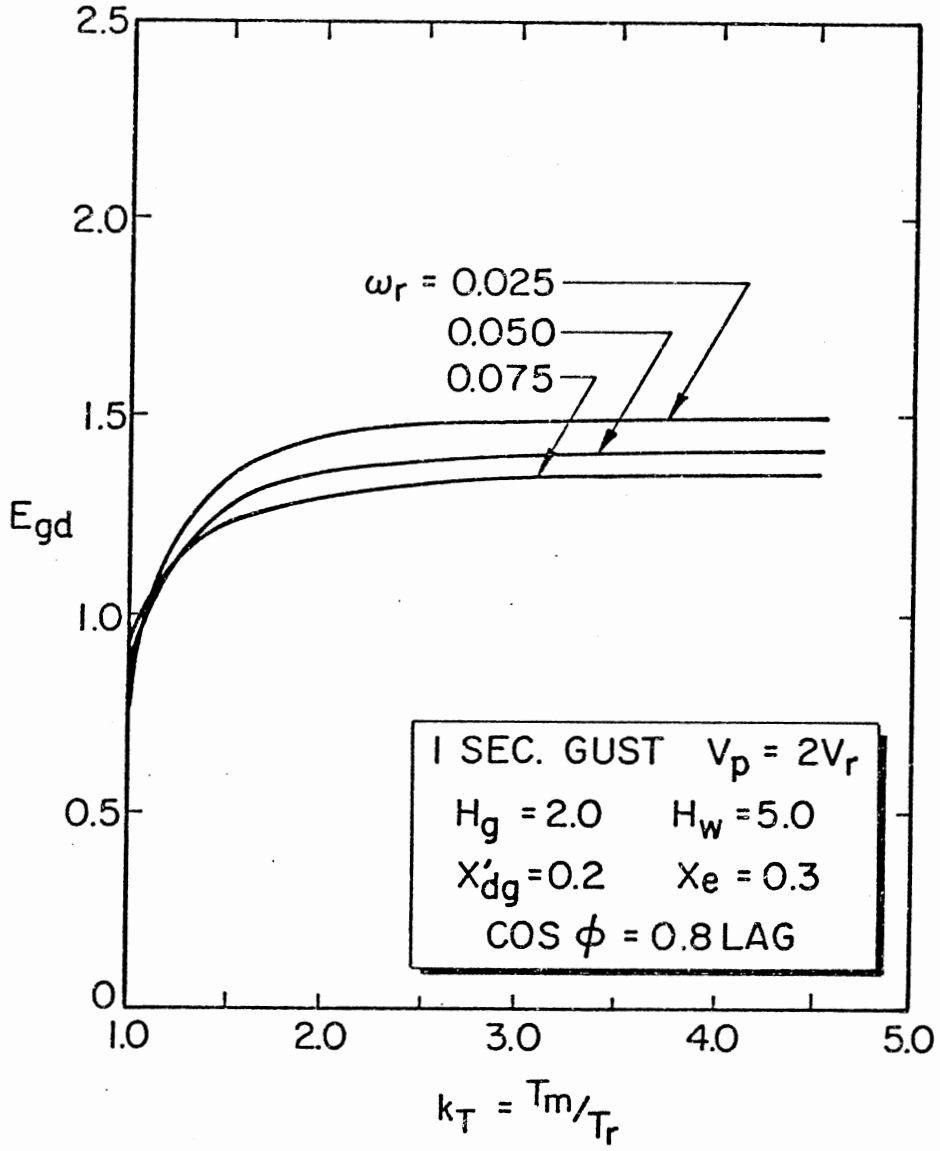

Figure 36. Non-dimensional (E_{gd} versus k) Curves Showing Effect of k_T and ω_r on E_{gd}; One Second Gust ($V_p = 2V_r$)

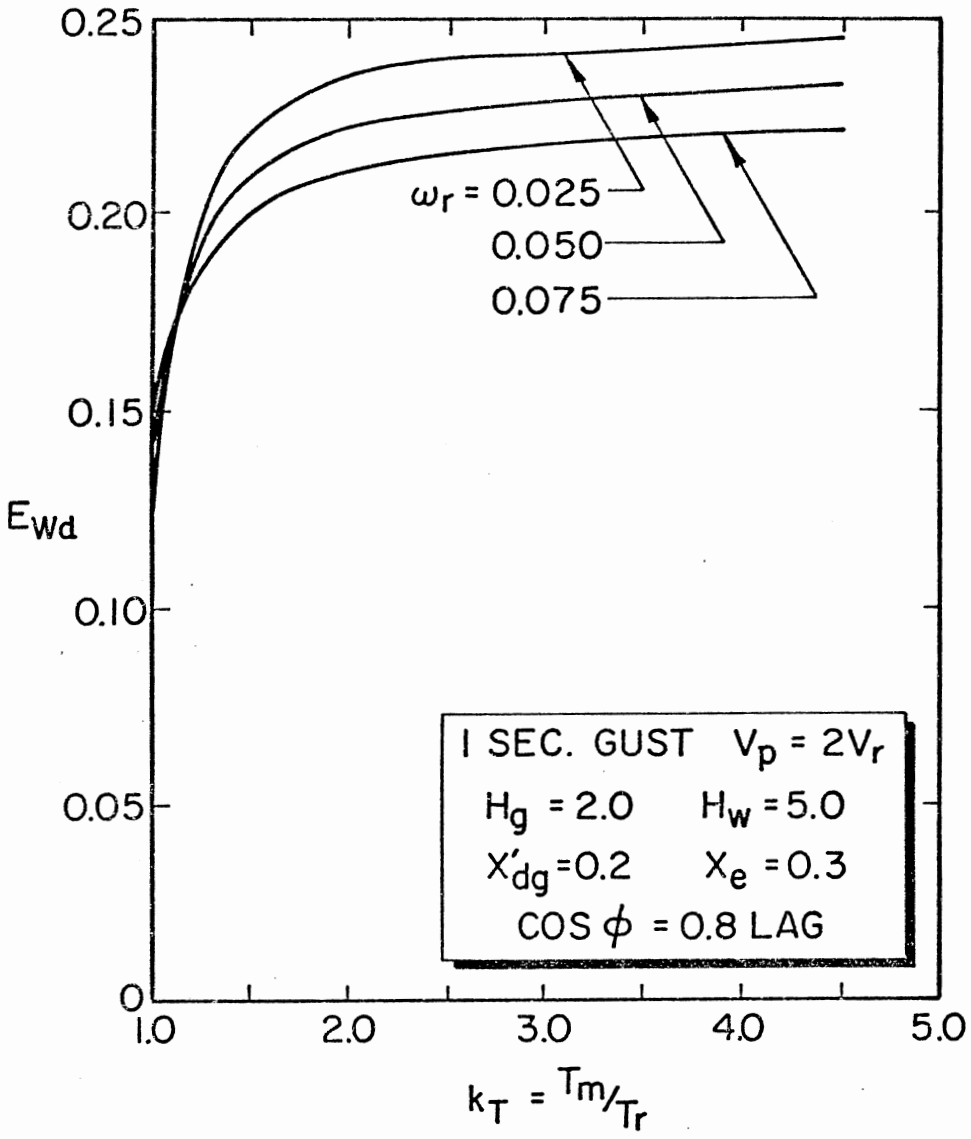

Figure 37. Non-dimensional (E_{wd} versus k_T) Curves Showing Effect of k_T and ω_r on E_{wd}; One Second Gust ($V_p = 2V_r$)

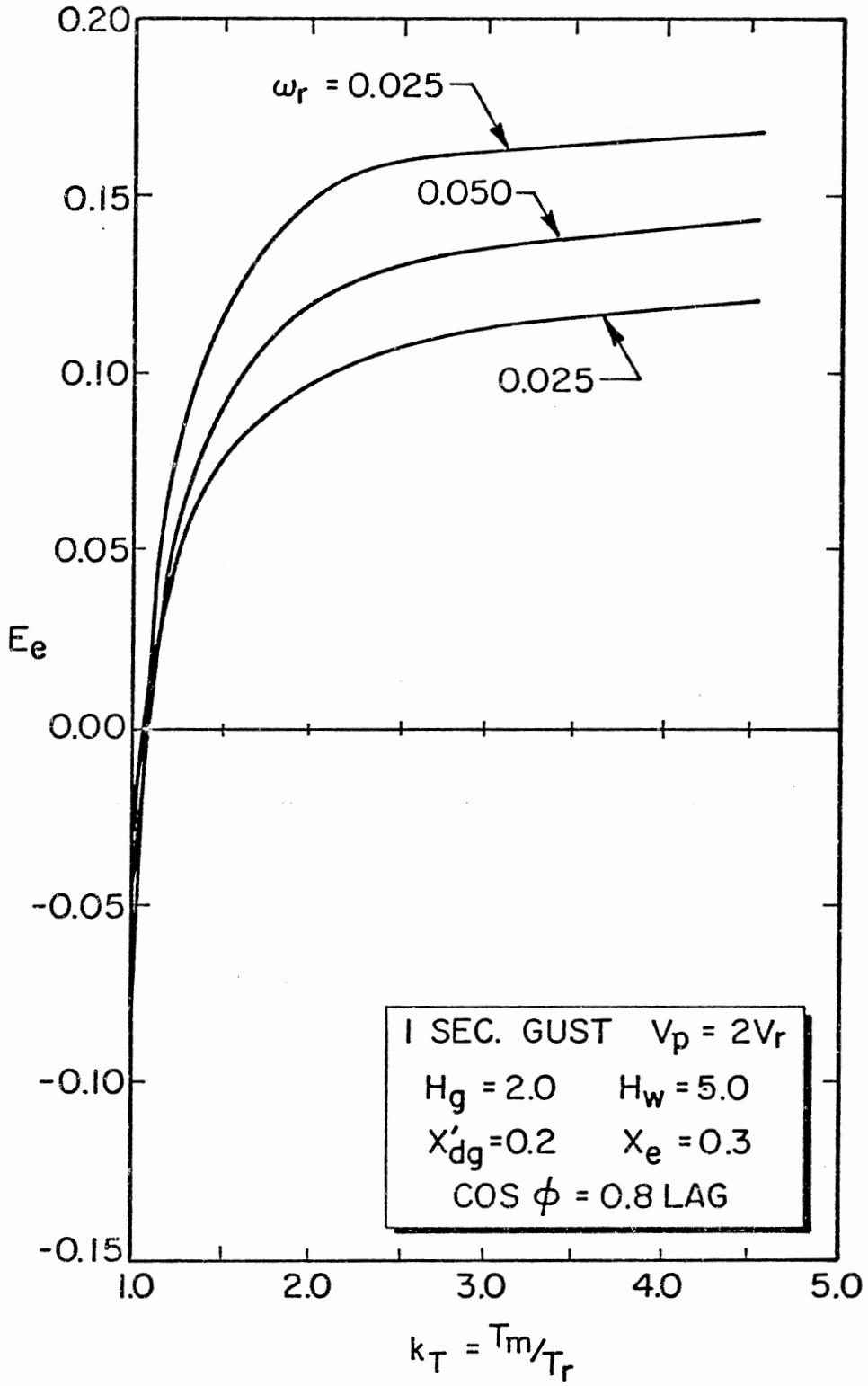

Figure 38. Non-dimensional (E_e versus k_T) Curves Showing Effect of k_T and ω_r on E_e; One Second Gust ($V_p = 2V_r$)

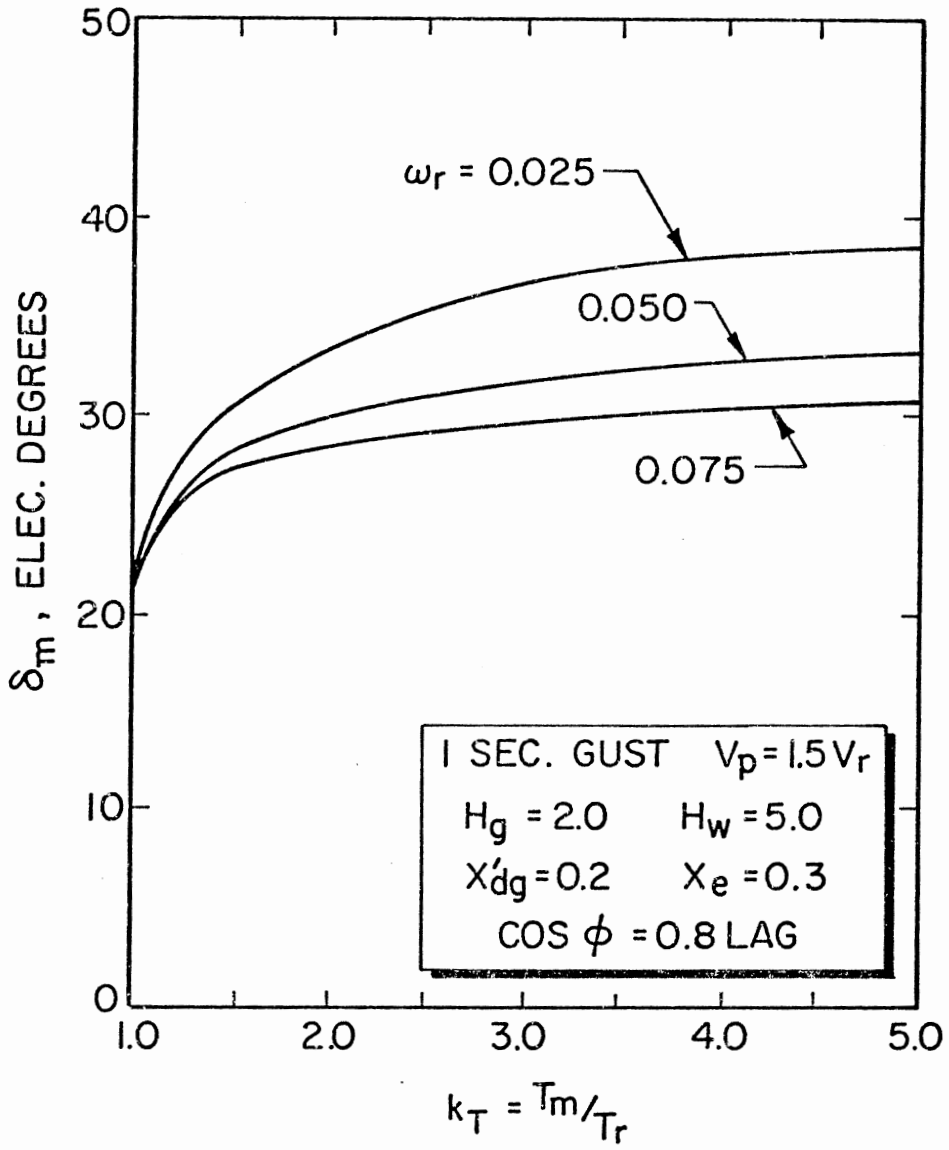

Figure 39. Effect of k_T and ω_r on Maximum Rotor Angle δ_m; One Second Gust ($V_p = 1.5V_r$)

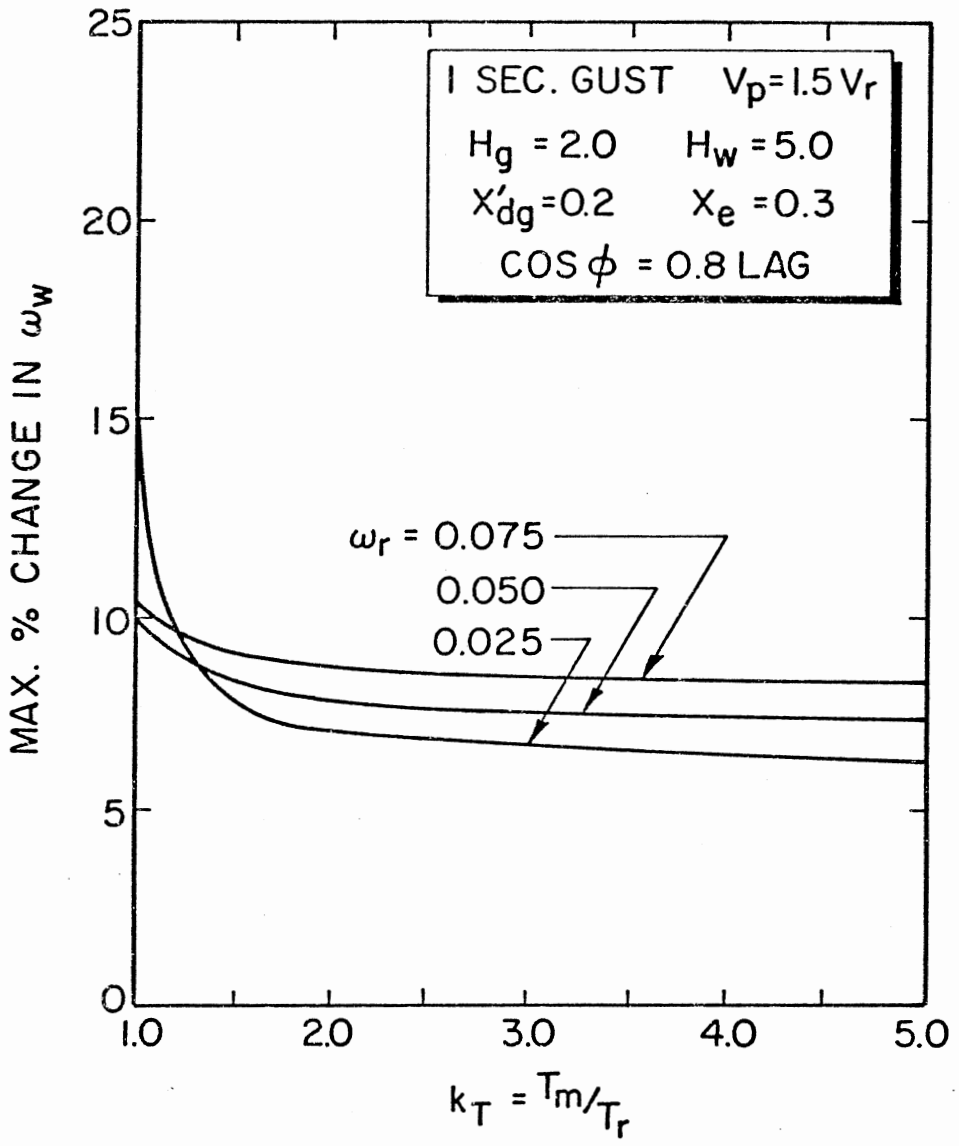

Figure 40. Effect of k_T and ω_r on Speed Variations of Wind Rotor ω_w; One Second Gust (V_p = 1.5V_r)

All the couplings considered ensure safe and stable operation for k_T between 2.0 to 3.0 (compare Figures 34 with 39 and 35 with 40) however more lossy couplings (ω_r = 0.05 and ω_r = 0.075) will pose potential cooling problems in wind energy systems with recurring gusts.

In terms of energy collection and conversion, an examination of E_{wd} curves (compare Figure 37 with 42) shows that the overall energy conversion efficiencies are higher for the gust with a lower peak (V_p = $1.5V_r$) than for a gust with higher peak (V_p = $2V_r$). On a three-second basis this value is 0.294 (V_p = $1.5V_r$) as compared to 0.239 (V_p = $2V_r$) for k_T = 2.5 and ω_r = 0.025. This pattern is repeated for the higher values of rated slips and same discussion is valid.

Similar behavior is exhibited by E_e. Once again these ratios are higher for all three couplings for V_p equal to $1.5V_r$ than for V_p equal to $2V_r$ (compare Figure 38 with 43). Point to note is that curves tend to level off in the range of k_T = 2.0 to k_T = 3.0 leading to the inference as regards the design value of k_T. Apparently the favorable regime of k_T lies between 2.0 to 3.0.

E_{gd} curves (compare Figures 36 and 41) exhibit similar behavior but inference is entirely opposite. The gains in E_{gd} are relatively higher for V_p equal to $2V_r$ than for V_p equal to 1.5 V_r, clearly indicating that though the overall conversion efficiencies (E_{wd}) are lower for V_p equal to $2V_r$ as compared to those for V_p equal to $1.5V_r$ yet net energy delivered to the grid is significantly more for V_p equal to $2V_r$ as compared to V_p equal to $1.5V_r$. This is due to the fact that there is lot more energy contained in the gust with V_p equal to $2V_r$ as compared to the gust with V_p equal to $1.5V_r$ in the same interval of time. Higher angles δ are reached for V_p equal to $2V_r$ as compared to V_p

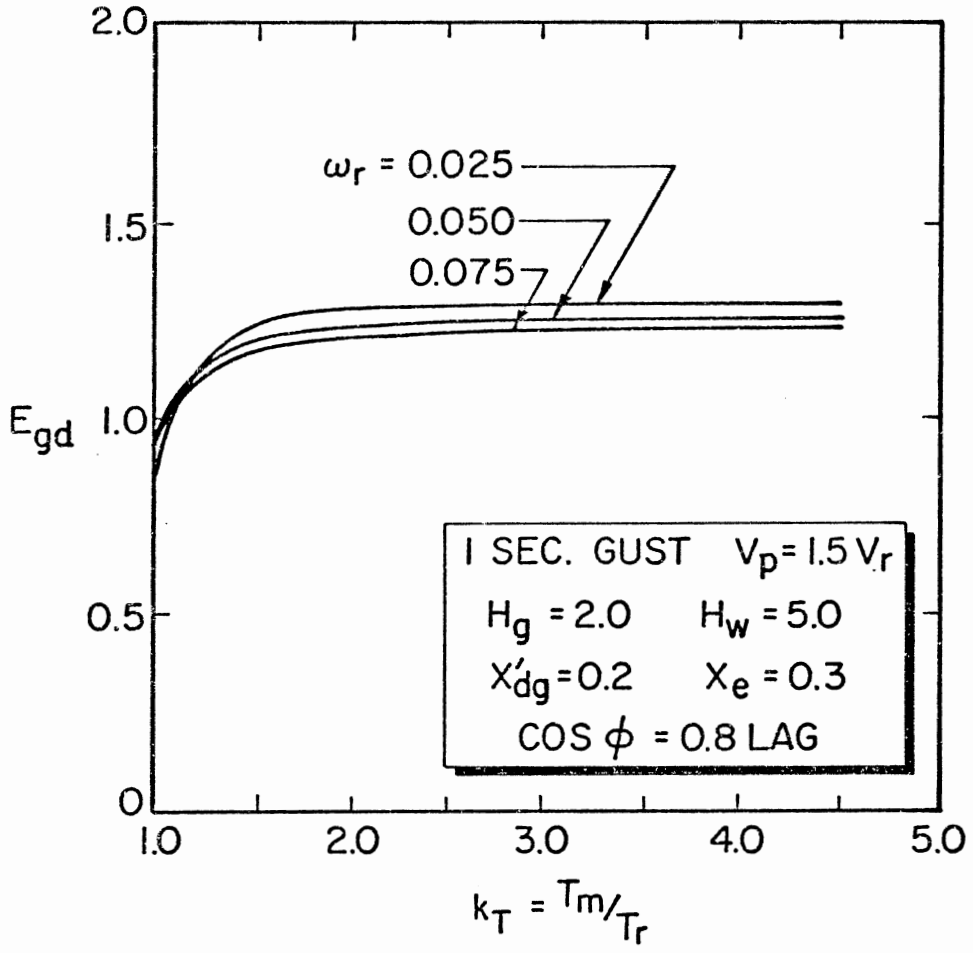

Figure 41. Non-dimensional (E_{gd} versus k_T) Curves Showing Effect of k_T and ω_r on E_{gd}; One Second Gust ($V_p = 1.5V_r$)

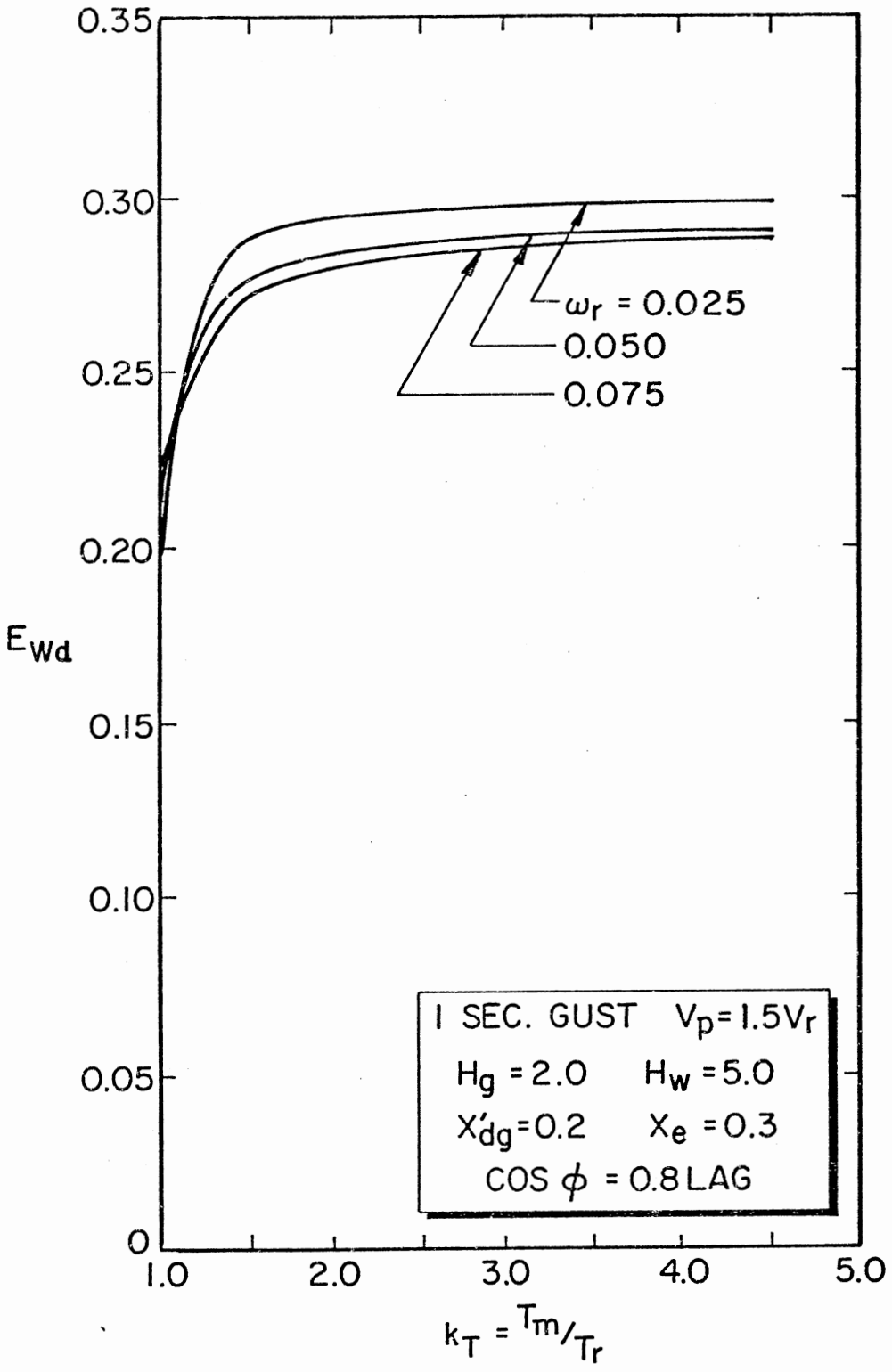

Figure 42. Non-dimensional (E_{wd} versus k_T) Curves Showing Effect of k_T and ω_r on E_{wd}; One Second Gust (V_p = 1.5V_r)

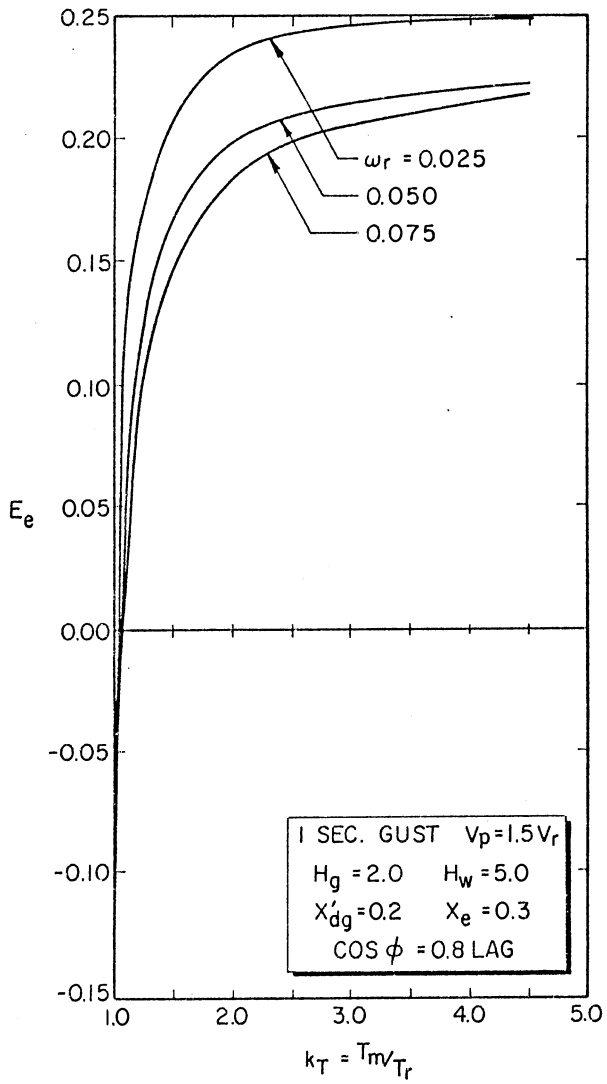

Figure 43. Non-dimensional (E_e versus k_T) Curves Showing Effect of k_T and ω_r on E_e; One Second Gust ($V_p = 1.5V_r$)

equal to $1.5V_r$, consequently more energy flows to the grid.

The case for which $T_m = T_r$ ($k_T = 1$) needs a special mention. For this case the torque T_2 is less than T_m (= T_r) for most of the time. This is evident from the Torque-slip curves (see Figures 31, 32, 33). Torque transmitted to the generator is less than the rated torque. Hence the maximum angle δ_m reached is equal to δ_o and the energy of the gust is taken up by the wind rotor (refer Figures 35 and 40). This results in the highest speed build up of the wind rotor. For ω_r = 0.025; speed rise above normal is of the order of 20 percent for the case when V_p equal to $2V_r$ and 15 percent above normal when V_p equal to $1.5V_r$. For values of k_T greater than 1.0; accelerating torque on the wind rotor is reduced and instead starts building upon the generator rotor for all investigated values of ω_r. Moreover for $k_T = 1.0$, E_{gd} is less than 1 (refer Figures 36 and 41) indicating that for $k_T = 1.0$, the energy delivered to the grid is less than normal (for no gust E_{gd} = 1.0) and such a performance is undesirable. Values of E_{wd} are substantially lower, indicating severe reductions in the overall conversion effeciency of the system (refer Figures 37 and 42). Ratios E_e are negative (refer Figures 38 and 43) indicating that with additional inputs due to the gusts; additional outputs (over and above normal) are negative. This means that outputs are less than those expected with normal wind and gust is of no value and is harmful for values of k_T = 1.0.

4.7.3 Two-Second Ideal and Actual Gusts ($V_p = 2V_r$)

Typical curves of δ versus t and percent change in ω_w versus t are shown in Figures 44 and 45 for an actual (zig-zag) wind gust of

two-seconds duration. Three curves are presented in Figure 44, wherein the effect of changing the mechanical interface (type of coupling) on the system behavior is shown. It is obvious from these plots that the eddy-current coupling not only prevents the loss of synchronism but limits the torque angle deviations to very small values. A simple comparison of the three curves (for stiff coupling, flexible coupling with damping and eddy-current coupling) shows that the eddy-current coupling is the only and superior choice. Due to the non uniformity of the gust (refer Figure 18), oscillations in δ (for eddy-current coupling) are no longer regular and smooth as before. For V_p equal to $2V_r$, curves of δ_m versus k_T tend to level off for values of k_T greater than 3.0 (compare Figures 34, 46 and 51), and hence, as said before, for values up to k_T = 3.0 generator angle δ is held at a reasonably good level irrespective of the shape of the gust and highest angle for k_T = 3.0 being 50.8 (refer Figure 51). Longer gusts appear to have greater accelerating influence on the wind rotor as well as the generator rotor for the same value of k_T (compare Figures 34 with 51 and 35 with 52). Influence of ideal two-second gust ($V_p = 2V_r$) is more pronounced than that of two-second actual zig-zag model.

Curves of E_{gd} vs k_T are similar for one-second and two-second gusts ($V_p = 2V_r$). E_{gd} is much higher for two-second ideal gust ($V_p = 2V_r$) as compared to that for actual model (compare Figures 48 and 53) for a given value of k_T and ω_r. Again, the curves tend to level off for k_T values in the range of 2.0 to 3.0 and the gains in E_{gd} sharply level off for the values of k_T greater than 3.0. This also gives an indication for selecting the k_T value. Overall system efficiencies (E_{wd}) exhibit almost the same behavior for k_T ranging from 2.0 to 3.0

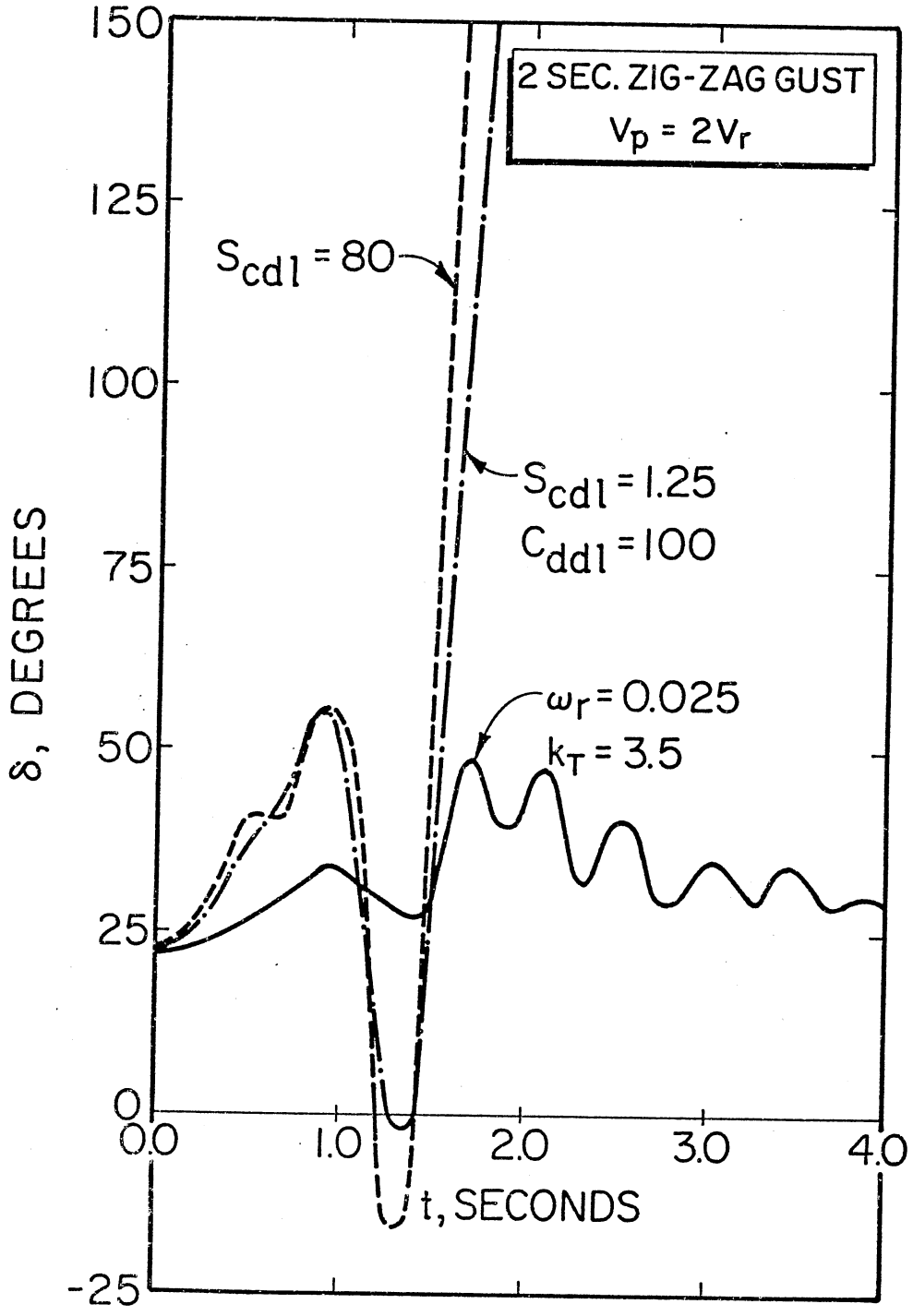

Figure 44. Typical Swing (δ versus t) Curves of a System Employing Various Coupling

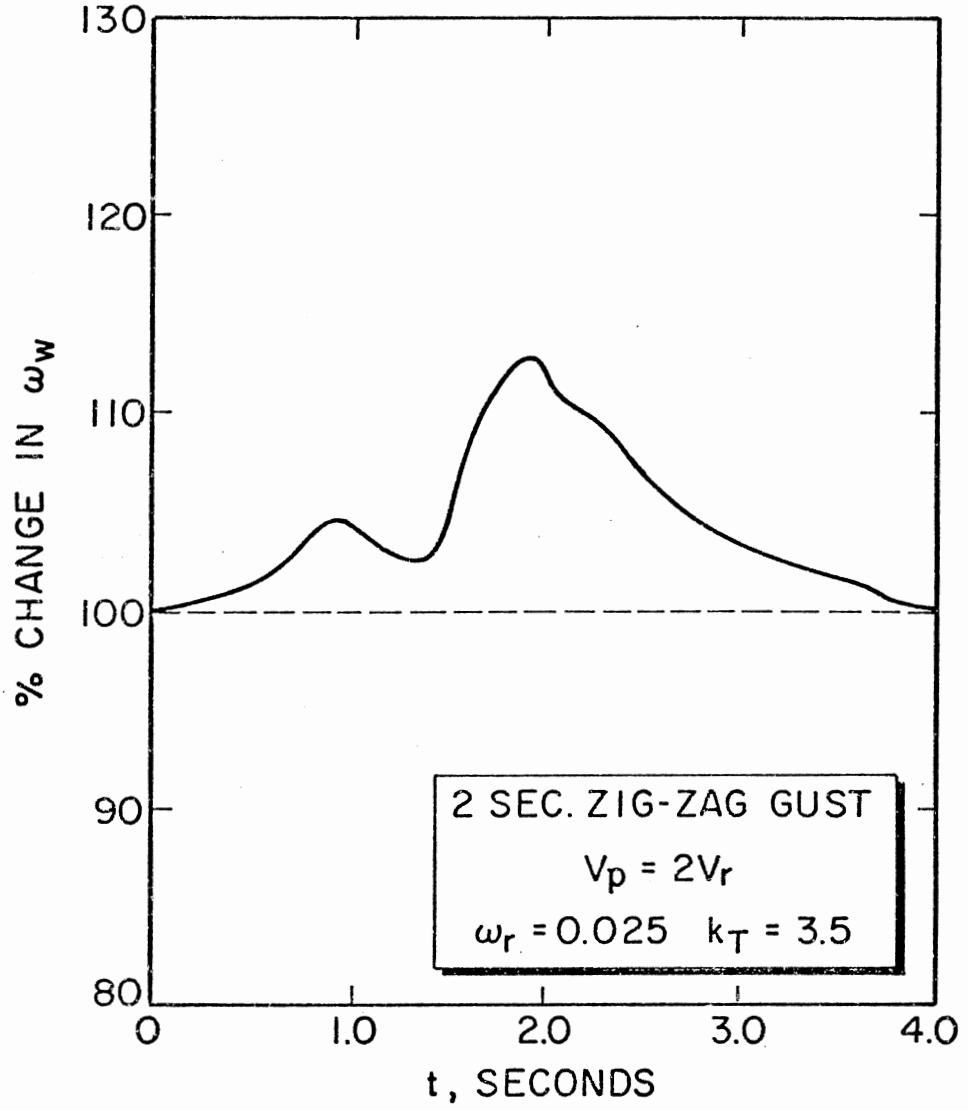

Figure 45. Typical % Change in ω_w versus t Curve for a System Employing Eddy Current Coupling

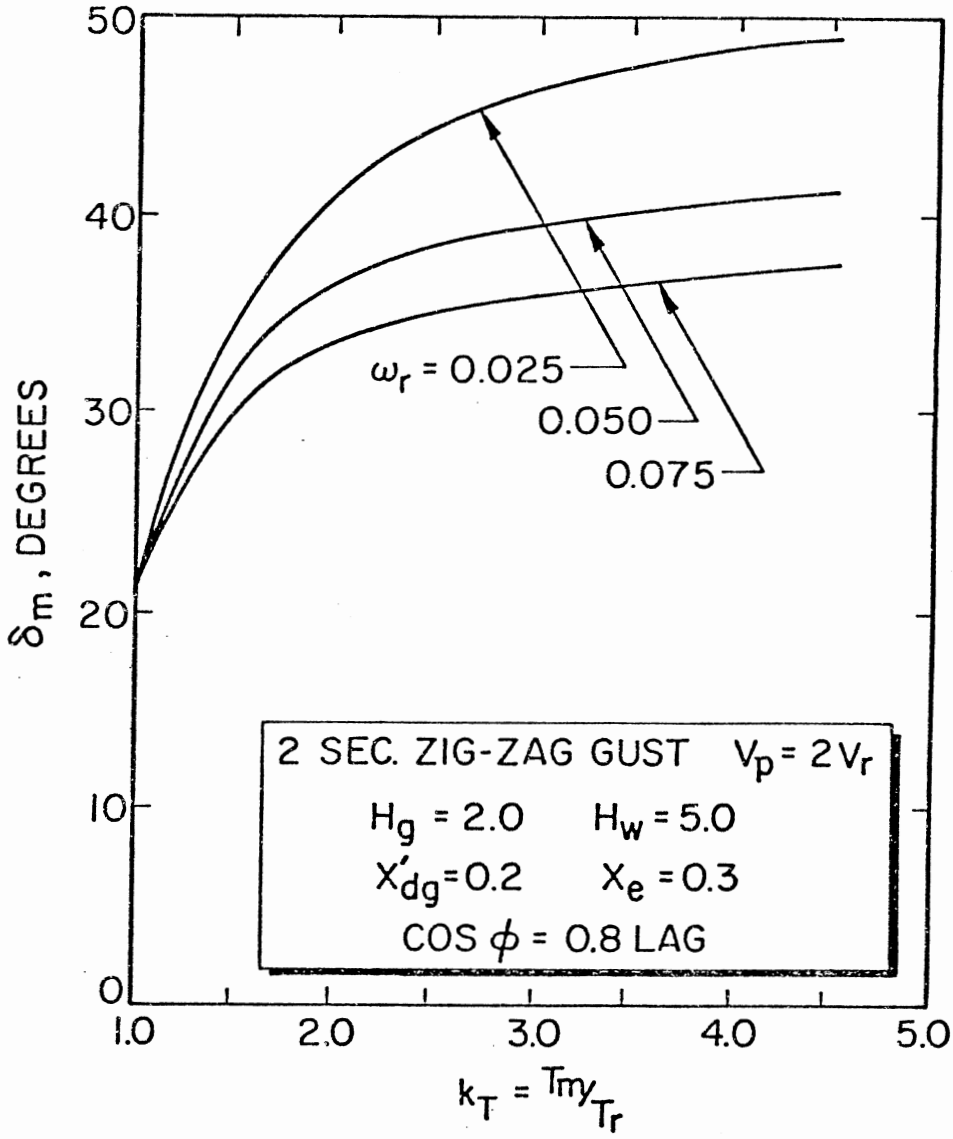

Figure 46. Effect of k_T and ω_r on Maximum Rotor Angle δ_m; Zig-Zag Gust ($V_p = 2V_r$)

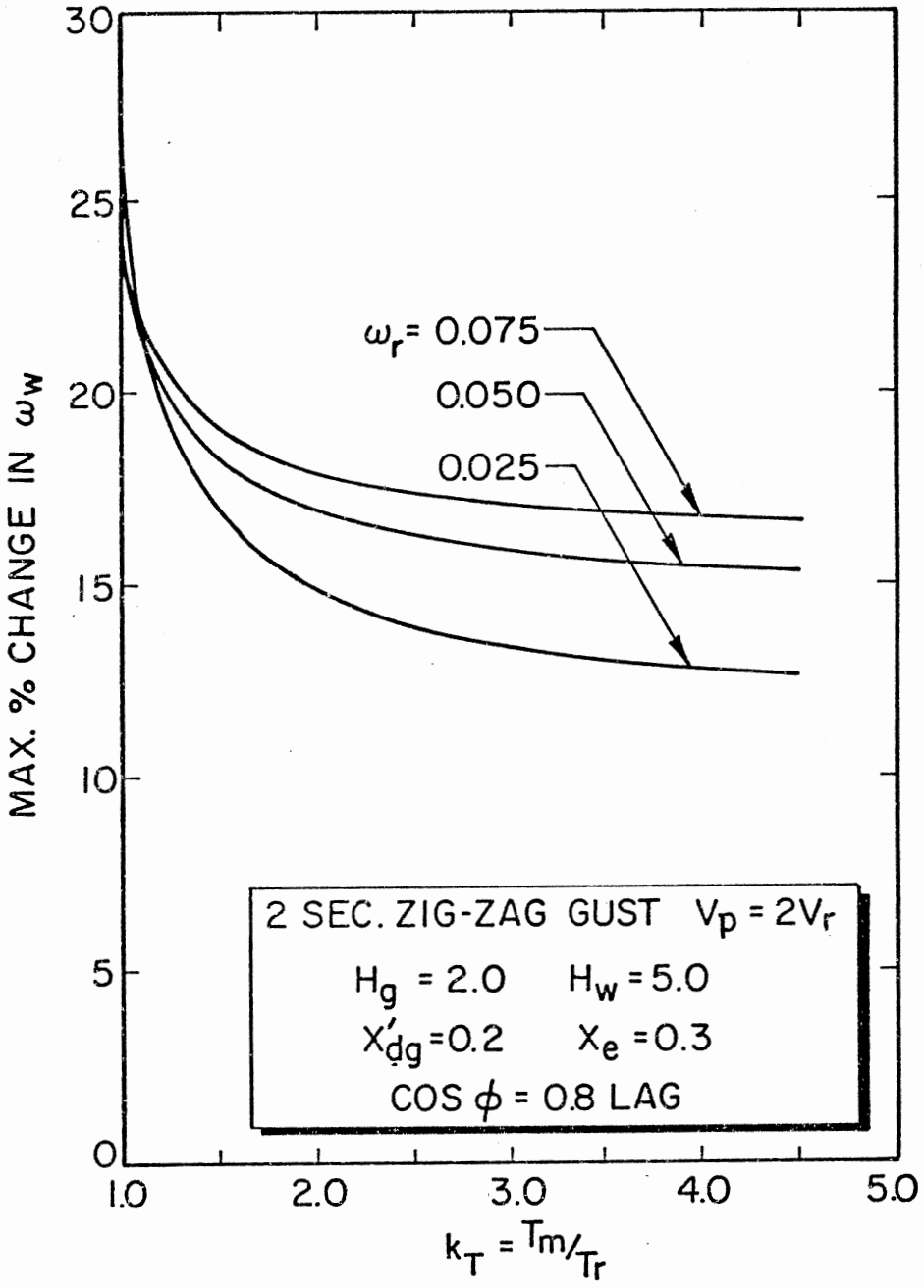

Figure 47. Effect of k_T and ω_r on Speed Variations of Wind Rotor ω_w; Zig-Zag Gust ($V_p = 2V_r$)

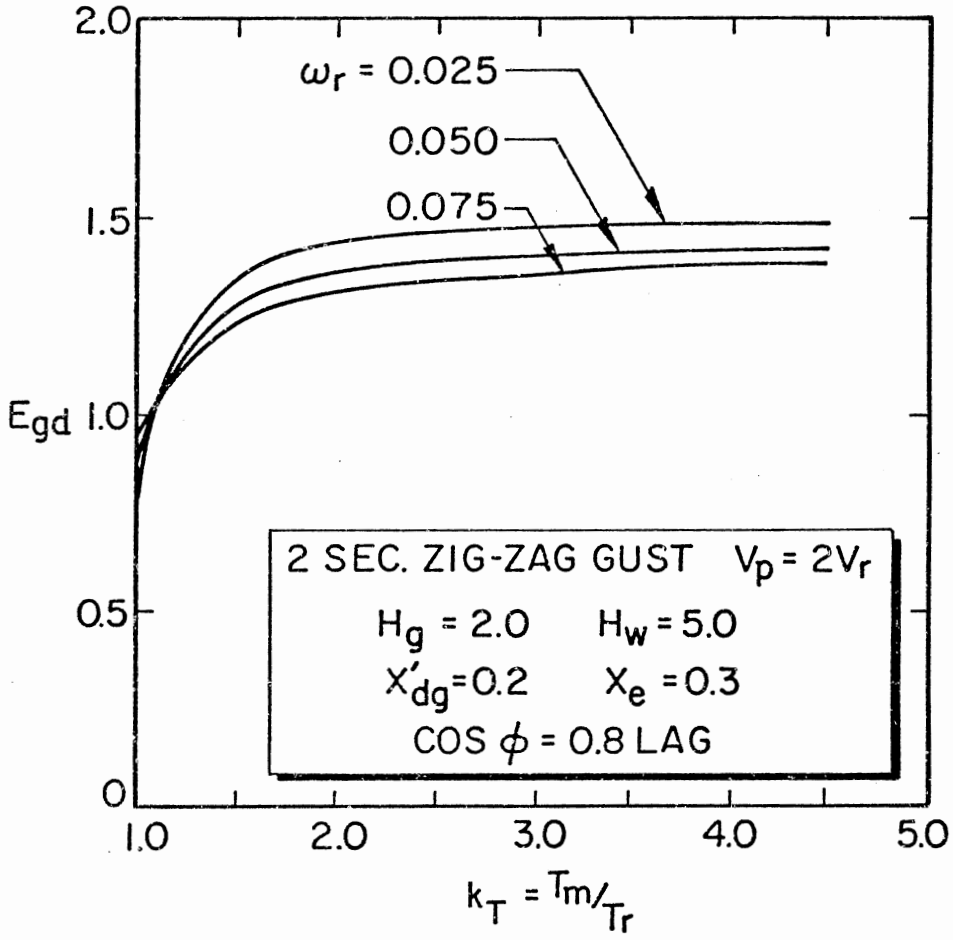

Figure 48. Non-dimensional (E_{gd} versus k_T) Curves Showing Effect of k_T and ω_r on E_{gd}; Zig-Zag Gust ($V_p = 2V_r$)

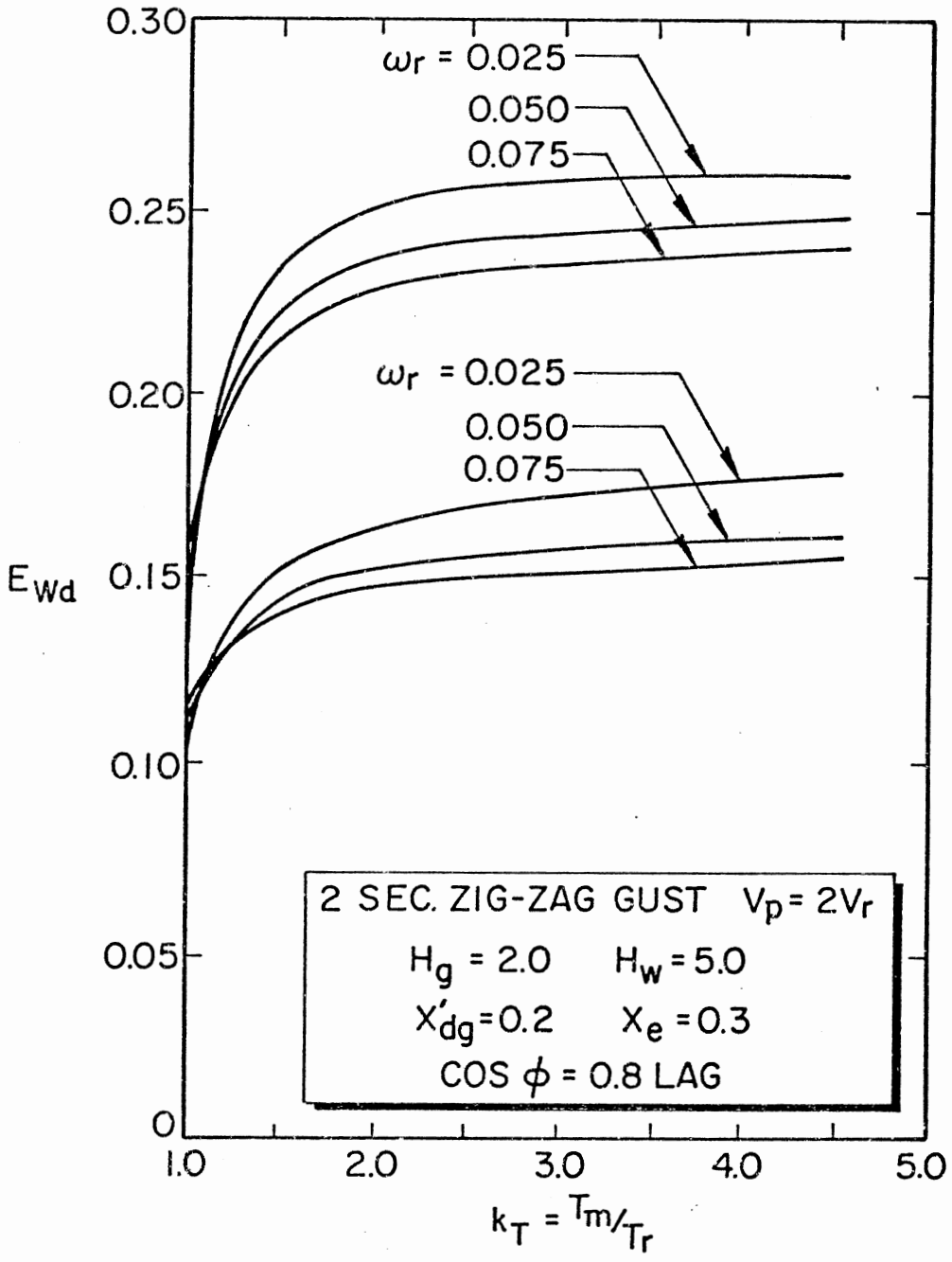

Figure 49. Non-dimensional (E_{wd} versus k_T) Curves Showing Effect of k_T and ω_r on E_{wd}; Zig-Zag Gust ($V_p = 2V_r$)

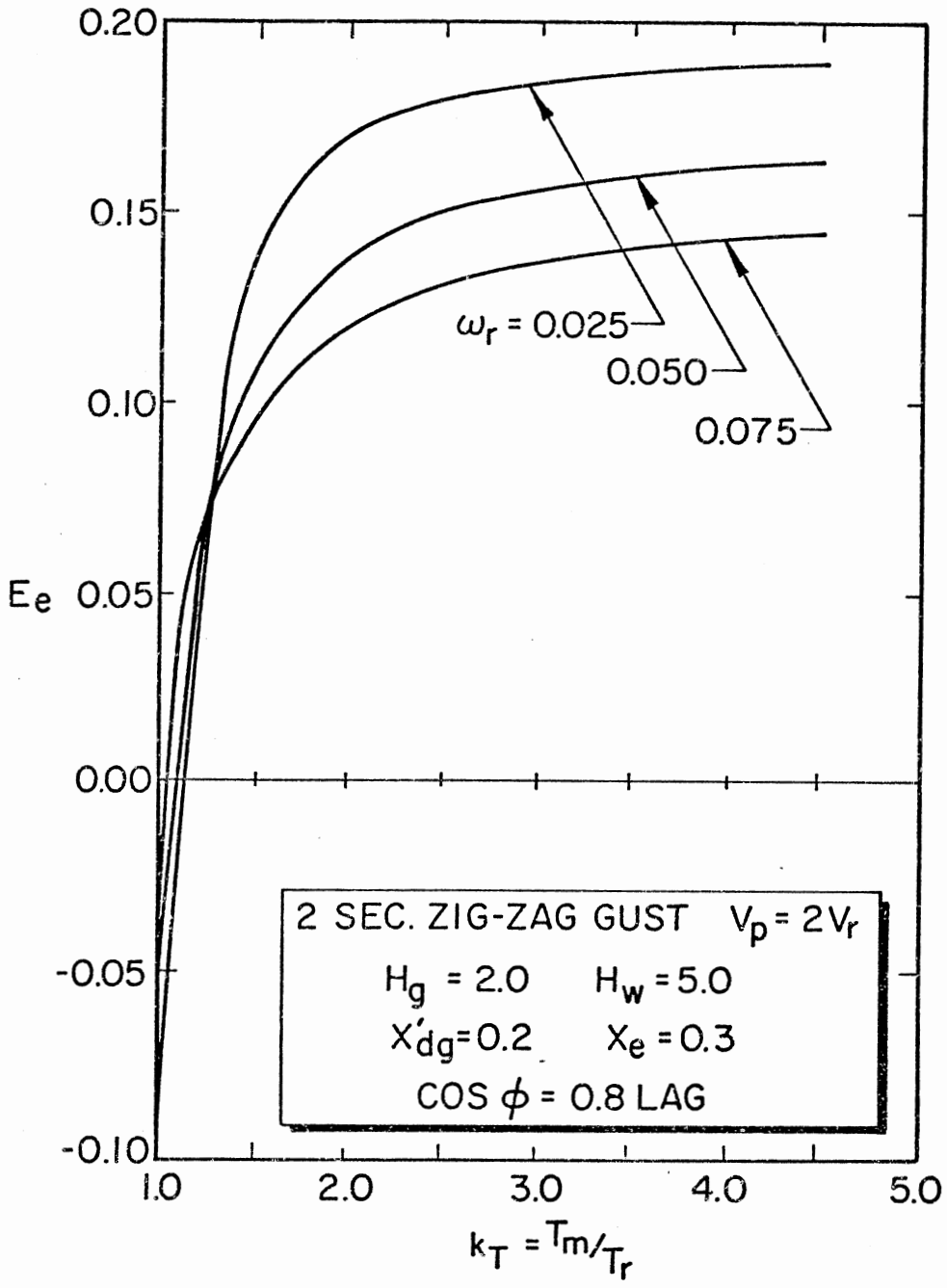

Figure 50. Non-dimensional (E_e versus k_T) Curves Showing Effect of k_T and ω_r on E_e; Zig-Zag Gust ($V_p = 2V_r$)

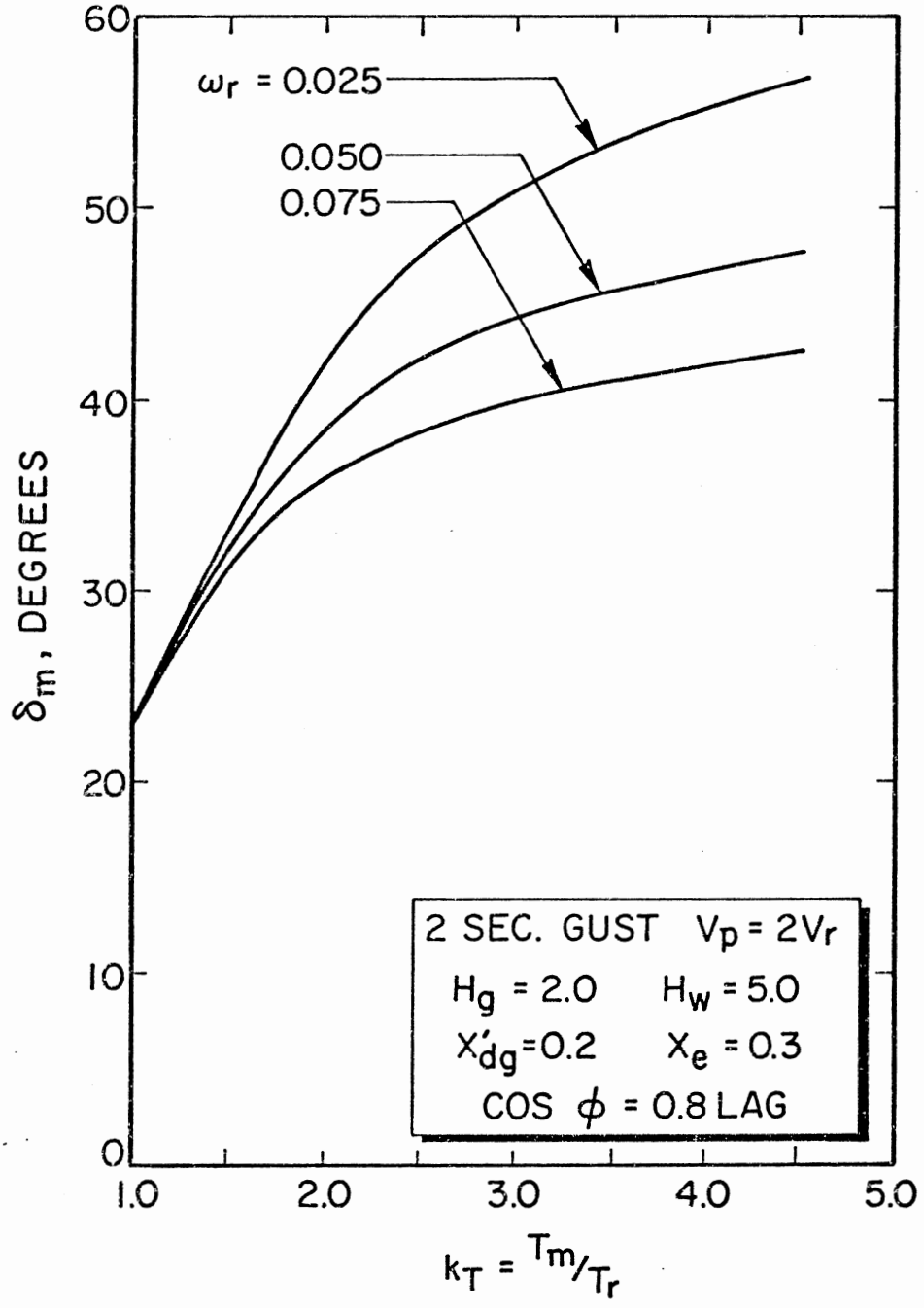

Figure 51. Effect of k_T and ω_r on Maximum Rotor Angle δ_m; Two Second Gust ($V_p = 2V_r$)

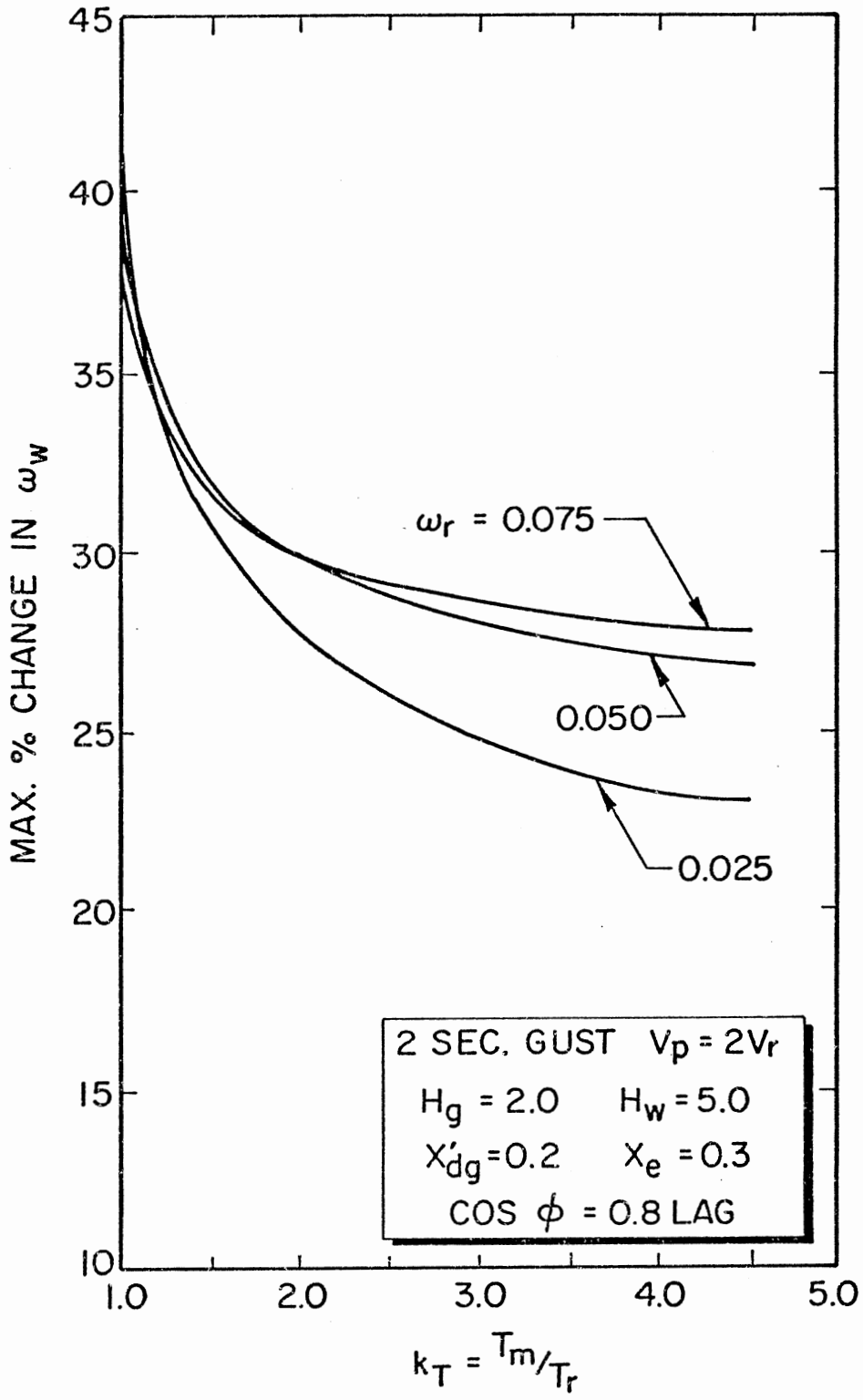

Figure 52. Effect of k_T and ω_r on Speed Variations of Wind Rotor ω_w; Two Second Gust ($V_p = 2V_r$)

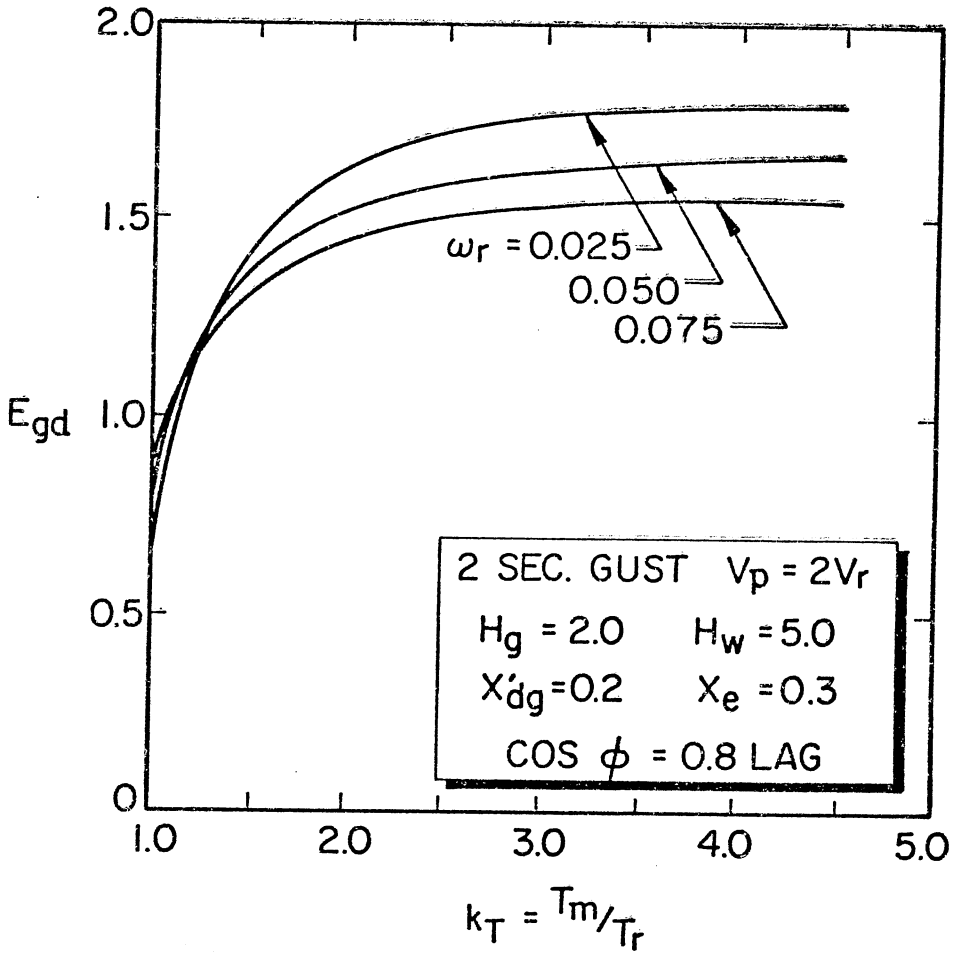

Figure 53. Non-dimensional (E_{gd} versus k_T) Curves Showing Effect of k_T and ω_r on E_e; Two-Second Gust ($V_p = 2V_r$)

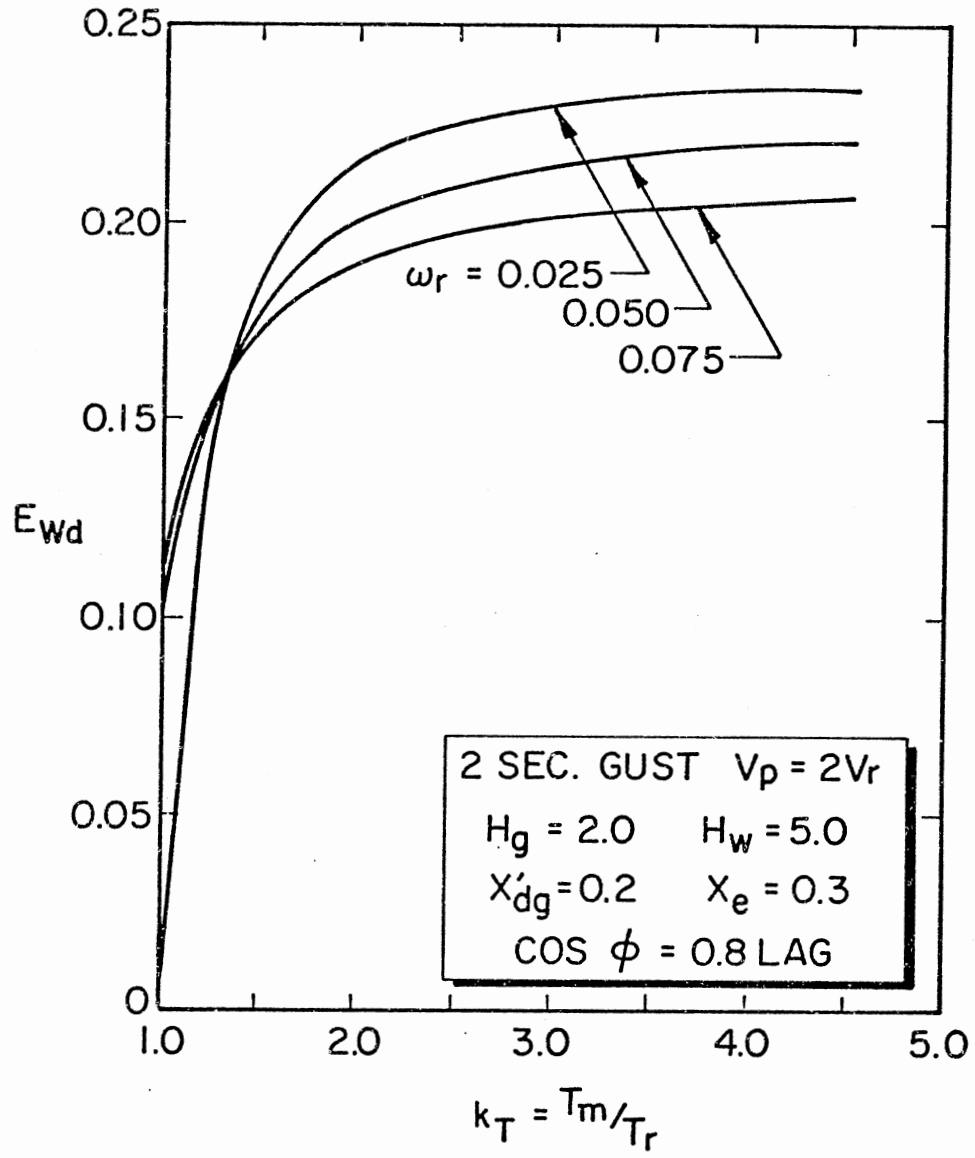

Figure 54. Non-dimensional (E_{wd} versus k_T) Curve Showing Effect of k_T and ω_r on E_{wd}; Two Second Gust ($V_p = 2V_r$)

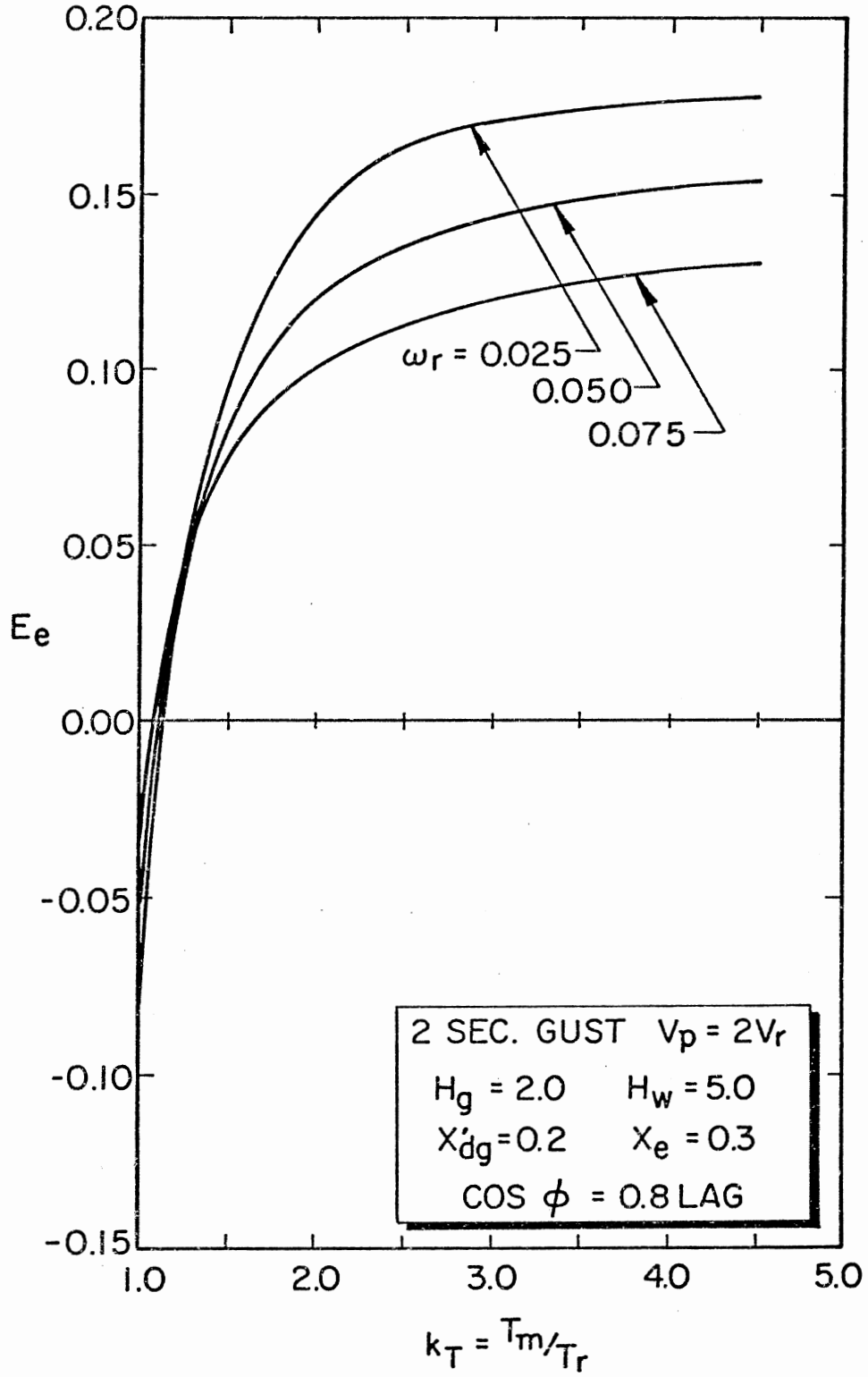

Figure 55. Non-dimensional (E_e versus k_T) Curves Showing Effect of k_T and ω_r on E_e; Two Second Gust ($V_p = 2V_r$)

and the curves level off thereafter. Operation with k_T = 1.0 very adversely affects the E_{gd} and E_{wd} and values of the same are very low (refer Figures 48, 49, 53 and 54). Such an operation is highly undesirable and be avoided, by increasing the excitation and operating on better Torque-slip speed characteristic. Curves of E_e vs k_T (V_p = $2V_r$) are similar to those for one-second gust and the gains are almost of the same order (compare Figures 38 and 55). Curves start leveling off for values of k_T greater than 3.0.

4.8 Concluding Remarks on Chapter IV

The following conclusions can be drawn from the results and discussion presented in this chapter.

i. Eddy-current couplings can be effectively used to limit the input torques of wind-driven synchronous machines.

ii. The ratio (k_T) of maximum torque to rated torque and the ratio of V_p to V_r are the most significant parameters to be taken into consideration.

iii. General stability level worsens with the increasing peak of the gust, but the coupling characteristics keep δ_m within reasonably safe limits. Motoring is completely prevented.

iv. Generator speed variations are negligible but the dynamic interactions cause pronounced speed build up of the wind rotor (41% above normal in the worst case when k_T = 1.0).

v. Of all the cases investigated, coupling with k_T = 2 to 3 and ω_r = 0.025 turns out the best performance irrespective of the type, peak and duration of the gust.

vi. Best gains in E_{gd}, E_{wd} and E_e are obtained in the range of

k_T = 2.0 to k_T = 3.0; for this range of k_T, δ_m is of the order of 40 to 45 electrical degrees.

vii. Operation with coupling designed for k_T = 1.0 is highly undesirable from the view points of accelerating torque on the wind rotor and reduction of energy delivered to the grid.

viii. Influence of the system reactance is not as significant as in the case of the stiff coupling and flexible coupling with damping from view point of stability.

CHAPTER V

BEHAVIOR OF WIND DRIVEN SYNCHRONOUS MACHINES UNDER SIMULTANEOUS GUSTS AND FAULTS

The last three chapters of this thesis have been exclusively devoted to the studies on wind driven synchronous machines employing different types of couplings, when such systems are subjected to the wind gusts of various types and durations. Though the wind gusts are undoubtedly the most frequent phenomenon causing disturbance in such systems, there are other disturbances which, though not so frequent, deserve consideration and study. A typical example of such a disturbance is the occurrence of faults in nearby circuits, followed by the opening and reclosing of the transmission circuits. It is with this view in perspective that an attempt is made in this chapter to undertake a preliminary study of such a case comprising of the simultaneous gusts and faults.

5.2 System Configuration and Governing Equations

The system under study comprises of an aeroturbine, a step up gearing mechanism, an eddy-current coupling and a synchronous generator connected to an infinite bus through a step up transformer, double circuit line and a step down transformer. Schematic of the system is shown in Figure 56. Performance equations for this model

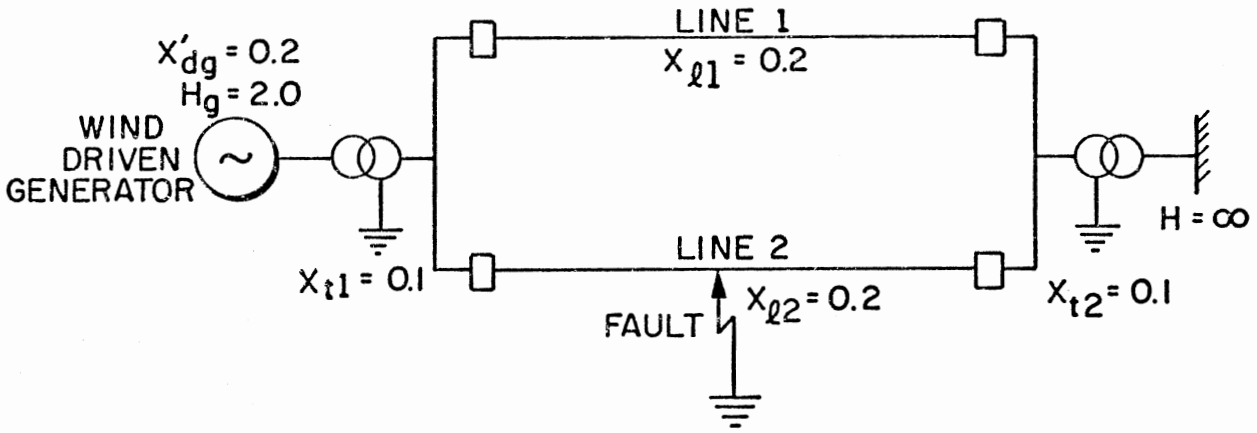

Figure 56. Schematic of the Power System Showing Electrical Components and Fault Location

are the same as given by equations (4.12) and (4.13), excepting that P_s and P_d are now given by the following equations:

$$P_s = \frac{E_i' E \sin \delta_i}{x_d'} \tag{5.1}$$

$$P_d = F_D \dot{\delta}_i \tag{5.2}$$

5.3 Computer Simulation

Computer simulation is carried out exactly in the same way as described in earlier chapters. Wind gust models and physical test data given in section 3.7 are used. The program is modified to conform with the modified equations (5.2) and (5.2). In this study, it is assumed that the voltage (E_i') behind the system direct axis transient reactance is constant during simulation with one-second gusts. The program is further modified to handle gusts and faults at the same time. The fault, removal of the fault (clearing of fault) and reclosing of the line are represented by changing the system reactances appropriately with time. Details of the network reduction and fault representation are not given here since such procedures are well known in power system work as described in the literature (refer (19)). The synchronous generator is replaced by its transient reactance, with a voltage behind the transient reactance, fixed in magnitude and at an angle corresponding to the initial machine kVA loading and infinite bus conditions. The disturbance is applied next. In the case of simultaneous gust and fault, both conditions are created by simulating a proper wind velocity and a new system reactance during the fault. New power output is calculated for the machine using initial machine

internal voltage (E_i'), new x_d' and the initial angle δ_i. Knowing the input, the accelerating power is computed which is then used to find the new rotor angle. In the succeeding interval, the newly computed machine angle is used to compute the new output power. Accelerating power is again computed and in turn the change in machine angle is obtained. This procedure is repeated until the duration of the fault clearing time (t_{sc}) is completed. The switching operation is now introduced by changing the system reactance x_d' (calculated for post fault conditions) and the process is repeated for the durations of reclosing time (t_{rc}), and the study duration thereafter, with appropriate system transient reactance x_d'.

The fault clearing time t_{sc} is taken as 0.1 second which is typical of fast acting relays. The circuit breaker reclosing time (t_{rc}) is taken as 0.3 second to allow for the extinction of the electric arc. A three-phase-to-ground fault in the middle of one of the lines (see Figure 56) is assumed in the study. Such a fault is quite severe (as compared to single phase faults) and will lead to conservative results. Removal of the fault and reclosing of the line are achieved by automatic opening and reclosing of the faulted line by the suitable action of the circuit breakers located at the two ends of the line.

Simulations are carried out for two values of k_T (2 and 2.5) and one value of ω_r (0.05). The system damping is separately included and the value of the damping constant (F_D) is taken as 1.0. Simulations are carried out for three system conditions: (a) when the system is subjected to gust only (b) when the system is subjected to simultaneous gust and three-phase-to-ground fault occurring at the beginning of

the gust, and (c) same conditions as in (b) except that the occurrence of the fault coincides with the peak of the gust (severest condition).

5.4 Results and Discussion

Computer simulation results are presented in the form of the swing (δ versus t) curves.

An overall examination of the curves shows that the system is stable and maintains its synchronism under the stipulated conditions. Conditions however can become critical if any electrical disturbance, subsequent to the one being studied, takes place. Such a subsequent electric disturbance (such as another fault) has the potential to throw the system out of synchronism. It should be mentioned here that the system would be stable (stay in synchronism) if the subsequent disturbance is mechanical and is on the wind rotor side of the mechanical interface (for example subsequent gust).

For the gust with higher peak ($V_p = 2V_r$), δ_m values are approximately the same for the two values of k_T (2.0 and 2.5) selected. It is obvious from the plots (compare Figures 57 and 58) that a three-phase-to-ground fault occurring at the peak of the gust causes severe oscillations in δ and the value of δ_m reached is about 67 to 70^o (initial angle δ_o being 14^o). The system oscillates for a long time and mild motoring (of the order of 2^o) is encountered indicating an underdamped condition. The results of the simulation, when the system is subjected to a three-phase-to-ground fault occurring at the beginning of the gust, show a milder response and the values of δ_m reached is 46^o (δ_o being 14^o). There is no motoring but, again, the oscillations appear to die slowly. The peak of the gust is the most influential external variable.

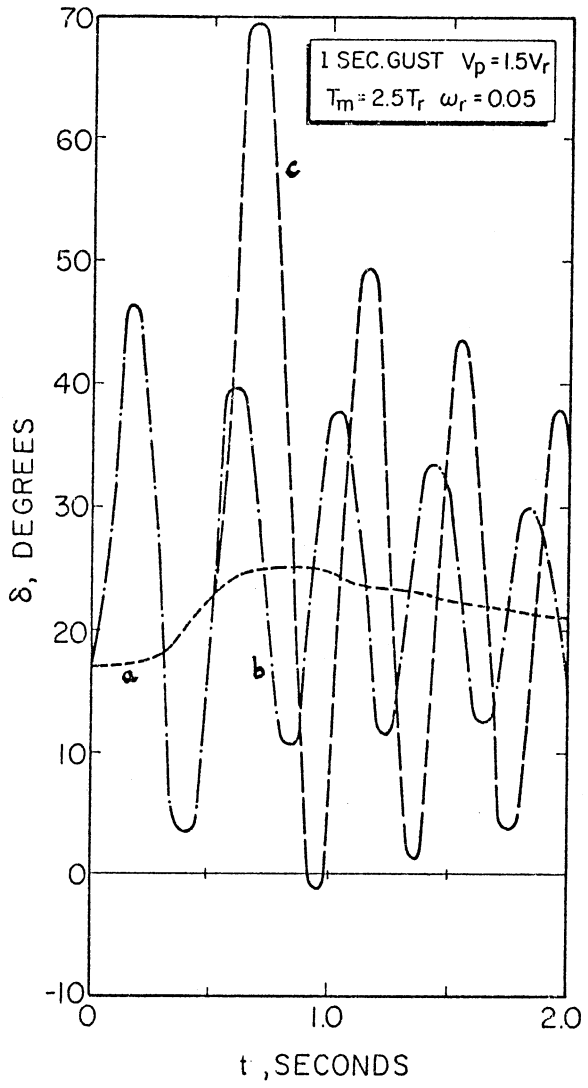

Figure 57. Swing Curves of the Investigated System
(a) Gust only
(b) Fault at Beginning of the Gust
(c) Fault at the Peak of the Gust

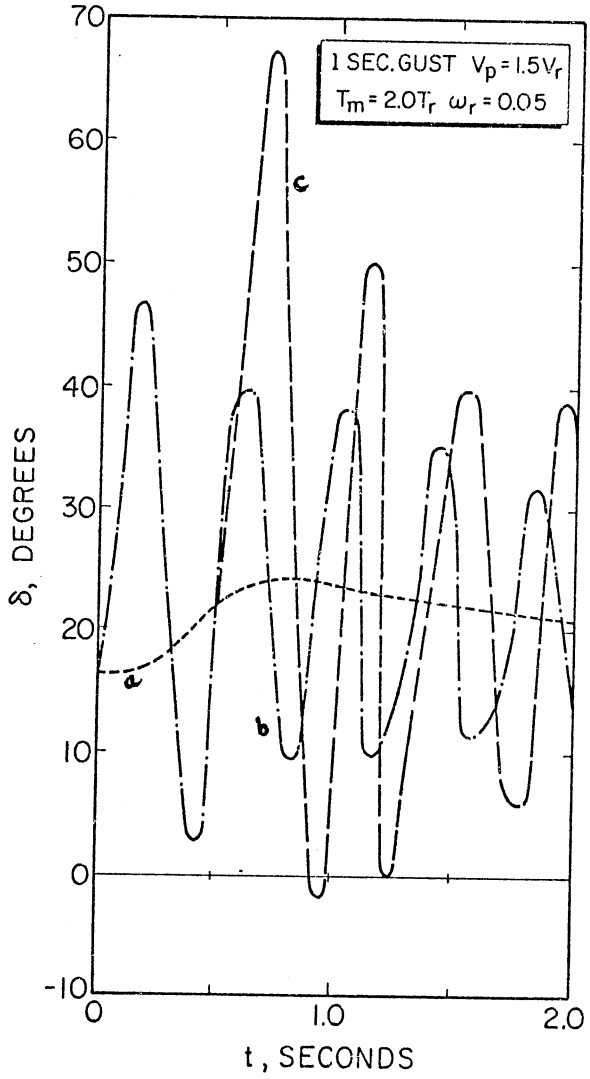

Figure 58. Swing Curves of the Investigated System
(a) Gust only
(b) Fault at Beginning of the Gust
(c) Fault at the Peak of the Gust

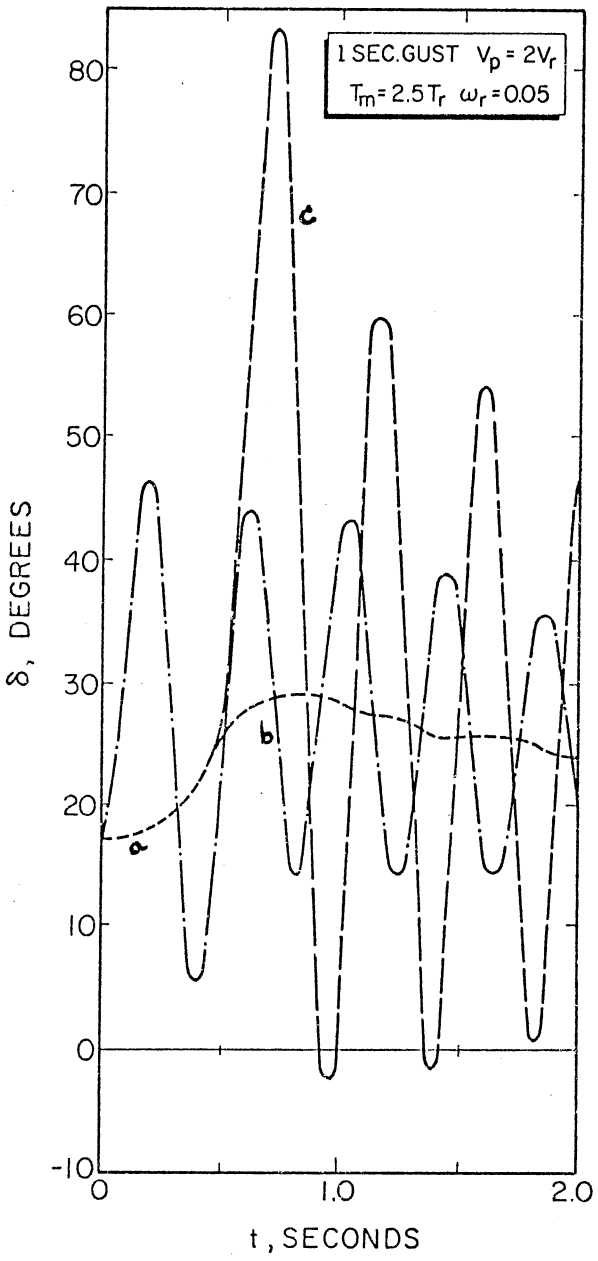

Figure 59. Swing Curves of the Investigated System
(a) Gust only
(b) Fault at Beginning of the Gust
(c) Fault at the Peak of the Gust

This fact is clearly indicated in Figure 59. For the same values of T_m (=2.5) and ω_r (=0.05), the maximum generator rotor angle reached is 83^o (δ_o being 14^o) in the case of $V_p = 2V_r$ as compared to 69^o in the case of $V_p = 1.5V_r$.

5.5 Concluding Remarks on Chapter V

The following preliminary conclusions can be drawn from the results and discussion presented in this chapter.

(i) The peak of the gust appears to be the most influential external variable.

(ii) The system employing an eddy-current-coupling appears to maintain stability even when subjected to simultaneous gusts and faults of the type studied.

(iii) Three-phase-to-ground fault occurring at the peak of the gust is more severe than the same occurring at the beginning of the gust.

(iv) Eddy-current coupling prevents the loss of system synchronism by limiting the input power under the conditions of gusts and faults occurring simultaneously.

CHAPTER VI

SUMMARY AND CONCLUSIONS

6.1 Summary of Results and Conclusions

The primary objective of this thesis was to examine the transient behavior of wind driven synchronous machines, under the conditions of wind gusts and faults for various system configurations.

This task has been performed in the following steps: (i) formulate the mathematical model for each system configuration, (ii) solve the sets of non-linear differential equation by employing an appropriate numerical technique and digital simulation, (iii) present the results in the form of curves, (iv) interpret these curves and (v) draw some useful conclusions.

Three chapters of this work (Chapters II, III, IV) deal extensively with the behavior of wind-driven synchronous machines under gusting conditions. Chapter V briefly describes the approach to handle simultaneous gusts and faults. Some useful conclusions have been drawn and these have been presented in the concluding section of each chapter.

These conclusions will now be consolidated, summarized and presented in a serial order.

(i) Dynamic behavior of wind driven synchronous-machines operating in parallel with infinite bus bars is analogous to the behavior of conventional prime-mover driven systems.

(ii) The amplitude and the duration of the gust are the most important external (input) variables determining the behavior and stability of wind-electric systems and as such wind gust models should be defined clearly and realistically.

(iii) The system reactance is the most influential electrical parameter in determining the system behavior and as such it should be kept as low as possible by selecting machines with low transient reactances.

(iv) Very soft couplings with damping ($S_{cdl} \simeq 1.25$; $C_{ddl} \simeq 100$) appear to be very effective from the view point of reducing the generator rotor angle and damping the oscillations subsequent to the maximum swing. Satisfactory performance can be obtained by combining very soft couplings with damping ($S_{cdl} \leq 1.25$; $C_{ddl} \geq 100$) along with a low system reactance ($x'_{dq} \leq 0.2$; $x_e \leq 0.2$) and by carefully selecting excitation control parameters. A typical set of recommended control parameters is given below.

$$500 \leq K_{ex} \leq 1000$$

$$0.05 \leq K_{st} \leq 0.075$$

$$0.05 \leq T_{ex} \leq 0.3$$

$$1.0 \leq T_{st} \leq 2.0$$

(v) Damped flexible couplings ($S_{cdl} = 80$; $C_{ddl} = 25$) can be employed in systems in which the total system reactance is very low ($x'_d = 0.3$) and in locations where wind gusts are mild ($V_p < 1.5\ V_r$) and infrequent.

(vi) The families of non-dimensional ($\hat{\delta}$ versus k) curves developed in this thesis provide design information useful for the

selection of

(a) the synchronous machine transient reactance (x'_{dg})

(b) the system external reactance (x_e) for a given type of coupling.

This information will enable a system designer to optimize a wind generating system from the view point of electrical stability.

(vii) Of all the couplings considered, eddy-current coupling has turned out the best performance in terms of system stability and energy delivered to the grid. This coupling is therefore strongly recommended for application in wind energy systems. The recommended values of design parameters for such couplings are:

k_T = 2.0 to 3.0 and ω_r = 0.025 to 0.05

(viii) In locations with frequent and severe gusting, only eddy-current coupling (or similar rate couplings) should be used to achieve satisfactory operation and to prevent the loss of synchronism.

(ix) The families of non-dimensional (E_{gd} vs k_T, E_{wd} vs k_T and E_e vs k_T) curves computed and presented provide valuable information on energy collection and energy delivery aspects of wind electric systems employing eddy-current couplings.

(x) Eddy-current couplings can be effectively employed in wind generator systems to maintain synchronism and to ensure reliable operation even when such systems are subjected to conditions of simultaneous faults and gusts.

(xi) For excitation systems, recommended values of ceiling voltage

ratio (CVR) lie between 2.0 and 3.0 for operation well below the 'critical line' (refer Figure 28). For systems which are expected to operate near the 'critical line', recommended values of CVR lie between 5.0 and 7.0.

6.2 Suggestions for Future Work

As a result of the present work, several problems in the field of stability of wind electric conversion systems worthy of future research have been identified. Specifically, the following areas are suggested for future research.

(i) Stability studies with a complete and refined machine representation as suggested by Olive (Reference (31). Non-dimensional parametric analyses of the type conducted in this thesis could be extended for this case also.

(ii) Extension of the present work, including complete machine representation and high performance blade pitch feed-back control loop is in order. Such studies assume special importance in the case of large (2 to 5 MW and above) systems when the wind gusts are frequent and their durations are long.

(iii) In this work, only a single parameter was varied at a time to lay the ground work and to develop a feeling for the system behavior and operation. Multiparameter variations may be necessary to optimize the system design from operational and stability view points.

(iv) This work has included only very preliminary studies on simultaneous gusts and faults. Extensive studies are suggested on

the less severe and unsymmetrical faults along with the occurrence of gusts as such conditions are more probable in practice.

(v) The present study has considered only one machine connected to a utility grid of infinite capacity. It is very likely in the future that a group of interconnected machines located in a windmill farm will supply wind generated electrical energy to a utility grid of infinite capacity, through a transmission link. Studies on such interconnected machines pose challenging problems from the view point of stability. This problem deserves very special attention.

(vi) As wind energy systems grow in size and in numbers, their penetration can no longer be considered small and the remaining system cannot be treated as infinite. Studies on the dynamics of wind driven synchronous machines operating in parallel with finite capacity networks are required to assess the stability of such systems under conditions of a variety of transient disturbances.

SELECTED BIBLIOGRAPHY

1. Fischer, J. "Past and Future of Wind Energy in Denmark." Proceedings, Second Workshop on Wind Energy Conversion Systems, Washington, D. C. (June, 1975), p. 162.

2. Putnam, P. C. Power From the Wind. New York: D. Van Nostrand Company, Inc. 1948.

3. Juul, J. "Design of Wind Power Plants in Denmark." Proceedings, United Nations Conference on New Sources of Energy, Vol. VII, Rome, Italy (August, 1961), pp. 229-241.

4. Simmons, D. M. Wind Power. Park Ridge, New Jersey: Noyes Data Corporation, 1975.

5. Hütter, U. "Influence of Wind Frequency on Rotational Speed Adjustments of Windmill Generators." NASA Technical Translation NASA-TT-F 15184 (November, 1973), pp. 1-16.

6. Hütter, U. "The Aerodynamic Layout of Wind Blades of Wind Turbines with High Tip-Speed Ratio." Proceedings, United Nations Conference on New Sources of Energy, Vol. VII, Rome, Italy (August, 1961), pp. 217-228.

7. Golding, E. W. Generation of Electricity by Wind Power. London: E. and F. N. Spon., Ltd., 1955.

8. Bonefille, Rene. "French Contribution to Wind Power Development-By EDF 1958-1966." Proceedings, Workshop on Advanced Wind Energy Systems, Stockholm, Sweden (August, 1974).

9. Ramakumar, R. "Wind Electric Conversion Utilizing Field Modulated Generator Systems." Proceedings, Sharing the Sun 76 - Solar Technology in the Seventies Conference, Winnipeg, Manitoba, Canada, Vol. 7 (August, 1976). pp. 215-229; to appear in Solar Energy.

10. Thomas, R., R. Puthoff and J. Savino. "Plans and Status of The NASA-Lewis Research Center Wind Energy Project." NASA Technical Memorandum. NASA TMX-71701 (1975).

11. Federal Wind Energy Program. Summary Report Washington, D.C., ERDA-77-32 (January 1, 1977).

12. Banas, J. F. and W. N. Sullivan. "Sandia Vertical-Axis Wind Turbine Program." Technical Quarterly Report, SAND 76-0036 (October/December, 1975).

13. Wetherholt, L. Proceedings, Vertical Axis Wind Turbine Technology Workshop, Albuquerque, New Mexico, SAND 76-5586 (May, 1976).

14. Ramakumar, R., H. J. Allison and W. L. Hughes. "Prospects for Tapping Solar Energy on a Large Scale." Solar Energy Journal, Vol. 16, No. 2 (October, 1974), pp. 107-115.

15. Ramakumar, R., H. J. Allison and W. L. Hughes. "Solar Energy Conversion and Storage Systems for the Future." IEEE TRANSACTIONS on Power Apparatus and Systems, Vol. PAS-94, No. 6 (November/December, 1975), pp. 1926-1934.

16. Reitan, D. K. "A Progress Report on Employing a Non-Synchronous AC/DC/AC Link in a Wind-Power Application." Proceedings, Second Workshop on Wind Energy Conversion Systems, Washington, D. C. (June, 1975), pp. 290-297.

17. Jayadev, T. S. "Induction Generators for Wind Energy Conversion Systems." Report Submitted to ERDA, Division of Solar Energy (February, 1976).

18. Smith, R. T. "Analysis of Polyphase Commutator Generators for Wind-Power Applications." IEEE Trans. Aerospace and Electronic Systems, Vol. AES-12, No. 1 (January, 1976), pp. 39-41.

19. Kimbark, E. W. Power System Stability. Vol. I and Vol. III, New York: John Wiley and Sons, Inc., 1956.

20. Stevenson, W. D. Elements of Power System Analysis. 3rd Ed. New York: McGraw-Hill, 1975, p. 367.

21. Romanelli, P. J. "Electrical Generating Equipment and Electric Utility Requirements for High Power Wind Generator Systems." Tenth Inter-Society Energy Conversion Engineering Conference Record, Newark, Delaware (August, 1975), pp. 1251-1257.

22. Elgerd, O. I. Electric Energy Systems Theory. New York: McGraw-Hill, 1971, p. 483.

23. Johnson, C. and R. T. Smith. "Dynamics of Wind Generators on Electric Utility Networks." IEEE Transactions on AES., Vol. AES-12, No. 4 (July, 1976), pp. 483-493.

24. Park, R. H. "Two Reaction Theory of Synchronous Machines-Generalized Method of Analysis-Part I." AIEE Transactions, Vol. 48 (February, 1929), pp. 716-730.

25. Park, R. H. "Two Reaction Theory of Synchronous Machines-II." AIEE Transactions, Vol. 52 (June, 1933), pp. 352-355.

26. Pantalone, D. K. and A. G. Potter. "Application of Wind Power to the Electric Power System." Proceedings, Frontiers of Power Technology Conference, Sec. 6, Stillwater, Oklahoma (October, 1976), pp. 1-10.

27. Martinez and Sanchez. Synchronous Alternators for Wind Energy Conversion. Cambridge, Massachusetts: Progress Report ERDA/NSF/00826-75/2 (February 15, 1976), pp. 24-46.

28. Lingelbach, D. D. "Simulation of Wind Turbine Generator System Power Flow Dynamics." Proceedings Workshop on Electrical Engineering Aspects of Wind Energy Systems, Sec. 7, Stillwater, Oklahoma (October, 1976), pp. 1-31.

29. Hwang, H. H. and L. J. Gilbert. "Random Synchronization of the ERDA/NASA 100 k W Wind Turbine Generator with Large Utility Networks." IEEE Control of Power Systems Conference Record, No. 77 CH 1168-4 REG. 5, College Station, Texas (March, 1977), pp. 26-30.

30. Hwang, H. H. and L. J. Gilbert. "Synchronization of Wind Turbine Generators against an Infinite Bus under Gusting Conditions." IEEE Power Engineering Society Paper No. F 77 6/5-2, presented in the 1977 Summer Power Meeting, Mexico City, Mexico (July, 1977), to appear in IEEE Transactions on Power Apparatus and Systems.

31. Olive, W. D. "Digital Simulation of Synchronous Machine Transients." IEEE Transactions on Power Apparatus and Systems, Vo. PAS-87, No. 8 (August, 1968), pp. 1669-1675.

32. Crary, S. B. Power System Stability. Vol II, New York: John Wiley and Sons, Inc., 1947.

33. Stagg, G. W. and A. H. El-Abiad. Computer Methods in Power System Analysis. New York: McGraw-Hill, 1968, pp. 366-368.

34. Lapidus, L. and J. H. Seinfeld. Numerical Solutions of Ordinary Differential Equations. New York: Academic Press, 1971, pp. 267-292.

35. Gerald, C. F. Applied Numerical Analysis. Reading, Massachusetts: Addison-Wesley, 1973, pp. 118-119.

36. Bronson, R. Theory and Problems of Modern Introductory Differential Equations. New York: Shaum's Outline Series, McGraw-Hill, Inc., 1973, pp. 223-231.

37. Puthoff, R. L. "Status of 100 kW Experimental Wind Turbine Generator Project." Proceedings, Second Workshop on Wind Energy Conversion Systems, Washington, D. C. (June, 1975), pp. 21-36.

38. Wright, S. H. "Determination of Synchronous Machine Constants by Tests." AIEE Transactions, Vol. 50 (December, 1931), pp. 1331-1351.

39. Park, R. H. and E. H. Bunkers. "System Stability as a Design Problem." AIEE Transactions, Vol. 48 (January, 1929), pp. 175-179.

40. Furst, B. G. "Effect of Synchronous Reactance and Excitation Parameters on Transient Stability." Transactions of the Institution of Engineers, Australia (March, 1968), pp. 135-140.

41. Fitzgerald, A. E. and C. Kingsley, Jr. Electric Machinery. New York: McGraw-Hill, 1961, pp. 543-546.

42. Kozdron, J. Introduction To Torsional Vibrations Eaton Corporation, Industrial Drives Division Cleveland, Ohio, 1976, pp. 1-37.

43. Diesel and Gas Turbine Worldwide Catalog. Vol. 42 (1977), Oshkosh, Wisconsin, 1977.

44. Dodge Engineering Catalog. D-63, Mishakawa, Indiana, 1963.

45. Byerly, R. T. and E. W. Kimbark. Stability of Large Electric Power Systems. IEEE Press, New York: 1974, pp. 50-54.

46. Gibbs, W. J. "Tooth-Ripple Losses in Unwound Pole-Shoes." Institution of Electrical Engineers Journal, Vol. 94, Part II (1947), pp. 2-12.

47. Glazenko, T. A. "Some Problems in the Design of an Asynchronous Clutch with a Monolithic Rotor." Automation and Remote Control (Avtomatika i Telemekhanika), Vol. 19, Part II (April, 1959), pp. 783-790.

48. Davies, E. J. "An Experimental and Theoretical Study of Eddy-Current Couplings and Brakes." IEEE Transactions on Power Apparatus and Systems, Vol. PAS-82 (August, 1963), pp. 401-419.

49. Flack, R. F., W. T. Grant and C. Parker. "Application for Eddy-Current Couplings." Electrical Times (April 17, 1969) pp. 52-54.

50. Shackshaft, G. "General-Purpose Turbo Alternator Model." Proceedings, I.E.E., Vol. 110, No. 4 (April, 1963), pp. 703-713.

51. Lokay, H. E. and R. L. Bolger. "Effect of Turbine-Generator Representation in System Stability Studies." IEEE Transactions on Power Apparatus and Systems, Vol. PAS-84, No. 10 (October, 1965), pp. 933-942.

52. Olive, D. W. "New Techniques for the Calculation of Dynamic Stability." IEEE Transactions on Power Apparatus and Systems, Vol. PAS-85, No. 7 (July, 1966), pp. 767-777.

53. Lewis, W. A. The Principles of Synchronous Machines. Chicago, Illinois: I.I.T. Press, 1949.

54. Concordia, C. Synchronous Machines. New York: John Wiley, 1951.

55. Prabhashankar, K. and W. Janischewsyj. "Digital Simulation of Multi-machine Power Systems for Stability Studies." IEEE Transactions on Power Apparatus and Systems, Vol. PAS-87, No. 1 (January, 1968), pp. 73-80.

56. Dineley, J. L. and A. J. Morris. "Synchronous Generator Transient Control: Part I." Proceedings Seventh PICA Conference, Boston, Massachusetts (May, 1971), pp. 182-192.

57. Kimbark, Edward W. Personal Correspondence, August 8, 1977.

58. Hwang, H. H. Personal Correspondence, July 27, 1977.

APPENDIX

SYNCHRONOUS MACHINE MODELS

SYNCHRONOUS MACHINE MODELS

(A) Machine Representations

Over the past several decades, many models have been proposed to represent synchronous machines in system studies. The complexity of the model used depends on the nature of the system disturbances studied. Any model is based on a certain set of idealizing assumptions and the researcher has to pick a model that will provide the information sought for, without compromising the basic behavior of the system.

When the electrical transients (electrical faults, synchronizing transients, etc.) are of interest, a detailed machine representation is essential and this fact has been recognized by many researchers in the past. A wealth of information is available in the literature pertaining to this topic.

One of the best treatises on modeling turbo-alternators is presented by Shackshaft (50). This paper deals extensively with the development of a mathametical model which includes mechanical and electrical damping, flux variations, iron saturation and saliency; it also permits the inclusion of the voltage regulator and steam turbine governer action. In this treatise, special mention of the iron saturation effects is made and a technique for taking it into account is suggested. Analog computer is used to solve the set of appropriate equations. Results of anolog simulations are compared with experimental data obtained using a 30 MW turbo-generator. As the treatise is extremely

complex, the author recommends a first order simplification by neglecting $p \Psi_d$ and $p \Psi_q$ (changes in the stator flux linkage) terms assuming speed variations to be negligible and introducing a separate damping term.

Lokay and Bolger (51) also emphasize the need for a detailed turbine generator representation. They present system simulation results obtained by using varying degrees of refinements in machine representation. The advantage of complete machine representation is clearly brought out. Nine test cases are considered and the results are compared and discussed. One of the cases, case ix, includes transient saliency, flux linkage variation, machine saturation, machine and system damping, speed governer action and excitation control. The paper concludes with a suggestion of not using a complete machine representation (unless absolutely necessary) from computional point of view and availability of data. The authors also emphasize the importance of machine damping and excitation control.

Olive (52), in an excellent treatment on the subject of the system stability, stresses the need for more involved machine representation in a philosophic manner. In his above quoted paper, a reasonable treatment is accorded to the machine and excitation voltage control with special attention to saturation. Damping is included separately, to account for negative sequence damping, direct current braking and positive sequence damping. Stator flux linkage variations ($p \Psi_d$ and $p \Psi_q$) are neglected. The theory and the underlying assumptions, voltage regulator and governer representations and the computational techniques, are discussed. This paper is essentially a first order simplification of the complete machine representation.

In his second paper (see reference 31), which is essentially a philosophic extension of his earlier paper on the subject (previously quoted reference 52) Olive discusses in a very qualitative manner the need and application of d, q, o transformation. Starting from a general machine model with three stator windings and four rotor windings placed around the air-gap periphery (two windings on each axis), he develops the flux linkage and voltage equations which are similar in form to those given by Park (references 24 and 25), Lewis (53) and Concordia (54). Formulae for input torque and electrical torque are also given. By properly defining some new variables he proceeds to convert the earlier set of variables into a new set in which all quantities are in per-unit and the new set of equations is readily adaptable to digital simulation. He concludes that at the present stage in stability analysis the procedure of neglecting $p \Psi_d$ and $p \Psi_q$ terms and correcting for (damping) torques appears to yield sufficiently accurate results and is very effective in the reduction of computer time.

Prabhashankar and Janischewsyj (55) in their excellent paper propose a digital simulation technique for detailed stability analysis on an extensive power system. Synchronous machine model is developed in the form of Park equations, in per-unit. Relations between self, mutual and leakage reactances are laid out. Provision for saturation is made by making proper assumptions and introducing a multiplying factor for mutual reactances. Control and speed governer equations are given along with the mechanical equations of the machine. Equations are manipulated to conform to a form suitable for digital simulation.

Dinely and Morris (56) in a valuable paper on the same subject

describe mathematical models of varying complexity for the digital simulation of the transient behavior of synchronous generators and motors in a power system. The results of various models are compared with a laboratory test model. It has been remarked that inclusion of $p\,\Psi_d$ and $p\,\Psi_q$ terms require an integration step of very small size ($\leq$ 0.0005s).

(B) Justification of the Model Used

The synchronous machine model used in section 2.2 of this thesis is originally due to Park, subsequently reduced and simplified by Kimbark. It has been assumed in this model that the transformer voltage ($p\,\Psi$) terms are very small as compared to terms with ω in them (speed voltage terms) and changes in ω are small ($\leq$ 3.5%). The above mentioned model, takes into account, the effect of saliency, effect of the damping (by including a separate damping term), change in E'_q (which depends on the change in the field flux linkage Ψ_f). The effect of excitation voltage control have been included in the model by expanding the state vector $\vec{Z}(t)$.

This model has been adopted in this work mainly because of the following reasons.

a. The major part of this thesis deals with system behavior when subjected to the wind gusts and the consequent mechanical transients. Mechanical variable δ (generator torque angle) is of major interest in determining the stability of the proposed wind driven systems. When mechanical transients of the power systems (mechanical oscillations of δ) are studied, it is reasonable to omit $p\,\Psi_d$ and $p\,\Psi_q$ terms and to assume $\frac{\omega}{\omega_r} = 1$.

This opinion has been expressed by Kimbark (57), Hwang (58) and Prbhashankar (see Discussion of reference 31). Omission of $p\Psi$ (changes in stator flux linkages) is equivalent to neglecting the direct current component and harmonic components of the armature currents, which are necessary if it is desired to compute the electrical phenomena in the system.

b. The exclusion of $p\Psi_d$ and $p\Psi_q$ terms in the model does have dramatic effect on the permissable calculation interval. A fifty-fold reduction in the step size has been found possible as a result of the exclusion of these terms (see Discussion of Reference 31).

c. Excellent results have been reported with this model in the past, especially with the salient pole machines with low synchronous reactances (as is the case in the present study).

VITA

Abdul Qavi Qazi

Candidate for the Degree of

Doctor of Philosophy

Thesis: TRANSIENT BEHAVIOR OF WIND DRIVEN SYNCHRONOUS MACHINES

Major Field: Electrical Engineering

Biographical:

Personal Data: Born on March 12, 1940, in Hyderabad, Sind, Pakistan, the son of Mr. and Mrs. Zubeda Abdul Haye Qazi.

Education: Attended primary, secondary and I. Sc. Schools in Hyderabad, Sind, Pakistan; received the Bachelor of Engineering degree in Mechanical and Electrical Engineering from University of Karachi, Karachi, Pakistan, in May, 1964; received the diploma of Magister Electro-Energeticae from the University of Zagreb, Zagreb, Yugoslavia, in December, 1967; completed requirements for the Doctor of Philosophy degree at Oklahoma State University, Stillwater, Oklahoma, in December, 1977.

Professional Experience: Junior Engineer, West Pakistan WAPDA (Electricity), November, 1963 to July, 1964: Training Engineer, Institute of Electro-economics, Zagreb, Yugoslavia, January, 1968 to June, 1968; Project Engineer, Energo invest, Sarajevo, Yugoslavia, July, 1968 to December, 1968; Senior Lecturer and Reader in Electrical Engineering, Sind University Engineering College, Jamshoro, Sind, Pakistan, February, 1969 to March, 1971; Professor in Electrical Engineering, NED University of Engineering and Technology, Karachi, Pakistan, April, 1971 to present (on leave abroad in U.S.A.).

Professional Organizations: Student Member of the Institute of Electrical and Electronics Engineers of U.S.A.